

27<sup>th</sup>  
ACSSSC



## Program and Abstracts

---





# Contents

---

Foreword.....	2
Preface .....	3
Campus Map .....	4
Sponsors.....	5
Students Bursaries .....	6
Previous Conferences .....	8
List of Participants.....	9
Scientific Program .....	11
Conference Awards.....	16
Abstracts – The TW Healy Centre Plenary Lecture .....	17
Abstracts – Oral Presentations .....	18
Poster Index .....	57
Abstracts – Posters .....	59
Experimental Techniques.....	83
Index of Presenters .....	96

# Foreword

---

Welcome to the 2010 Australian Colloid and Surface Science Student Conference, the 27<sup>th</sup> of its kind since they began in 1968.

Like many of the academics (and possibly one or two of the students) in the wonderful world of colloid and surface science, I've been looking forward to the ACSSS conference for some time. For me, it's the 'perfect meeting'. Firstly, I don't have to prepare a talk. Secondly, I get to catch up with all of my friends who have come from interstate, overseas, or just from over the other side of my own city. Finally, and most importantly, I get to hear about the latest research in our field, presented by energetic and enthusiastic people who, in a few years, will take the place of the current academics in pushing back the frontiers of science, while we more senior folk shuffle off to the Australian Research Council-funded Colloid and Surface Science Maximum-Security Twilight Home.

I realize, however, that many of the postgraduate students, particularly the 'first-timers', might view the ACSSS Conference in a very different light to me. There may be some nervousness about having to present the work, uneasiness about the questions that may be asked (and, more importantly, who might ask them), and depression created by the suggestions of further work that really needs to be done when you thought you had completed THAT section of the experimental work.

We 'non-students' understand these uneasy feelings. To some, it may come as a surprise that we weren't born with a PhD testamur sticking out of our left nostril. Even the follicle-challenged of us once faced the daunting prospect of having to stand up in front of a similar community as this, at an earlier time, to present our research. We survived (well, most of us did), and I have no doubt that this year's students will too (well, most of them).

Students - you will gain the valuable experience that this conference offers to each of its speakers; the chance to present your work to a group of genuinely interested scientists in an extremely supportive environment. If you are lucky, you will also get to experience pure 'post-talk euphoria', which often blends into 'morning-after hangover'. The elements are an important part of the student conference experience.

In 2008, the surface and colloid science community celebrated the 40<sup>th</sup> Anniversary of this conference, but now we've hit the 'magic 42', and I doubt that I need to remind people of the significance of this number. At the 40<sup>th</sup> Anniversary event, however, I noted that the ACSSSC was for me, as a student, 'the equivalent of receiving a scientific vitamin shot. I returned from each student conference with a renewed enthusiasm for my research, and re-focused on completing my PhD studies'.

I trust that the students will view this conference the same way. Have a great meeting, and enjoy your 2010 scientific vitamin shot!

*Russell Crawford*

# Preface

---

The Australian Colloid and Surface Science Conference has a special place in the hearts and minds of the Australian colloid community, having endured for more than 40 years since its inception by the wizened heads of Bob Hunter and Tom Healy. The ACS SSC provides an invaluable forum for “young” researchers to present their work for review by their peers and the broader community. In today’s world where the number of conferences continues to expand at a rapid pace, this reflects the strong collegial spirit of the local colloid community and remains a challenge for the next generation to maintain.

This, the 27<sup>th</sup> Australian Colloid and Surface Science Student Conference, is proudly hosted by the Ian Wark Research Institute, University of South Australia. The organising committee would like to welcome the **68** students attending the conference from near and afar (China, Poland, Sweden and Switzerland) particularly those who have not been to an ACS SSC previously; we hope you enjoy both the academic and social activities planned. We also welcome Dr Ramón Pericet Cámara from Switzerland and Prof Mark Rutland from Sweden for travelling to be with us, to present the plenary and conference dinner talks, respectively. We would also like to thank the **59** staff members representing Universities, CSIRO and companies from across Australia for attending the conference.

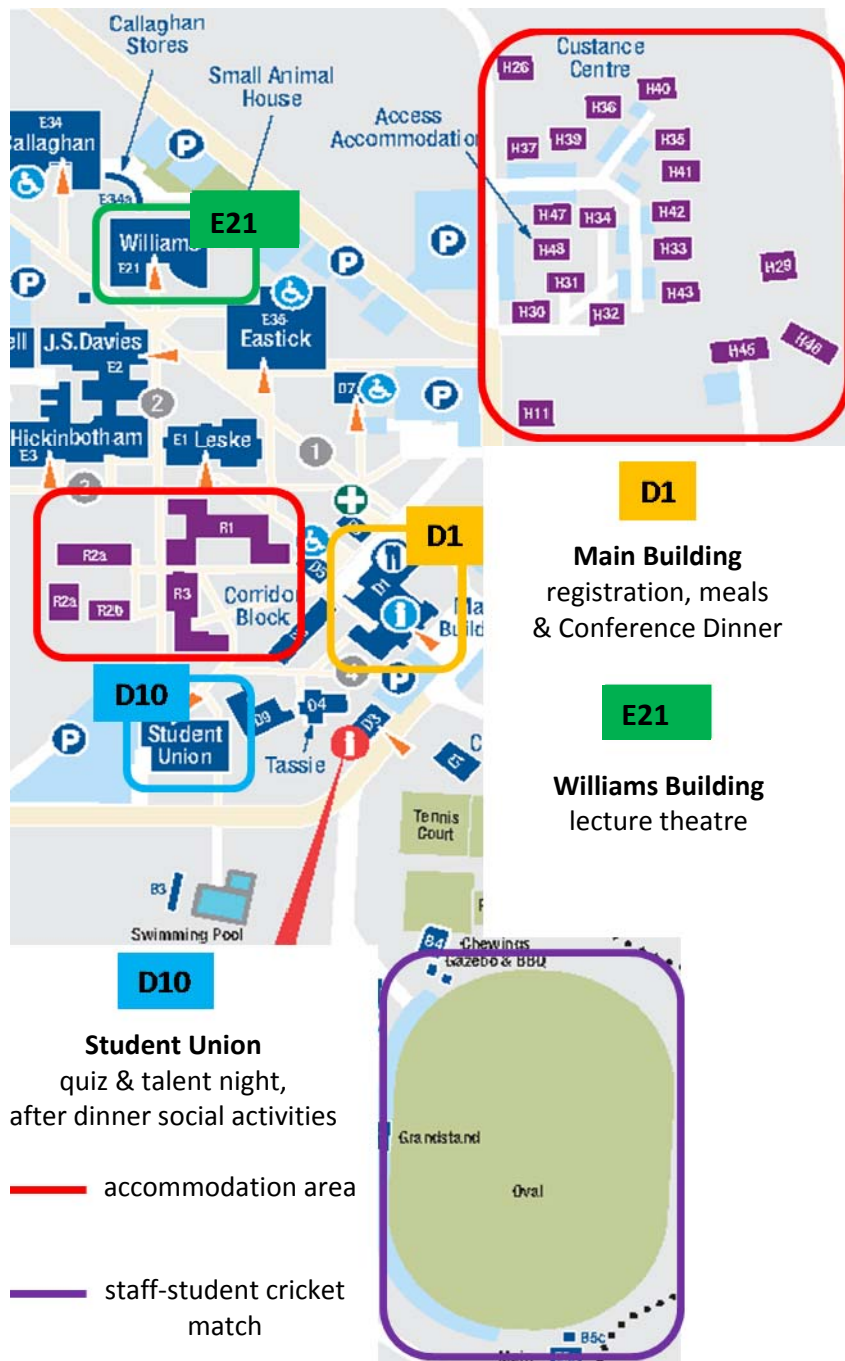
Finally, we must also acknowledge the sponsors of this conference, without your generous support it would not be possible to keep this conference affordable for students. Thank you also to the student committee members for your invaluable assistance in organising the conference, in particular Valentin Vancea (AV, Web design & maintenance), Muireann O’Loughlin (Abstracts), Melanie Ramiasa (Quiz), and also to those of you who provided experimental descriptions for the Book of Abstracts.

We hope that you enjoy the tranquillity of the Roseworthy campus of Adelaide University, please make full use of the Student Union bar and pool facilities (although not at the same time ☺), and enjoy the company of your colleagues from across Australia and around the world.

*Jonas Addai-Mensah, Tim Barnes and Marta Krasowska*

Conference Co-Chairs, 27<sup>th</sup> ACS SSC

# Map & Info



## Warnings:

1. The rooms are fitted with extremely sensitive thermal fire alarms – smoking, incense, candles, etc can all trigger the alarm. The charge of SA CFS response to trigger alarms will be passed on those who trigger the alarm.
2. The only licensed place on the campus is Student Union (D10). Alcohol consumption in any other areas is prohibited.
3. The swimming pool is not a public pool and therefore no swimming is permitted unless lifeguard or first aid officer is present. No glass is permitted in swimming pool area.
4. Do not lose your keys, if you do so the cost of replacement will be passed on you.

# Sponsors

---

The conference committee thanks the following organisations for their generous support of 27<sup>th</sup> ACSSC 2010:

## Platinum Sponsor:



## Gold Sponsors:



## Silver Sponsors:



# Student Bursaries

---



**Ian Wark Research Institute International Student Bursaries** were awarded to:

1. Hanne Evenbratt (Chalmers University of Technology, Sweden)
2. Anna Niecikowska (Institute of Catalysis and Surface Chemistry PAS, Poland)



**AINSE Interstate Student Travel Bursaries** were awarded to:

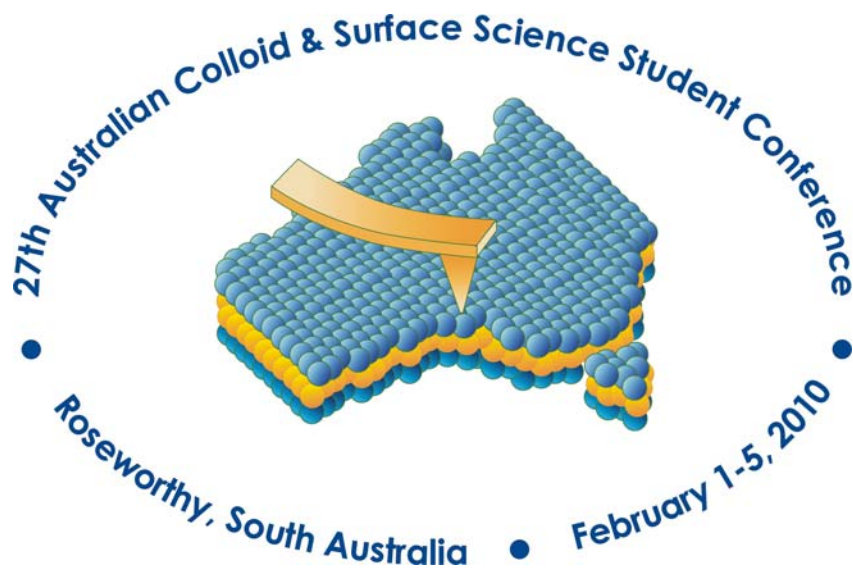
1. Thakshila Balasuriya (University of Melbourne)
2. Hannah Lockie (University of Melbourne)
3. Annette Haebich (University of Melbourne)
4. Connie Liu (The University of Sydney)
5. Liwen Zhu (The University of Sydney)
6. Deborah Wakeham (The University of Newcastle)
7. Robert Hayes (The University of Newcastle)
8. E-Jen Teh (The University of Western Australia)
9. Jie Fang (East China University of Science and Technology & The University of Western Australia)



Australian Government  
Australian Research Council

**ARCNN Student Conference Bursaries** were awarded to:

1. Rick Walsh (Australian National University)
2. Lorena Del Castillo (IWRI, University of South Australia)
3. Stefanie Sham (University of Melbourne)
4. Lauren Palmer (University of Melbourne)
5. Zhengfei Chen (University of Melbourne/CSIRO)
6. Adam John Tilley (Monash University)
7. Wye Khay Fong (Monash University)
8. Aurelia Dong (Monash University/CSIRO)
9. Josephine Chong (CSIRO)
10. Shuhua Peng (CSIRO Molecular and Health Technologies)
11. Rodney Chen (CSIRO Molecular and Health Technologies)
12. Khwanrat Chatjaroenporn (The University of Sydney)



The 27<sup>th</sup> Australian Colloid and Surface Science Student Conference is proudly hosted by



**Organising Committee:**

**Chair:** Jonas Addai-Mensah

**Co-chairs:** Tim Barnes & Marta Krasowska

**Committee Members:**

Valentin Vancea  
Muireann O'Loughlin  
Melanie Ramiasa  
Lorena Del Castillo  
Li Jiang  
Hua Li

# Previous Conferences

---

Year	Location	Total number of participants
1967	Melbourne	-
1968	Sydney	-
1970	Melbourne	14
1972	Sydney	-
1973	Melbourne/Blackwood	30
1974	Sydney/Woy Woy	39
1976	Canberra	33
1977	Melbourne/Blackwood	34
1978	Yarrowood	-
1980	Kioloa	50
1982	Mt. Eliza	75
1983	Yarrowood	51
1985	Roseworthy	49
1987	Kioloa	55
1988	Albury	107
1990	Camden	-
1991	Roseworthy	118
1993	Deakin University	144
1995	Fairy Meadow	185
1996	Murramarang	118
1998	Hahndorf	141
1999	Morpeth	143
2001	Bendigo	110
2002	Lake Hume	114
2004	Sunset Cove	116
2006	Beechwood	135
2008	Warrnambool	126
<b>2010</b>	<b>Roseworthy</b>	<b>127</b>

# List of Participants

---

## **Australian National University**

Ponlawat Tayati  
Rick Walsh

## **Chalmers University of Technology**

Hanne Evenbratt

## **CSIRO**

Marcus Zipper  
Calum Drummond  
Nicholas Tse  
Miao Chen  
Su Nee Tan  
Wei Min Zeng  
Yansheng Zhang  
Rodney Chen  
Zhengfei Chen  
Shuhua Peng  
Chantelle Driever  
Josephine Chong  
Patrick Hartley  
Feng Goh  
Darrell Wells

## **École Polytechnique Fédérale de Lausanne**

Ramon Pericet-Camara

## **Institute of Catalysis and Surface Chemistry**

### **Polish Academy of Sciences**

Anna Niecikowska

## **Monash Institute of Pharmaceutical Sciences,**

### **Monash University**

Ben Boyd  
Ian Larson  
Aurelia Dong  
Adam John Tilley  
Wye Khay Fong

## **NewSpec**

Neil McMahon  
Thomas Zhang

## **Ian Wark Research Institute, University of South Australia**

Jonas Addai-Menash  
Tim Barnes  
Marta Krasowska  
Valentin Vancea  
Muireann O'Loughlin  
Melanie Ramiasa  
Moom Aw  
Susana Isabel Lima Goncalves Brito e Abreu  
Danfeng Xu  
Xun Bian  
Hua Li  
Lee San Puah  
Mani Nath Paneru  
Bogale Tadesse  
Wendy Harrington  
Lorena Del Castillo  
Li Jiang  
William Skinner  
Satomi Onishi  
Ataollah Nosrati  
Yang Yu  
Jason Connor  
Feng Park  
John Ralston  
Trent Albrecht  
Maria Sinche Gonzalez  
Daniel Chipfunhu  
Terry Dermis  
Kai Ying Yeap  
Clive Prestidge  
David Beattie  
Luke Parkinson  
Rossen Sedev  
Craig Priest  
Catherine Whitby  
Jingfang Zhou  
Sarah Harmer  
Igor Ametov  
Daniel Fornasiero  
Sin Ying Tan  
Vera Lockett

**The University of Melbourne**

Tom Healy  
John-Paul O'Shea  
Hannah Lockie  
Thakshila Balasuriya  
MD Hemayet Uddin  
Scott McLean  
Stefanie Sham  
Stephen Tanurdjaja  
Chayuda Chuanuwatanakul  
Carolina Tallon  
Paul Mulvaney  
Annette Haebich  
Ben van Deventer  
Ashish Kumar  
Josephine Lim  
Feng Qian  
Peter Scales  
Lauren Palmer  
Kwun Lun Cho  
Derek Chan  
Ofer Manor  
George Franks  
Elizaveta Forbes  
Mirijam Zobel  
Rico Tabor  
Raymond Dagastine  
Anthony Stockland

**The University of Adelaide**

Mark Biggs  
Matthew Penna

**Deakin University**

Roger Horn

**Research Laboratories of Australia**

Drew Evans

**RMIT University**

Benjamin Kent

**Swinburne University of Technology**

Adoracion Pegalajar Jurado  
Russell Crawford  
Sally McArthur  
Hayden Webb

**Royal Institute of Technology**

Mark Rutland

**The University of Sydney**

Bob Hunter  
Muay Chatjaroenporn  
Natalie Baptista  
Connie Liu  
Liwen Zhu  
Xiaoli Zhang  
Gregory Warr  
Thomas Lee  
Chiara Neto

**The University of Newcastle**

Erica Wanless  
Grant Webber  
Rob Atkin  
Deborah Wakeham  
Oliver Werzer  
Robert Hayes  
Jacob Smith

**Victoria University**

Gayle Morris

**East China University of Science and Technology**

Jie Fang

**Veeco**

Angus Tsang  
Ian Armstrong

**The University of Western Australia**

E-Jen Teh

# Scientific Program

Time	Monday 1.02.2010	Tuesday 2.02.2010	Wednesday 3.02.2010	Thursday 4.02.2010	Friday 5.02.2010
7:00-8:30	<b>Breakfast (café)</b>	<b>Breakfast (café)</b>	<b>Breakfast (café)</b>	<b>Breakfast (café)</b>	<b>Breakfast (café)</b>
9:00	 <b>Veeco workshop on AFM 9am-1pm</b>	<b>O 05</b> E-J. Teh	<b>Talent Night Preparation</b>	<b>O 23</b> A. Nosrati	<b>Departure</b>
9:20		<b>O 06</b> K.Y. Yeap		<b>O 24</b> Y. Zhang	
9:40		<b>O 07</b> W. Harrington		<b>O 25</b> W. Zeng	
10:00		<b>O 08</b> J. Lim		<b>O 26</b> T. Dermis	
10:20		<b>Morning Tea</b>	<b>Morning Tea</b>	<b>Morning Tea</b>	
10:50		<b>O 09</b> O. Manor	<b>O 18</b> A. Haebich	<b>O 27</b> T. Balasuriya	
11:10		<b>O 10</b> L. Del Castillo	<b>O 19</b> H. Lockie	<b>O 28</b> R. Chen	
11:30		<b>O 11</b> D. Xu	<b>O 20</b> A.W. Dong	<b>O 29</b> Ch. Driever	
11:50		<b>O 12</b> A. Niecikowska	<b>O 21</b> C. Liu	<b>O 30</b> H. Evenbratt	
12:10		<b>O 13</b> L. Jiang	<b>O 22</b> K. Chatjaroenporn	<b>O 31</b> B. Kent	
12:30	<b>Lunch (café)</b>	<b>Lunch (café)</b>	<b>Lunch (café)</b>		
1:00	<b>Lunch (café)</b>	<b>O 14</b> R. Hayes	<b>Staff-Students Cricket Match</b>	<b>O 32</b> R.B. Walsh	
2:00	<b>Welcome</b>	<b>O 15</b> Z. Chen		<b>O 33</b> S. Sham	
2:20	<b>Invited Lecture R. Pericet-Camara</b>	<b>O 16</b> D. Wakeham		<b>O 34</b> J. Fang	
2:40	<b>Afternoon Tea</b>	<b>O 17</b> H. Li		<b>O 35</b> Ch. Chuanuwatanakul	
3:00	<b>Afternoon Tea</b>	<b>Poster Session</b>		<b>Afternoon Tea</b>	
3:20	<b>O 01</b> M. Paneru			<b>O 36</b> D. Chipfunhu	
4:00	<b>O 02</b> K.L. Cho			<b>O 37</b> S. Brito e Abreu	
4:20	<b>O 03</b> L. Palmer		<b>O 38</b> Y. Yu		
4:40	<b>O 04</b> LS. Puah		<b>O 39</b> F. Qian		
5:00	<b>Free time</b>		<b>Free time</b>		
5:20	<b>Dinner (café)</b>	<b>Dinner (café)</b>	<b>Dinner (café)</b>	<b>Conference Dinner (café)</b>	
6:00	<b>Pool Party</b>	<b>Quiz Night (Tavern)</b>	<b>Talent Night (Tavern)</b>		
8:30 - 2:00					

## Monday 1.02.2010

2:20pm	WELCOME	J. Addai-Mensah
2:40-3:20pm	The TW HEALY Centre Plenary Lecture <i>Mighty Microdrops Deforming and Restructuring Polymer Surfaces</i> R. Pericet-Camara	Chair: R. Dagastine
3:20-4:00pm	Afternoon Tea	
4:00-5:20pm	Oral Presentations	Chair: C. Priest Co-chair: M. Ramiasa
4:00pm	<i>Influence of Molecular Structure on the Electrowetting of Ionic Liquids</i> M. Paneru, C. Priest, R. Sedev and J. Ralston	page 18
4:20pm	<i>Transparency in the Face of Roughness</i> K. L. Cho, I. I. Liaw, A. H-F. Wu and R. N. Lamb	page 19
4:40pm	<i>Wetting of Self-Assembled Monolayers – A SAXS and AFM Study</i> L. Palmer, P. Mulvaney, D. Cookson and R. Lamb	page 20
5:00pm	<i>Influence of Solution pH on the Static and Dynamic Wetting in Titania/Glycerol-Water/Vapour System</i> L. S. Puah, R. Sedev, D. Fornasiero and J. Ralston	page 21
6:00pm	Dinner	
8:30pm	Pool Party	

## Tuesday 2.02.2010

7:00-8:30am	Breakfast	
9:00-10:20am	Oral Presentations	Chair: S.N. Tan Co-chair: T. Dermis
9:00am	<i>High Yield Stress in Alumina Dispersions due to Capillary Attraction caused by Adsorbed Low Molecular Weight Dicarboxylic Acids</i> E-J. Teh, Y-K. Leong, Y. Liu, V. S. J. Craig, R. B. Walsh and S. C. Howard	page 22
9:20am	<i>Effect of Temperature-Sensitive Poly(N-isopropylacrylamide) Adsorption and Flocculation Conditions on the Dewaterability of Talc Suspensions</i> K. Y. Yeap, J. Addai-Mensah, D. A. Beattie and A. Mierczynska-Vasilev	page 23
9:40am	<i>Dispersants-Mediated Control of Pigmentary TiO<sub>2</sub> Interfacial Chemistry and Particle Interactions in Aqueous Media</i> W. J. Harrington, W. Skinner, and J. Addai-Mensah	page 24
10:00am	<i>The Role of Cementation Process in Controlling Non-Swelling Clay Behaviour in Suspension</i> J. Lim, Ross G. de Kretser and P. J. Scales	page 25
10:20-10:50am	Morning Tea	
10:50-12:30pm	Oral Presentations	Chair: M. Krasowska Co-chair: H. Lockie
10:50am	<i>Contribution of Polymeric Brush Layers to the Force between Colliding Drops</i> O. Manor, T. T. Chau, G. Stevens, F. Grieser, R. R. Dagastine and D. Y. C. Chan	page 26
11:10am	<i>Effects of Salt Concentration and Speed of Approach on Bubble Coalescence</i> L. Del Castillo, S. Ohnishi and R. Horn	page 27

<b>11:30am</b>	<i>Effect of Dynamic Wettability on Detachment of Coarse Particles from Bubbles</i> D. Xu, I. Ametov and S. R. Grano	page 28
<b>11:50am</b>	<i>Mutual Interdependences of Electrostatic Interactions and Hydrophobicity for Three Phase Contact Formation at Titania Surface</i> A. Niecikowska, M. Krasowska, J. Ralston and K. Malysa	page 29
<b>12:10pm</b>	<i>Interaction between a Fine Alumina Particle and an Air Bubble</i> L. Jiang, M. Krasowska, D. Fornasiero and J. Ralston	page 30
<b>12:30-2:00pm</b>	Lunch	
<b>2:00-3:20pm</b>	<b>Oral Presentations</b>	<b>Chair: R. Atkin</b> <b>Co-chair: C. Liu</b>
<b>2:00pm</b>	<i>The Smallest Sponge: Nanostructure in Ionic Liquids</i> R. Hayes, S. Imberti, G. G. Warr and R. Atkin	page 31
<b>2:20pm</b>	<i>Nanocrystalline TiO<sub>2</sub> from Hydrothermal Treatment with Various Ionic Liquids</i> Z. Chen, T. Greaves, R. A. Caruso and C. J. Drummond	page 32
<b>2:40pm</b>	<i>Surfactant Adsorption at the Ethylammonium Nitrate–Air Interface: An X-ray and Neutron Reflectivity and Vibrational Sum Frequency Spectroscopy Study</i> D. Wakeham, P. Niga, A. Nelson, G. G. Warr, M. Rutland and R. Atkin	page 33
<b>3:00pm</b>	<i>Spreading of Ionic Liquids on a Hydrophobic Surface</i> H. Li, J. Ralston and R. Sedev	page 34
<b>3:20-4:00pm</b>	Afternoon Tea	
<b>4:00-5:20pm</b>	<b>Poster Session sponsored by CSIRO</b>	
<b>6:00pm</b>	Dinner	
<b>8:30pm</b>	Quiz Night	

### Wednesday 3.02.2010

<b>7:00-8:30am</b>	Breakfast	
<b>9:00-10:20am</b>	Talent Night Preparation	
<b>10:20-10:50am</b>	Morning Tea	
<b>10:50-12:30pm</b>	<b>Oral Presentations</b>	<b>Chair: C. Whitby</b> <b>Co-chair: O. Manor</b>
<b>10:50am</b>	<i>Enantioselective Adsorption of a Racemic Mixture of Surfactants at a Chiral Film monitored by ATR-FTIR</i> A. Haebich, G. Qiao and W. Ducker	page 35
<b>11:10am</b>	<i>Tailoring Self-assembled Thiol Monolayers to Facilitate Measurement of Tetradecane Micro-Droplet Interactions with AFM</i> H. Lockie, G. Stevens, D. Y. C. Chan, F. Grieser and R. R. Dagastine	page 36
<b>11:30am</b>	<i>Application of PALS to Understand Structure in Self-Assembled Systems: Investigations with a Dilutable Microemulsion</i> A. W. Dong, B. J. Boyd, A. J. Hill and C. J. Drummond	page 37
<b>11:50am</b>	<i>Lyotropic Liquid Crystalline Phases in Surfactant Biomineralisation Precursors</i> C. Liu and G. G. Warr	page 38
<b>12:10pm</b>	<i>Rearrangement of Micelle Structures during Polymerization</i> K. Chatjaroenporn, R. W. Baker, P. A. FitzGerald and G. G. Warr	page 39

<b>12:30-2:00pm</b>	Lunch
<b>2:00-5:20pm</b>	Staff-Students Cricket Match
<b>6:00pm</b>	Dinner
<b>8:30pm</b>	Talent Night

## Thursday 4.02.2010

<b>7:00-8:30am</b>	Breakfast	
<b>9:00-10:20am</b>	<b>Oral Presentations</b>	<b>Chair: J. Connor</b> <b>Co-chair: E-J. Teh</b>
<b>9:00am</b>	<i>Influence of Hydrolysable Metal Ions on the Interfacial Chemistry and Particle Interactions of Aqueous Muscovite Dispersions</i> <u>A. Nosrati</u> , J. Addai-Mensah and W. Skinner	page 40
<b>9:20am</b>	<i>Electrochemistry Study of Chalcopyrite with Different Phase</i> <u>Y. Zhang</u> , M. Chen, W. Qin, W. Zeng and J. Liu	page 41
<b>9:40am</b>	<i>Characterization of Extracellular Polymeric Substances Extracted from the Mineral Surface during Bioleaching of Chalcopyrite Concentrate</i> <u>W. Zeng</u> , M. Chen, G. Qiu, H. Zhou, W. Chao and Y. Zhang	page 42
<b>10:00am</b>	<i>An Investigation of the Pulp Chemistry and Structural Network of an Isothermally Leached Muscovite Clay Suspension</i> <u>T. Dermis</u> , W. M. Skinner and J. Addai-Mensah	page 43
<b>10:20-10:50am</b>	Morning Tea	
<b>10:50-12:30pm</b>	<b>Oral Presentations</b>	<b>Chair: T. Barnes</b> <b>Co-chair: A. Dong</b>
<b>10:50am</b>	<i>Nano-Mechanical Behaviour of Living Cancer Cell Surface Using Atomic Force Microscopy</i> <u>T. Balasuriya</u> , G. Stevens, F. Grieser, M. de Silva, E. Williams and R. R. Dagastine	page 44
<b>11:10am</b>	<i>Multifunctional Polymeric Surface Coatings via Brominated Plasma Polymers</i> <u>R. Chen</u> , B. W. Muir, G. K. Such, A. Postma, R. A. Evans, K. M. McLean and F. Caruso	page 45
<b>11:30am</b>	<i>Controlling Burst Release of Cubosomes Through Nano-Encapsulation</i> <u>Ch. Driever</u> , X. Mulet, A. Johnston, H. Thissen, F. Caruso and C. Drummond	page 46
<b>11:50am</b>	<i>In Vivo Study of Lipid-Water Cubic Formulation for Drug Delivery in Photodynamic Therapy</i> <u>H. Evenbratt</u> , Ch. Jonsson, J. Faergemann, M. B. Ericson and S. Engström	page 47
<b>12:10pm</b>	<i>Effects of Sugars on Bilayer to Non-Bilayer Phase Transitions in Biological Membranes during Dehydration</i> <u>B. Kent</u> , C. J. Garvey and G. Bryant	page 48
<b>12:30-2:00pm</b>	Lunch	
<b>2:00-3:20pm</b>	<b>Oral Presentations</b>	<b>Chair: B. Boyd</b> <b>Co-chair: S. Sham</b>
<b>2:00pm</b>	<i>Ultra-Smooth Titania Surfaces for Surface Force Analysis</i> <u>R. B. Walsh</u> and V. S. J. Craig	page 49
<b>2:20pm</b>	<i>Synthesis and Mechanical Characterization of Hollow Silica Shells – for the use in Total Internal Reflection Microscopy (TIRM)</i> <u>S. Sham</u> and R. R. Dagastine	page 50

<b>2:40pm</b>	<i>Facile One-Pot Method to Synthesize Koosh Ball-Shaped Magnetite/ Lanthanide Phosphate Nanocomposites</i> J. Fang, M. Saunders, Y. Guo, G. Lu, C. L. Raston and K. Swaminathan Iyer	page 51
<b>3:00pm</b>	<i>Highly Porous Alumina Bodies from Ceramic Particle Stabilized Foams</i> Ch. Chuanuwatanakul, C. Tallon, D. E. Dunstan and G. V. Franks	page 52
<b>3:20-4:00pm</b>	Afternoon Tea	
<b>4:00-5:20pm</b>	<b>Oral Presentations</b>	<b>Chair: D. Beattie Co-chair: L. Palmer</b>
<b>4:00pm</b>	<i>The Dependency of the Critical Contact Angle of Flotation on Particle Size - Evidence for the Non-Floatability of Fine Particles</i> D. Chipfunhu, M. Zanin and S. R. Grano	page 53
<b>4:20pm</b>	<i>Method for Determination of The Contact Angle of Individual Particles by ToF-SIMS Surface Analysis</i> S. Brito e Abreu and W. Skinner	page 54
<b>4:40pm</b>	<i>Developing Natural Diatomaceous Earth (DE) Particles for Process Water Treatment Application</i> Y. Yu, J. Addai-Mensah and D. Losic	page 55
<b>5:00pm</b>	<i>Dewatering of Cyanobacteria-Rich Sludges</i> F. Qian, P. J. Scales, D. R. Dixon and G. Newcombe	page 56
<b>5:20pm</b>	CLOSING REMARKS	
<b>6:00pm</b>	Conference Dinner sponsored by Ian Wark Research Institute	

# Conference Awards

---



**Healy-Hunter Award** – the most outstanding oral presentation will be awarded the Healy-Hunter Award. This award consists of a commemorative medal and a contribution (\$1500) towards the travel costs of attending an international conference. Students enrolled at an Australian university are eligible candidates for this award. All staff members attending the student conference are eligible to vote. Supervisors may vote for their own PhD students if so desired.

**Best Poster Award** – the most outstanding poster presentation will be awarded the Best Poster Award. This award is a prize of \$300 cash and is voted by eligible staff.

**The Most Probing Question and the Most Memorable Moment Awards** – as a part of the tradition, there will be a presentation of specially designed trophies for both the Most Probing Question and the Most Memorable Moment witnessed at the conference. To be eligible, the event is nominated and a winner decided by a carefully chosen panel of judges. The prize – embarrassment and notoriety!

# Abstracts

---



## Mighty Microdrops Deforming and Restructuring Polymer Surfaces

Ramon Pericet-Camara

*Max Planck Institute for Polymer Research, Mainz, Germany*

&

*Laboratory of Intelligent Systems, Swiss Federal Institute of Technology in Lausanne – EPFL, Lausanne, Switzerland*

ramon.pericet@epfl.ch

A sessile droplet can deform the surface of a soft solid not only with its weight. For instance, the surface tension pulls up at the perimeter of the drop forming a ridge, and the capillary pressure embosses a quasi-spherical dimple under the contact area. Moreover, if the liquid is a solvent for the surface, some other interrelated physicochemical processes occur, and the drop may even restructure the surface permanently. The deformation of soft surfaces by sessile drops has already been predicted in literature by theoretical studies or with numerical simulations, but only partially observed in experiments. Furthermore, some important aspects like the effect of drop capillary pressure had not been verified *in situ* so far. The interest on these systems has increased due to a range of potential applications, such as the use of microdrops as agents for micro- and nanopatterning of surfaces or for printable electronics. Additionally, these experiments may help in the understanding of wetting phenomena on deformable surfaces.

Herein, the effect of microdrops on deformable surfaces is analyzed experimentally. On one hand, the deformation of elastic polymer layers by non-evaporating microdrops is studied by confocal microscopy techniques. It is demonstrated the presence of strain in the micrometer range, that is, the liquid droplet generates a depression on the elastic surface due to its capillary pressure, and a ridge at the three-phase contact line. The deformation is inversely proportional to the elastic modulus of the surface material, and proportional to the thickness of the soft layer below a certain threshold that will be discussed. On the other hand, we study the effect of solvent microdrops deposited by inkjet printing on polymer surfaces. In this case, the evaporated drop causes a permanent restructuring of the substrate, which shape depends on the parameters of deposition and on the material properties of the surface. The use of solvent microdrops on polymer surfaces as a technique to fabricate arrays of microlenses will also be shown.

## Influence of Molecular Structure on the Electrowetting of Ionic Liquids

Mani Paneru, Craig Priest, Rossen Sedev and John Ralston

*Ian Wark Research Institute, University of South Australia, Mawson Lakes, SA, 5095, Australia*

Mani.Paneru@postgrads.unisa.edu.au

We studied the electrowetting of imadizolium based ionic liquids (ILs) on Teflon in an ambient phase of hexadecane. Our aim was to relate electrowetting parameters to the chemical composition of ILs. The insulated electrode was a layer of indium tin oxide, electrically insulated from the droplet of IL (1-10  $\mu\text{l}$ ) by a layer (1-4  $\mu\text{m}$ ) of an amorphous fluoropolymer (Teflon AF1600), and entirely immersed in hexadecane. A platinum wire was used to electrically connect the droplet and apply an external DC potential. Contact angle and base area of the droplet were measured using the sessile drop and capacitance techniques.

The nature of ILs had a strong influence on the electrowetting behaviour. The initial contact angle (zero applied potential) decreased with the size of the anion. Contact angles decreased with applied voltage (by more than  $90^\circ$ ), in accordance with the Young-Lippmann equation, and saturated at about  $50^\circ$ , for all ILs studied. The saturation voltage decreased when the anion and/or cation size increased. In all cases, solid-liquid-liquid electrowetting showed excellent reversibility and minimal contact angle hysteresis ( $2^\circ$ ). Dewetting (the IL receding) was always slower than wetting (the IL advancing) by a factor of 1.5. The characteristic wetting time was strongly influenced by the viscosity of the IL, though prominent exceptions indicated the correlation is not universal.

Our results may be used as references to select task-specific ILs for electrowetting based applications. They can also be useful in elucidating the mechanism of contact angle saturation.

## Transparency in the Face of Roughness

Kwun Lun Cho, Irving I. Liaw, Alex Hing-Fai Wu and Robert N. Lamb

*School of Chemistry, University of Melbourne, VIC, 3010, Australia*

k.cho@pgrad.unimelb.edu.au

Superhydrophobic thin films with  $\theta > 170^\circ$  were fabricated through the cross-linking of silica particles with sizes ranging from 7 – 40 nm [1]. Such surfaces are ultra-rough as seen by high resolution SEM, however AFM quantification indicates average roughness (Ra) of only 1  $\mu\text{m}$ . Using Synchrotron Small Angle X-ray Scattering (SAXS), more detailed surface roughness analysis is possible.

The aim of this project is to create superhydrophobic thin films which also optically transparent. This requires careful control of film and surface architecture. A novel fabrication process has been developed which involves the addition of mono-disperse latex spheres (400 – 800 nm) to the silica nanoparticles hybrid mixture. During processing, these latex particles are removed resulting in roughness (Ra) controlled formation of microvoids within the film.

At visible wavelength ( $\lambda = 500\text{nm}$ ) void-free coatings (Ra = 1  $\mu\text{m}$ ) are opaque. By comparison the microvoid coatings (Ra = 200 nm), show 90% transparency. Clearly there is a region where the film exhibits both superhydrophobicity and optical transparency. In both cases, SAXS experiments indicate a surface fractal dimension of 2.8. Theoretical studies reveal that Ra = 200 nm is the upper limit of roughness for optical transparency. SAXS measurements indicate a surface fractal dimension of 2.8 is required for maximum superhydrophobicity, regardless of roughness (Ra).

1. R. Lamb; H. Zhang; C. Raston. "Hydrophobic coatings", AU (1997) European PATENT 0969934 (2002)

## Wetting of Self-Assembled Monolayers – A SAXS and AFM Study

Lauren Palmer<sup>1</sup>, Paul Mulvaney, David Cookson<sup>2</sup> and Rob Lamb

<sup>1</sup>*School of Chemistry, University of Melbourne, Parkville, VIC, 3010, Australia*

<sup>2</sup>*Australian Synchrotron, Clayton, VIC, 3168, Australia*

l.palmer4@pgrad.unimelb.edu.au

The structure of increasingly hydrophobic interfaces in ethanol/water solutions were examined using Atomic Force Microscopy (AFM) and synchrotron based Small Angle X-Ray Scattering (SAXS).

Recent research on the hydrophobic effect has led to the proposal that the long-range force is caused by “nanobubbles” developing on the surface of the sample. AFM imaging [1] has suggested the existence of nanobubbles. In addition SAXS has recently been used to investigate nanowetting of rough surfaces.[2]

We combine these two techniques to examine three Self-Assembled Monolayers: 11-Bromo-1-undecanethiol {1} (water contact angle ( $\theta$ ) = 90°), 1-Octadecanethiol {2} ( $\theta$  =108°), and Heptadecafluoro-1-decanethiol {3} ( $\theta$  =114°).

SAXS results demonstrate that when ethanol is injected into the system there is a decrease in the measured scattering intensity suggesting a wetting phenomenon. This is particularly strong for hydrophilic surfaces; however, this drop in intensity is substantially less for hydrophobic surfaces, suggesting decreasing wetting most likely due to air on the surface or trapped within the SAMs.

The AFM results suggest that with increasing water composition the average adhesive force and van der Waals force for {2} and {3} increases; at 80% water in ethanol, the van der Waals interaction increases dramatically.

When combining the SAXS and AFM measurements; deviation from the typical van der Waals interaction is not a true hydrophobic force, but rather, suggests trapped air at the nanoscale.

1. Zhang, L.; Zhang, Y.; Zhang, X.; Li, Z.; Shen, G.; Ye, M.; Fan, C.; Fang, H.; Hu, J., *Langmuir*, **2006**, 22, (19), 8109.
2. Zhang H, Lamb R, Cookson D., *Appl. Phys. Lett*, **2007**, 91, 254106.

## Influence of Solution pH on the Static and Dynamic Wetting in Titania/Glycerol-Water/Vapour System

Lee San Puah, Rossen Sedev, Daniel Fornasiero and John Ralston

*Ian Wark Research Institute, University of South Australia, Mawson Lakes, SA, 5095, Australia*

LeeSan.Puah@postgrads.unisa.edu.au

The static and dynamic wetting properties of a titania surface, partially covered with octadecyltrihydrosilane, were investigated as function of solution pH. The results showed that surface charge affects both static wettability and wetting kinetics. The static contact angle of water substantially decreased above and below the isoelectric point of the titania surface. This was reflected in the dependence of the dynamic contact angle on wetting velocity. The molecular-kinetic theory accounted for the results over the full range of wetting velocities studied. The frequency of molecular displacement, the distance of molecular displacement, and contact line friction strongly vary with pH. The influence of surface charge on both static and dynamic contact angles can be rationalised through a free energy argument including the effect of the electrical double layer. The predicted relation between contact line friction and work of adhesion is followed. The estimated value of the volume of unit flow suggests that a small cluster of liquid molecules, rather than a single molecule, are displaced at the moving contact line. This work provides a better understanding of the wetting on metal oxide surfaces.

## High Yield Stress in Alumina Dispersions due to Capillary Attraction caused by Adsorbed Low Molecular Weight Dicarboxylic Acids

E-Jen Teh<sup>1</sup>, Yee-Kwong Leong<sup>1</sup>, Yinong Liu<sup>1</sup>, Vincent S. J. Craig<sup>2</sup>, Rick B. Walsh<sup>2</sup> and Shaun C. Howard<sup>2</sup>

<sup>1</sup> Department of Mechanical Engineering, The University of Western Australia, Crawley, WA, 6009, Australia

<sup>2</sup> Department of Applied Mathematics, Research School of Physical Sciences and Engineering, The Australian National University, Canberra, ACT, 0200, Australia

ejen@mech.uwa.edu.au

Adsorbed low molecular weight charged molecules are known to change the rheological behaviour of oxide dispersions dramatically. The isomers of muconic acid were used to investigate the effect of molecular structure and solubility on the bulk properties of alumina dispersions and the nanoscale interactions between alumina surfaces. The surface forces in dispersions were characterized by yield stress while atomic force microscopy (AFM) was used to directly measure the force between a single alumina particle and an alumina substrate. Both (*trans, trans*) *TT* and (*cis, cis*) *CC* muconic acid were found to increase the yield stress of alumina slurries significantly at low pH when compared to that of the pure alumina (Fig.1). *TT* muconic acid achieved a much higher yield stress than that of *CC* at high additive concentration. AFM measurements revealed force-distance features that indicate a capillary-type attraction between the adsorbed layers of *TT* muconic acid at high surface coverage. The force-distance curve for the *CC* muconic acid system displayed a capillary force-mediated with an electrostatic force (Fig.2). At low pH, the muconic acids become less soluble in the confined space between the interacting surfaces resulting in the formation of an “oily” muconic acid phase between the interacting surfaces. This nanosized “oil” phase is the source of the capillary force. The capillary force at high concentration of *TT* and *CC* muconic acid observed during AFM measurements can account for the large increase of yield stress at low pH. The bridging mechanism applicable in other cases is not found to be operating at high concentration of adsorbed muconic acids. This study revealed that not only the molecular structure of these low molecular weight molecules plays a role in increasing the interparticle strength between metal oxide surfaces but also their solubility and concentration have a direct link in inducing an attraction between adsorbed surfaces.

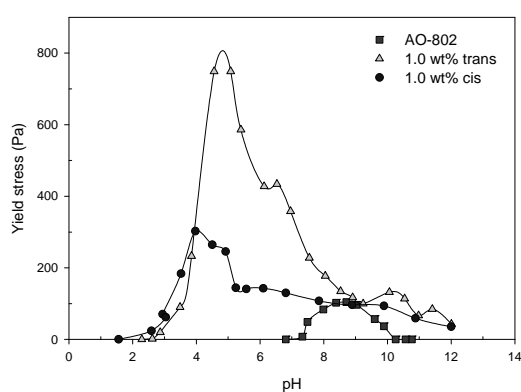


Fig. 1: Yield stress of AO-802 in the presence of *TT* and *CC* muconic acid.

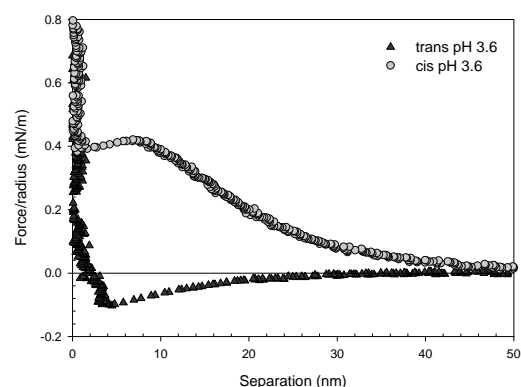


Fig. 2: Approach force curves between ALD alumina surfaces in  $10^{-3}$  M KCl,  $10^{-3}$  M *TT* and *CC* muconic acid at low pH

## Effect of Temperature-Sensitive Poly(N-isopropylacrylamide) Adsorption and Flocculation Conditions on the Dewaterability of Talc Suspensions

Kai Ying Yeap, Jonas Addai-Mensah, David A. Beattie and Agnieszka Mierczynska-Vasilev

*Ian Wark Research Institute, University of South Australia, Mawson Lakes, SA, 5095, Australia*

Kai.Yeap@postgrads.unisa.edu.au

Substantial amount of recyclable water is trapped in clay mineral waste tailings generated by the mining industry. Conventional polyacrylamide (PAM) flocculant-assisted dewatering in gravity thickeners leads to fast settling but low solid content sediment. Recently, for flocculant-mediated dewatering enhancement, significant interest has been focused on non-conventional, thermosensitive poly(N-isopropylacrylamide) (pNIPAM) which undergoes phase-transition from hydrophilic coiled state to hydrophobic globule state when temperature > lower critical solution temperature (LCST, ~35 °C), impacting on sediment consolidation [1, 2]

The main aim of the present work was to investigate the use of pNIPAM as a temperature responsive flocculant for improved dewatering of talc clay suspension. The links between pNIPAM interfacial conformation, adsorption behaviour, particle interaction force, flocculation and dewatering behaviour of talc dispersion (batch settling rate, supernatant clarity and sediment consolidation) at pH 7.5 have been investigated through the influence of temperature (22 – 50 °C), polymer dosage (100 – 500 g·t<sup>-1</sup> solid) and sonication. Higher temperature led to greater pNIPAM adsorption and greater attractive/adhesive forces between talc particles which resulted in faster settling behaviour but poorer supernatant clarity and lower sediment consolidation. Stronger pNIPAM mediated-interparticle adhesion mitigated compact consolidation. The enhanced settling behaviour at higher temperature is consistent with dramatic change in the adsorbed polymeric flocculant layer structure from hydrophilic to hydrophobic state above the LCST. The resulting attractive hydrophobic interaction is responsible for the improved settling rate. An optimum flocculant dosage of 100 g·t<sup>-1</sup> solid, reflecting maximum settling behaviour was observed. An increase of ~ 3-8 wt.% in solid loading was achieved upon application of ultra-sonication to pre-sedimented suspension for 30 min.

1. J.-P. O'Shea, H. Li, G. Qiao and G. Franks. *Chemeca*, **2008**, Newcastle, Australia (2008).
2. H. Li, J. Long, Z. Xu and J.H. *Masliyah.AIChE Journal*, **2007**, 53, 479.

## Dispersants-Mediated Control of Pigmentary TiO<sub>2</sub> Interfacial Chemistry and Particle Interactions in Aqueous Media

Wendy J. Harrington, William Skinner and Jonas Addai-Mensah

*Ian Wark Research Institute, University of South Australia, Mawson Lakes, SA, 5095, Australia*

Wendy.Harrington@postgrads.unisa.edu.au

TiO<sub>2</sub> is by far one of the most widely used white pigment materials due to its unique physico-chemical properties that facilitate diverse applications in a broad range of products. For the production of certain high quality products, it is necessary to coat the TiO<sub>2</sub> particles with inorganic oxide layers (SiO<sub>2</sub>, Al<sub>2</sub>O<sub>3</sub>, and ZrO<sub>2</sub>) to mask its deleterious photocatalytic activity. TiO<sub>2</sub> particles of interest to pigment manufacturers are of colloidal dimensions (250-350 nm) and hence, susceptible to aggregation during aqueous processing at certain pH values due to strong attractive particle interactions. Aggregation is undesirable during TiO<sub>2</sub> inorganic oxide coating process and its suppression, very important in defining the pigments physico-chemical performance. Furthermore, the surface chemistry of the TiO<sub>2</sub> particles has a profound impact on the interactions between particles and with the dissolved species in aqueous medium. In the present work, industrial-grade, colloidal TiO<sub>2</sub> particle interfacial chemistry modification, via anionic polymeric dispersants was investigated, and the impact on particle interactions quantified by dispersion rheology. Two conventional, low molecular weight (10<sup>4</sup> Da) polymers, polyacrylic acid (PAA) and polyacrylamide, were used as dispersants. Pristine TiO<sub>2</sub> particle bulk and surface analysis by several techniques (XRD, XRF, XPS, ToF-SIMS, Acousotizer) revealed the following results. The TiO<sub>2</sub> mineralogical structure was that of the rutile form, with the structure comprising predominantly TiO<sub>2</sub>, with ~1% Al<sub>2</sub>O<sub>3</sub> and ~0.15% SiO<sub>2</sub>. Surface sensitive techniques showed that the particle surface was six times more enriched with Al than the bulk. Furthermore, the particle zeta potential as a function of pH indicated an isoelectric point (iep) of pH 5.8 consistent with surface chemical analysis. The adsorption of the anionic dispersants, PAA and PAM showed strong pH and polymer structure dependency. At pH conditions, where the particle and polymer carried opposite charges, a greater adsorption density plateau was observed. Furthermore, the results also suggest that chemical factors contributed significantly to the adsorption mechanism. The PAM led to a greater adsorption density than that of the PAA without increased adsorption affinity. Both polymers exhibited Langmuir type adsorption behaviour and had similar influence on the TiO<sub>2</sub> particle zeta potential. Their specific adsorption led to TiO<sub>2</sub> particle charge reversal at acidic pH values and strong shifts in the iep to low pH values with increasing polymer dosage. Rheological investigations demonstrated that both polymer dosage and pH strongly effected particle interactions and stabilisation. Polymer induced electro-steric mechanisms played a significant role in the dispersion of TiO<sub>2</sub> at 10g/ton dispersant dosage.

## The Role of Cementation Process in Controlling Non-Swelling Clay Behaviour in Suspension

Josephine Lim, Ross G. de Kretser and Peter J. Scales

*Particulate Fluids Processing Centre, Department of Chemical and Biomolecular Engineering, University of Melbourne, VIC, 3010, Australia*

j.lim3@pgrad.unimelb.edu.au

Clays, which are often associated with mineral deposits, can be the source of significant problems in mineral processing operations. Their presence as the impurities in low grade ores can lead to issues such as high pumping energy, high water consumption and large volume of tailings.

Current strategies for dealing with clay related issues in mineral processing are all end-of-pipe in nature, in the sense that they all attempt to solve the problems relating to highly dispersed clays well after they have been created. For example, polymers or coagulants are often added into dilute tailings or high pressure dewatering equipment used to improve the extent and rate of tailings dewatering. However, the effectiveness of such strategies will always be limited due to the physical and chemical nature of clays. Far greater benefits could be generated through minimising the generation of clay related problems in the first place.

This study aims to develop a new paradigm for the minerals industry to control clay behaviour in suspensions using a start-of-pipe, or up front strategy that reduces the level of dispersion and break-up of the clays throughout the process. Through such a strategy, the occurrence of clay-associated problems could be anticipated and moderated at the front end of a processing plant. This can result in significant improvements in both rheology and dewaterability over the current end-of-pipe practice.

This paper will deal with the specific case of dispersion control of an as-mined Kaolin (non swelling) clay through cementation. This process involves the precipitation of Aluminium Hydroxide on the surface of the clay particles, via the addition of Aluminium Sulphate (alum) into the clay suspensions at pH 6.5. The results from adding the alum before (start-of-pipe strategy) and after (end-of-pipe strategy) shearing the suspensions with a shear rate of approx.  $1500\text{s}^{-1}$  were compared. The outcomes indicate that the deposition of aluminium hydroxide through start-of-pipe strategy assists in preventing the dispersion of as-mined clay, resulting in a moderate improvement on the dewaterability. Additionally, an optimum dewaterability is observed at alum to clay ratio of 2.5 wt%. The occurrence of this optimum point implies that the nature of the aluminium hydroxide precipitation changes from surface to self precipitation as the alum to clay ration is increased. In this context, surface precipitation is defined as the adsorption / precipitation of aluminium hydroxide species directly onto the surface of clay particles and self precipitation is defined as the precipitation / coagulation of free aluminium hydroxide species within the suspending medium.

## Contribution of Polymeric Brush Layers to the Force between Colliding Drops

Ofer Manor<sup>1</sup>, Tam T. Chau<sup>1</sup>, Geoffery Stevens<sup>1</sup>, Franz Grieser<sup>1</sup>, Ray R Dagastine<sup>1</sup> and Derek Y C Chan<sup>1,2</sup>

<sup>1</sup>*Particulate Fluids Processing Centre, University of Melbourne, Parkville, VIC, 3010, Australia*

<sup>2</sup>*National University of Singapore, 117543, Singapore*

o.manor@pgrad.unimelb.edu.au

We present static and dynamic atomic force microscopy (AFM) force measurements between two decane drops coated with a polymer brush in electrolyte (10mM and 1M Sodium Chloride). The polymer brush is an irreversibly adsorbed block co-polymer, Pluronic F-108, composed of an anchoring block of a polypropylene oxide between two ethylene oxide stabilizing blocks. The drops are immobilized on the end of the AFM cantilever or the solid substrate. The measured dynamic forces are used to characterize the steric forces between the drops and the hydrodynamic drainage inside and outside the polymer brush layers in the nanometer thick intervening aqueous film. With a theoretical model fitted to the experiment we are able to deduce the permeability of the polymer brush layers, which is measured as the aqueous film “effective thickness for free flow” in the brushes. We find that the effective thickness for free flow changes with electrolyte concentration. This is explained by dehydration and partial collapse of the ethylene oxide block buoy with an increase in electrolyte concentration. Thus, the AFM force measurement allows us to quantitate the contribution of the aqueous flow in the polymer brush layers to the hydrodynamic resistance between the two approaching and retracting drops.

## Effects of Salt Concentration and Speed of Approach on Bubble Coalescence

Lorena Del Castillo<sup>1</sup>, Satomi Ohnishi<sup>1</sup> and Roger Horn<sup>2</sup>

<sup>1</sup>*Ian Wark Research Institute, University of South Australia, Mawson Lakes, SA, 5095, Australia*

<sup>2</sup>*Research Training, Deakin University, Ea2-52 Burwood Campus, Burwood Highway, VIC, 3125, Australia*

Lorena.Delcastillo@postgrads.unisa.edu.au

When two bubbles in a liquid medium approach each other, a thin film of liquid may form between them, which drains over time until the film is thin enough to rupture. This leads to the joining of the two bubbles to form a larger one, in a process called bubble coalescence.

Knowledge of the basic phenomena involved in bubble coalescence, like thin film drainage and the effects of various factors on the rate of coalescence, is important in understanding various gas-liquid systems which have a great number of industrial, environmental and biological applications. Because of its importance, the phenomenon of bubble coalescence has been the subject of intense research. The effects of electrolytes [1,2], surfactants [3], their concentrations [4,5], media [4], and bubble size [5] on coalescence and stability of a film between air-liquid interfaces have been reported. There have also been a few reports on the effect of approach velocity for bubble coalescence [6, 7], the first mention of which was in 1974 [6].

In this study we present results of experiments conducted to investigate the effects of salt concentration and speed of approach on bubble coalescence using a sliding bubble apparatus, in which mm-sized bubbles with different speeds approached the meniscus of the liquid at the end of an inclined closed glass cylinder. A high speed camera was used to measure the lifetime of the bubble contacting the meniscus. We confirmed that stable bubbles can be formed in purified water at very slow approach speeds [8]. However, the stability of bubbles depends significantly on the approach speed and on the salt concentration. We have found a critical speed of approach ( $V_c$ ) that determines bubble lifetimes before coalescence, and showed that  $V_c$  varies with salt concentration. For water, the critical speed was observed to be around 0.04 mm/s below which all bubbles are very stable, with lifetimes of a few minutes to more than an hour, but above which the lifetimes of the bubbles drop significantly to few seconds. There is also a second critical speed observed to be around 1.2mm/s above which all bubbles coalesce instantly upon touching the meniscus. This is consistent with the film stability observed by Yaminsky and co-workers [8] in thin film balance experiments. Details of other observations and comparisons with other studies will be reported in this presentation.

1. G. Marrucci, L. Nicodemo, *Chem. Eng. Sci.* 22, 1967, 1257-1265.
2. C. I. Henry, V.S. J. Craig, *Langmuir* 2008, 24, 7979-7985
3. K.D. Danov, D.S. Valkovska, I.B. Ivanov, *J. Colloid Interface Sci* 1999, 211, 291-303.
4. P.K. Weissenborn, R.J. Pugh, *Langmuir* 1995, 11(5), 1422-1426.
5. B. S. Chan, Y. H. Tsang, *J. Colloid Interface Sci*, 286 (2005) 410-413
6. D. Kirkpatrick and M. J. Lockett, *Chem. Eng. Sci.* 29 (1974) 2363-2373.
7. C.P. Ribeiro Jr and D. Mewes, *Chem. Eng. Sci.* 126 (2007) 23-33.
8. V.V. Yaminsky, S. Ohnishi, E.A. Vogler, R.G. Horn, (manuscript submitted to *Langmuir*)

## Effect of Dynamic Wettability on Detachment of Coarse Particles from Bubbles

Danfeng Xu, Igor Ametov and Stephen R. Grano

Ian Wark Research Institute, ARC Special Research Centre for Particle and Material Interfaces, University of South Australia, Mawson Lakes, SA, 5095, Australia

Danfeng.Xu@postgrads.unisa.edu.au

In mineral processing, disruption of bubble-particle aggregates in the turbulent zone is the main reason for the low recovery of coarse particles [1]. The detachment force acting on particle/bubble aggregates in a flotation cell has been simulated and studied by several methods including centrifugal methods [2] and vibrational methods [3].

In this work, detachment of particles from bubbles was investigated using a novel electro-acoustical technique. The experimental setup consisted of a loudspeaker connected to a computer through an amplifier. A teflon capillary tube was attached to the membrane of a loudspeaker. A bubble-particle aggregate on the other end of the capillary tube was subjected to vibration when the sinusoidal signal was transmitted to the loudspeaker. The detachment behaviour was investigated at different frequencies (30, 50, and 90 Hz) in water and 50/50 glycerol/water mixtures respectively in order to explore the effect of dynamic wettability on detachment. The critical amplitudes of particle detachment were determined and the experimental detaching force and theoretical adhesive force were compared.

The detachment experiments were conducted using model quartz particles of various hydrophobicities. Results showed that the detaching forces and maximum theoretical adhesive force (tenacity) showed good agreement for particles vibrated at low frequency and in low viscosity fluid (water). Both fluid viscosity and vibration frequency played a role in the movement of three phase contact line, and consequently influenced the detaching force required to detach the particle from the bubble. Thus, the greatest difference between the experimental detaching force and theoretical tenacity was observed at 90 Hz in 50/50 glycerol/water mixture (Fig. 1).

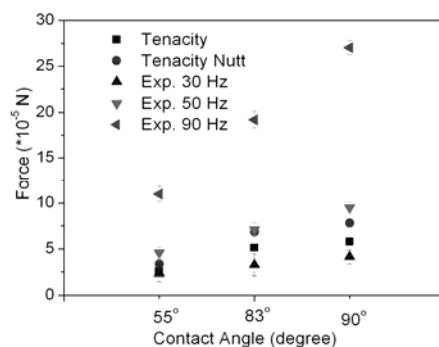


Fig. 1: Comparison of experimental detaching force and theoretical tenacity

1. Dai, Z, Fornasiero, D & Ralston, J 2000, 'Particle-bubble collision models - a review', *Advances in Colloid and Interface Science*, vol. 85, no. 2-3, pp. 231-256.
2. Schulze, HT, Wahl, B & Gottschalk, G 1989, 'Determination of adhesive strength of particles within the liquid/gas interface in flotation by means of a centrifuge method', *Journal of Colloid and Interface Science*, vol. 128, no. 1, pp. 57-65
3. Holtham, PN & Cheng, T-W 1991, 'Study of probability of detachment of particles from bubbles in flotation', *Trans. Instn. Min. Metall. (Sect. C: Mineral Process. Extr. Metall.)*, vol. 100, pp. C147-153.

## Mutual Interdependences of Electrostatic Interactions and Hydrophobicity for Three Phase Contact Formation at Titania Surface

Anna Niecikowska<sup>1</sup>, Marta Krasowska<sup>2</sup>, John Ralston<sup>2</sup> and Kazimierz Malysa<sup>1</sup>

<sup>1</sup> Institute of Catalysis and Surface Chemistry Polish Academy of Sciences, ul. Niezapominajek 8, 30-239 Cracow, Poland,

<sup>2</sup> Ian Wark Research Institute, University of South Australia, Mawson Lakes, SA, 5095, Australia

ncniecik@cyf-kr.edu.pl

Three phase contact (TPC) can be formed by bubble colliding with solid surface when thin liquid film (wetting film) between them ruptures. The surface chemistry, particularly the degree of hydrophobicity of solid and surface charge at liquid/solid and liquid/gas interfaces are main factors determining stability of such wetting film. Air bubbles in distilled water bear negative charge within wide range of pH, down to pH~2, while the isoelectric point (IEP) of titania surface is located at pH 4.7. Below the IEP of titania its surface is positively charged and an attractive electrostatic force occurs between the metal oxide/liquid and negatively charged liquid/vapor interfaces. That can lead to destabilisation of the wetting film. Hydrophilic titania surface can be easily modified with octadecylsilane (OTHS) in order to alter its hydrophobicity.

The paper presents results of studies on influence of titania surface charge on kinetics of the TPC formation at weakly hydrophobic (advancing contact angle ca. 40°) titania surface. The collision of bubbles of different size (bubble diameter varied from 0.4 to 1.48 mm) and kinetics of the TPC formation were studied using high speed camera. The experiments were carried without and with inert electrolyte (KCl) of concentration 0.01 M at pH =3.5; 4.0 and 5.8. It was found that for the same hydrophobicity the time of the TPC formation was highly affected by: i) electric charge at the wetting film interfaces affected by pH changes, ii) presence of the inert electrolyte, and iii) dimensions of the colliding bubbles (see Table I).

Table I

pH	Time needed for TPC formation in MilliQ water		
	d <sub>b</sub> =1,48 mm	d <sub>b</sub> =0,98 mm	d <sub>b</sub> =0,40 mm
5.8	462,02 ± 31,03	132,50 ± 30,76	9,62 ± 2,12
4	229,40 ± 32,31	94,81 ± 18,92	7,88 ± 1,56
3.5	92,21 ± 4,57	113,94 ± 39,17	6,94 ± 0,93

### Acknowledgement:

Scientific cooperation within COST Action P21 "Physics of droplets" is gratefully acknowledged. MK and JR acknowledge the financial support of the Australian Research Council Linkage Scheme, AMIRA International, and State Governments of South Australia and Victoria.

## Interaction between a Fine Alumina Particle and an Air Bubble

Li Jiang, Marta Krasowska, Daniel Fornasiero and John Ralston

*Ian Wark Research Institute, University of South Australia, Mawson Lakes, SA, 5095, Australia*

Li.Jiang@postgrads.unisa.edu.au

Interactions between an air bubble and an alumina particle of different hydrophobicity have been studied by colloidal probe atomic force microscopy (CP AFM) and single bubble flotation experiments. In our study particular attention was paid to the effect of the solution composition (e.g. ionic strength, pH etc.), because it affects the surface charge of the interacting interfaces, and therefore should influence the force acting between the particle and bubble. The isoelectric point (IEP) of  $\alpha$ -Al<sub>2</sub>O<sub>3</sub> particles used in our study was found to be around pH=9.1. Since it is well-known that the bubble surface bears a negative charge at pH above 3 [1], we were able to probe a wide range of pH values when a particle and a bubble surface were oppositely charged.

We also investigated the effect of salt concentration because it affects the magnitude of the surface potential, and hence the electrostatic interactions. For both hydrophilic and hydrophobic alumina particles, below the IEP the attractive force between the particle and bubble was stronger. This was also confirmed in a series of single bubble flotation experiments, where the attachment efficiency increased with decreasing pH. Similar behaviour, i.e. a stronger attractive force and higher attachment efficiency was observed with a decrease in salt concentration. For a hydrophobic particle, it was also found that the large adhesion appearing in the approach part of the force curve depended on the surface hydrophobicity, as did the attachment efficiency. As the surface hydrophobicity was increased, both the adhesion and attachment efficiency increased.

1. Brandon, N. P., Kelsall, G. H. *Journal of Applied Electrochemistry*, **1985**, 15 (4), 485.

## The Smallest Sponge: Nanostructure in Ionic Liquids

Robert Hayes<sup>1</sup>, Silvia Imberti<sup>2</sup>, Greg G. Warr<sup>3</sup>, and Rob Atkin<sup>1</sup>

<sup>1</sup> *The University of Newcastle, Australia*

<sup>2</sup> *ISIS Facility, Rutherford Appleton Laboratory, United Kingdom*

<sup>3</sup> *The University of Sydney, NSW, Australia*

Ionic Liquids (ILs) are a new and remarkable class of chemical solvents composed solely of ions. Unlike conventional solvents, ILs are structurally heterogeneous, with polar and apolar domains in the bulk. In this presentation, two structurally simple ILs, ethylammonium nitrate (EAN) and ethanolammonium nitrate (EtAN) will be investigated using small angle neutron diffraction and computer simulations. The results demonstrate EAN responds to the solvophobic effect and self-assembles into an  $L_3$ -sponge phase but with a domain size of only 1 nm. The addition of an alcohol (-OH) moiety disrupts solvophobic contact between cation alkyl chains and thus small clusters of ions appear in EtAN's bulk organization. These nanostructures are suggested to be key to many of EAN & EtAN's desirable physiochemical properties.

## Nanocrystalline TiO<sub>2</sub> from Hydrothermal Treatment with Various Ionic Liquids

Zhengfei Chen<sup>1,2</sup>, Tamar Greaves<sup>1</sup>, Rachel A. Caruso<sup>2,3</sup> and Calum J. Drummond<sup>1,3</sup>

<sup>1</sup>CSIRO Molecular Health and Technologies, Clayton, VIC, 3169, Australia

<sup>2</sup>School of Chemistry, The University of Melbourne, Parkville, VIC, 3010, Australia

<sup>3</sup>CSIRO Materials Science and Engineering, Clayton, VIC, 3169, Australia

zhengfei.chen@csiro.au

Ionic liquids, particularly room temperature ionic liquids (RTILs), have attracted a great deal of interest due to their unique properties. They are good solvents for a wide range of organic and inorganic materials, and can be chosen to be non-volatile, have excellent chemical and thermal stability, high polarity, good electrical conductivity and high ionic mobility [1,2]. Recently, TiO<sub>2</sub> nanomaterials have been synthesized in various ionic liquids [3-6], with unique morphologies obtained. This is attracting attention as nanocrystalline TiO<sub>2</sub> materials have many potential applications.

In this work, imidazolium based ionic liquids, such as 1-butyl-3-methylimidazolium hexafluorophosphate (Bmim [PF<sub>6</sub>]), 1-butyl-3-methylimidazolium tetrafluoroborate (Bmim[BF<sub>4</sub>]) and 1-butyl-3-methylimidazolium bromide (BmimBr), were used during the synthesis of TiO<sub>2</sub>. Firstly, titanium isopropoxide (TIP) was hydrolyzed in various ionic liquids to form amorphous TiO<sub>2</sub>-IL composites. These TiO<sub>2</sub>-IL composites were then solvothermally treated at 150 °C under natural and basic conditions using an autoclave. The ionic liquid used during synthesis as well as the solvent in the solvothermal treatment had an effect on the morphology, surface area and crystallinity of the final product. Well crystalline TiO<sub>2</sub> materials with high surface areas (up to 160 m<sup>2</sup>/g), and various morphologies were obtained after the solvothermal treatment. For example, the TiO<sub>2</sub> obtained from the TiO<sub>2</sub>-BmimBr composite showed a square-like morphology, while a flake-like morphology was observed when the TiO<sub>2</sub>-Bmim[PF<sub>6</sub>] composite was used, as shown in Fig. 1.

All ionic liquids were recycled from the reaction solutions after the hydrothermal treatment and it was found the ionic liquids containing F in the anions could not be reused as indicated by NMR spectra.

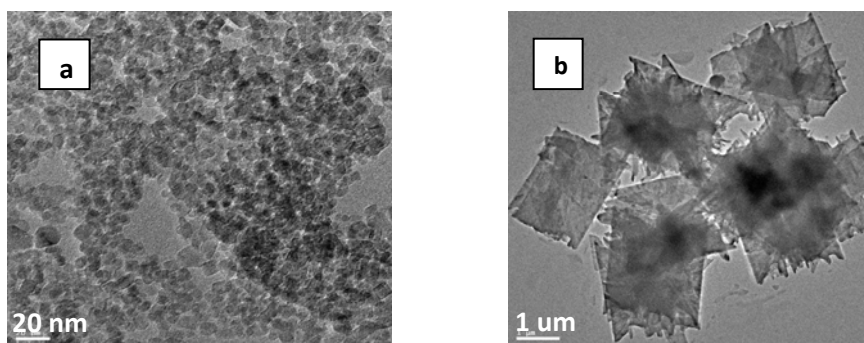


Fig. 1. TEM images of TiO<sub>2</sub> obtained using the a) TiO<sub>2</sub>-BmimBr composite and b) TiO<sub>2</sub>-Bmim[PF<sub>6</sub>] composite.

1. Welton, T. *Chemical Reviews* **1999**, *99*, 2071-2084.
2. Mikami, K. *Green Reaction Media in Organic Synthesis* **2005**
3. Kaper, H.; Endres, F.; Djerdj, I.; Antonietti, M.; Smarsly, B. M.; Maier, J.; Hu, Y. S. *Small* **2007**, *3*, 1753-1763
4. Zhou, Y.; Antonietti, M. *Journal of the American Chemical Society* **2003**, *125*, 14960-14961.
5. Zhai, Y.; Gao, Y.; Liu, F.; Zhang, Q.; Gao, G. *Materials Letters* **2007**, *61*, 5056-5058.
6. Yoo, K.; Choi, H.; Dionysiou, D. D. *Chemical Communications* **2004**, 2000-2001.

## Surfactant Adsorption at the Ethylammonium Nitrate–Air Interface: An X-ray and Neutron Reflectivity and Vibrational Sum Frequency Spectroscopy Study

Deborah Wakeham<sup>1</sup>, Petru Niga<sup>2</sup>, Andrew Nelson<sup>3</sup>, Gregory G. Warr<sup>4</sup>, Mark Rutland<sup>2</sup> and Rob Atkin<sup>1</sup>

<sup>1</sup> Centre for Organic Electronics, The University of Newcastle, Callaghan, NSW, 2308, Australia

<sup>2</sup> Department of Chemistry, Surface Chemistry, Royal Institute of Technology, Drottning Kristinas Väg 51, SE-100 44, Stockholm, Sweden

<sup>3</sup> Bragg Institute, Australian Nuclear Science and Technology Organisation, PMB 1, Menai, NSW, 2234, Australia

<sup>4</sup> School of Chemistry, The University of Sydney, NSW, 2006, Australia

deborah.wakeham@newcastle.edu.au

X-ray reflectivity and vibrational sum frequency spectroscopy are used to probe the structure at the air – liquid interface of ethylammonium nitrate (EAN), a protic ionic liquid, while neutron reflectivity and vibrational sum frequency spectroscopy are used to investigate the morphology of adsorbed layers of nonionic polyoxyethylene n-alkyl ether ( $C_nE_m$ ) surfactants at this interface. This work has revealed that the pure EAN – air interface is highly structured, and consists of alternating non-polar and charged layers that extend 19 Å into the bulk. The interfacial cations have their ethyl moieties oriented towards air, with the C3 axis of the cation terminal  $CH_3$  positioned approximately  $36.5^\circ$  from the interface normal. This structure is invariant in the temperature range 15 -  $50^\circ$ . Adsorbed  $C_{12}E_4$ ,  $C_{14}E_4$  and  $C_{16}E_4$  layers at the EAN – air interface have a head group layer that is thin and compact (only ~30% EAN by volume). The headgroups do not adopt a preferred orientation and are disordered within the interfacial layer. The surfactant tail groups have a significant number of gauche defects indicating a high degree of conformational disorder. The thickness of the tail layer thickens with increasing alkyl chain length, while the headgroup layer shows little change. Lowering the concentration of  $C_{12}E_4$ , from 1 wt% to 0.1 wt% decreases the surface excess, and the headgroup layer becomes thinner and less solvated, whereas  $C_{14}E_4$  and  $C_{16}E_4$  adsorbed layers are unaffected. When the temperature is increased to  $60^\circ C$ , the  $C_{16}E_4$  layer thickness increases and area per molecule decreases, but adsorbed layer structures of  $C_{12}E_4$  and  $C_{14}E_4$  are invariant. Both effects are attributed to surfactant solubility.

## O 17

### Spreading of Ionic Liquids on a Hydrophobic Surface

Hua Li, John Ralston and Rossen Sedev

*Ian Wark Research Institute, University of South Australia, Mawson Lakes, SA, 5095, Australia*

Hua.Li@postgrads.unisa.edu.au

The spontaneous spreading of ionic liquids on a hydrophobic surface (Teflon AF1600) was investigated by high-speed video microscopy. Six ionic liquids (EMIM BF<sub>4</sub>, BMIM BF<sub>4</sub>, OMIM BF<sub>4</sub>, EMIM TFSI, BMIM TFSI and HMIM TFSI) were used as probe liquids. The molecular-kinetic model provided a credible description of the spreading behaviour over the whole range of velocities investigated. The mean distance between two adsorption sites was predominantly determined by the properties of solid surface. The equilibrium displacement frequency was significantly influenced by the surface contribution of the activation free energy of wetting. The calculated volume of unit flow was close to the volume of a single ion, suggesting that the liquids move in single ions or ion pairs.

## Enantioselective Adsorption of a Racemic Mixture of Surfactants at a Chiral Film monitored by ATR-FTIR

Annette Haebich, Greg Qiao and William Ducker

*Department of Chemical & Biomolecular Engineering, The University of Melbourne, Parkville, VIC, 3010, Australia*

a.haebich@pgrad.unimelb.edu.au

Chiral compounds are molecules that cannot be superimposed with their mirror image, which results in two distinct isomers called enantiomers. An equimolar mixture of the two enantiomers is called a racemic mixture. Biological molecules like amino acids and sugars are chiral, and in nature nearly always appear as a single enantiomer.

In pharmacology only one enantiomer may be medically active, whilst the other may not be effective or even cause an adverse reaction. An enantiomerically pure synthesis is desirable but not always possible; so separation of the enantiomers is mostly done by chromatography, i. e. adsorption at a chiral stationary phase. The separation efficiency depends upon the column material and mobile phase used in a specific system.

To make the separation of chiral compounds more effective it is necessary to understand the interactions between chiral molecules with a chiral surface at a molecular level. Due to a lack of techniques that can distinguish between enantiomers adsorbed to a surface, not much research has been done in this field despite the need of more insight in the enantiospecific adsorption of enantiomers.

In this project the adsorption of amino acid surfactants and a chiral surface are studied by a surface sensitive infrared technique called Attenuated Total Reflection Infrared Spectroscopy (ATR-IR). The chiral surface is prepared by chemically attaching a chiral film to a silicon prism. Enantiomers of the amino acid surfactant are tagged by replacing the hydrogen atoms with deuterium which changes the frequency of IR absorption and thus makes the two enantiomers distinguishable by infrared spectroscopy. We could thus monitor the absorption of a racemic mixture in real-time. It was found that the enantiomeric excess i. e. the excess of one enantiomer over the other strongly depends on the density of chiral surface groups. The higher the density of chiral groups on the surface the higher the enantiomeric excess. The choice of solvent also had a great influence on chiral discrimination. Non-polar solvents facilitated enantiodiscrimination in this system and thus increased the enantiomeric excess.

## Tailoring Self-assembled Thiol Monolayers to Facilitate Measurement of Tetradecane Micro-Droplet Interactions with AFM

Hannah Lockie, Geoffrey Stevens, Derek Y. C. Chan, Franz Grieser and Raymond R Dagastine

*Particulate Fluids Processing Centre, University of Melbourne, Parkville, VIC, 3010, Australia*

hlockie@pgrad.unimelb.edu.au

Interactions between oil droplets in aqueous solutions, including the process leading to coalescence, is both difficult to measure and interpret theoretically due to the deformation of both interfaces. A novel AFM technique is presented here that facilitates accurate force measure of droplet-droplet interactions of oils in aqueous solutions. The technique involves tailoring of mixed self-assembled thiol monolayers (hydroxy-thiol combined with alkane-thiol) on gold to provide surfaces of the required hydrophobicity. The new system is then used to measure interactions between tetradecane droplets in SDS solution showing the transition from static to dynamic conditions at increasing velocity. Theoretically the system can be explained through earlier work performed by our group [1, 2] , that provides a mathematical explanation for the measured forces.

1. Carnie, S. L., D. Y. C. Chan, et al. (2005). "Modelling drop-drop interactions in an atomic force microscope." ANZIAM J 46(E): C805--C819
2. Dagastine, R. R., R. Manica, et al. (2006). "Dynamic Forces Between Two Deformable Oil Droplets in Water." Science (Washington, DC, United States) 313(5784): 210-213.

## Application of PALS to Understand Structure in Self-Assembled Systems: Investigations with a Dilutable Microemulsion

Aurelia W. Dong<sup>1,2</sup>, Ben J. Boyd<sup>2</sup>, Anita J. Hill<sup>3</sup> and Calum J. Drummond<sup>1,3</sup>

<sup>1</sup> CSIRO Molecular and Health Technologies, Clayton, VIC, 3168, Australia

<sup>2</sup> Drug Delivery, Dispositron and Dynamics, Monash Institute of Pharmaceutical Sciences, Monash University, Parkville, VIC, 3052, Australia

<sup>3</sup> CSIRO Materials Science and Engineering, Clayton, VIC, 3168, Australia

Aurelia.Dong@Pharm.monash.edu.au

Positron Annihilation Lifetime Spectroscopy (PALS) (Fig. 1) has been used extensively to characterize solid-state materials, such as the porosity in polymer membranes and physical defects in metals and ceramics [1]. Although PALS is a well established technique for characterizing solid materials, its application in nano-porous 'soft' matter materials such as amphiphile self-assembly systems is not yet established. Ordered amphiphile self-assembly systems are utilized in a wide variety of applications including drug delivery, personal care, structure templating, catalysis and energy storage. The properties of these systems play an important role in their application, and is dictated by the internal structure of the amphiphile self-assembly materials. Nano-scale physical and chemical interactions govern the packing of self-assembled amphiphilic molecules, resulting in thermodynamically stable phases of defined geometries. At present, small angle x-ray scattering (SAXS) has been the most common technique used to characterise the structure of self-assembled systems. PALS offers a possible alternative technique as it is shown to be sensitive to the molecular packing and mobility of the self-assembled lipid molecules in various lyotropic liquid crystalline phases [2]. Thus, in combination with SAXS, PALS may provide more detailed structural information about molecular level structure in the lipid domains, and trends in this structure with changes in composition and temperature. In this study the structure of a self-assembled amphiphile system, known to undergo a transition from inverse (water-in-oil, w/o) to normal (oil-in-water, o/w) micelles through a bicontinuous microemulsion with increasing water content (Fig. 2), has been systematically investigated. The dilutable microemulsion system comprised two surfactants (Labrasol + Plurol oleique), an oil (Isopropyl myristate) and water.

PALS investigation of the system where ortho-positronium (oPs) lifetime and intensity signatures were determined reveal differences between the various self-assembled phases. oPs lifetimes obtained from PALS were able to detect the phase transitions, and compositions correlated well to those determined by conductivity measurements.

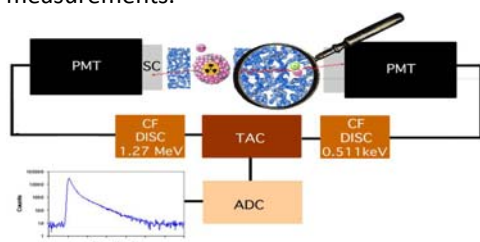


Fig. 1. Schematic of a PALS experimental setup. The <sup>22</sup>Na source is sandwiched in the sample which is contained in a specially designed sample holder. The emitted positrons from the decay of <sup>22</sup>Na interact with the material structure, emitting  $\gamma$ -rays at characteristic time scales indicative of nanostructure

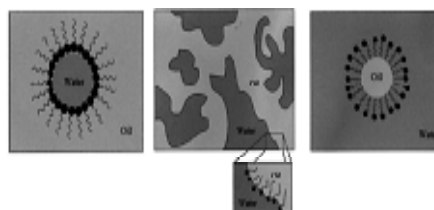


Fig. 2. Schematic representation of microemulsion structures: water-in-oil, bicontinuous, oil-in-water microemulsion [3].

1. Hulett, L. D. *et al.*, "Application of Positron Spectroscopy to material science," in *Advanced Materials Research*, vol 3, Switzerland: Scitec Publications, **1994**.
2. Dong, A. *et al.*, "Positron Annihilation Lifetime Spectroscopy as a characterization technique for Nanostructured Self-assembled Amphiphile Systems," *J. Phys. Chem. B* **2009**, 113, 84-91.
3. Lawrence, M. J. and Rees, G. D., "Microemulsion-based media as novel drug delivery systems," *Adv. Dru. Del. Rev.*, vol 45, **2000**, 89-121.

## O 21

### Lyotropic Liquid Crystalline Phases in Surfactant Biomineralisation Precursors

Connie Liu and Gregory Warr

*School of Chemistry, University of Sydney, NSW, 2006, Australia*

c.liu@chem.usyd.edu.au

Biogenic crystals such as calcium carbonate, calcium phosphate and calcium oxalate exhibit ordered microstructures for both functional and structural purposes. In nature, the mineral architecture is controlled on a micro-scale by a network of proteins and organic macromolecules.

Surfactants are candidate nano-scale templating agents due to their molecular dimensions and ability to spontaneously self assemble in solution into a variety of microstructures. Prior to the controlled fabrication of biomaterial, it is critical that the nature of the template is well understood such that manipulation of the template directly leads to desired properties in the biomaterial.

In this project, cationic (dodecyltrimethylammonium) surfactants have been prepared with hydrolysable carbonate and phosphate counterions. The self assembly of these surfactants in aqueous solution have been characterised by their critical micelle concentration (cmc), pH at various concentrations of the micellar solution and the microstructure of lyotropic surfactant phases have been studied by observing the optical texture under a polarising microscope and small angle x-ray scattering (SAXS). The microstructure formed as a result of the self assembly for all new surfactants varies from - micelles in solution to several liquid crystalline phases including cubic, hexagonal and lamellar geometries. In addition, a second cubic phase of 3D hexagonal close packed spheres (HCPS) has been identified for dodecyltrimethylammonium carbonate. The HCPS structure is rare in surfactant mesophases and has not been previously reported to form in cationic surfactant systems.

## Rearrangement of Micelle Structures during Polymerization

Khwanrat Chatjaroenporn, Robert W. Baker, Paul Anthony FitzGerald and Gregory G. Warr

*School of Chemistry F11, The University of Sydney, NSW, 2006, Australia*

muay@chem.usyd.edu.au

Using small angle neutron scattering (SANS), we studied the shape transition of micelles of the tail-polymerizable cationic surfactant 11-(methacryloyloxy)undecyltrimethylammonium bromide (MUTAB) as a function of polymer conversion. Previous studies of such systems have suggested kinetic “locking” of the micelle structure during polymerization, however, we found a transition from spheres (unpolymerized) to rods (at intermediate conversions) back to spheres (fully polymerized), see Fig. 1. By comparing these results to the micelle shapes formed by the mixtures of 100% polymerized and unpolymerized MUTAB, we show that the shape transitions observed during polymerization are due to equilibrium structures that undergo rearrangement as the composition changes.

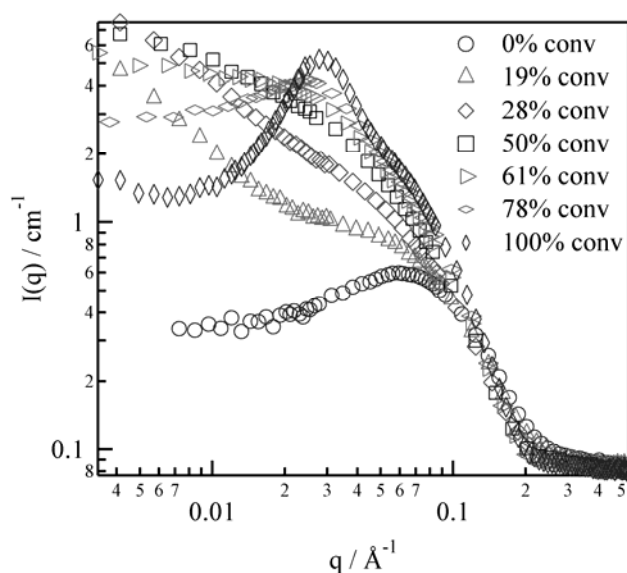


Fig. 1. Small angle neutron scattering from 1.9 w/v% MUTAB in D<sub>2</sub>O at various polymer conversions.

## Influence of Hydrolysable Metal Ions on the Interfacial Chemistry and Particle Interactions of Aqueous Muscovite Dispersions

Ataollah Nosrati, Jonas Addai-Mensah and William Skinner

*Ian Wark Research Institute, University of South Australia, Mawson Lakes, SA, 5095, Australia*

Ataollah.Nosrati@postgrads.unisa.edu.au

In a number of unit operations (e.g. leaching and dewatering) used for valuable metal (e.g., Cu, Ag, etc.) recovery from mineral ores, the interfacial chemistry and rheological behaviour of gangue clay minerals (e.g. muscovite) present may be a predominant issue. Depending upon the pH and behaviour of certain hydrolysable metal ions in feed process water or leached from the reactive clay particles may dramatically impact on pulp chemistry and particle interactions. In this study, the influence of hydrolysable metal ions (Al(III), Fe(III) and Cu(II)) on the interfacial chemistry and shear rheology of aqueous muscovite dispersions has been investigated at pH range 3 – 10 and 25 °C. Particle zeta potential analysis revealed strong metal ion type and pH-dependent behaviour, with striking impact on dispersion viscosity and yield stress. In  $10^{-3}$  M  $\text{KNO}_3$  background electrolyte, zeta potential profile from pH 10 to 3 showed an isoelectric point (iep) around pH 3 – 3.3 and 4 – 4.3 for dilute and concentrated dispersions, respectively. Subsequent measurements from low to high pH showed differing electrokinetic potentials with iep shift to higher pH values. The presence of Al(III) or Fe(III) or Cu(II) ions at different ionic strengths, led to a marked metal ion specific changes in the interfacial chemistry reflecting different zeta potential profiles. The concomitant dispersions shear yield stress analysis revealed similar, strong metal ion type and pH-dependency. Different maximum shear yield stresses were observed at iep for the dispersions with and without metal ions, indicating the attractive van der Waals and particle bridging forces which scaled with ionic strength. The results exemplify how different metal ions in the aqueous clay dispersions can significantly influence the particles' surface chemistry and control the pulps' rheological behaviour.

## Electrochemistry Study of Chalcopyrite with Different Phase

Yansheng Zhang<sup>1,2</sup>, Miao Chen<sup>1</sup>, Wenqing Qin<sup>2</sup>, Weimin Zeng<sup>1,2</sup>, and Jinfeng Liu<sup>1</sup>

<sup>1</sup> *CSIRO Processing Science and Engineering, Clayton South, VIC, 3169, Australia*

<sup>2</sup> *School of minerals processing and bioengineering, Central South University, Changsha, China*

Yansheng.Zhang@csiro.au

The phase transformation of chalcopyrite and the electrochemical behaviour of the different phase chalcopyrite electrode were investigated in 9K media at 30°C. The roasting of chalcopyrite was carried out at 200°C, 380°C and 552°C at which the chalcopyrite was stable as  $\alpha$  phase,  $\beta$  phase and  $\gamma$  phase. It was found that chalcopyrite crystal lattices increase with the roasting temperature by XRD analysis. Cyclic voltammetry and the linear polarization were employed to determine the electrochemical behaviours of the different phase chalcopyrite electrode. CV showed that the redox current increase and the oxidation potential move negatively, indicating the dissolution reaction occurs more easily. The corrosion kinetic studies using the linear polarization shows that the corrosion potential of the chalcopyrite electrode decrease with the roasting temperature and the corrosion current increased. It was demonstrated that the chalcopyrite in the  $\gamma$  phase and  $\beta$  phase was dissolved more easily compared with the nature chalcopyrite in  $\alpha$  phase.

## Characterization of Extracellular Polymeric Substances Extracted from the Mineral Surface during Bioleaching of Chalcopyrite Concentrate

Weimin Zeng<sup>1,2,3</sup>, Miao Chen<sup>1</sup>, Guanzhou Qiu<sup>2,3</sup>, Hongbo Zhou<sup>2,3</sup>, Weiliang Chao<sup>4</sup> and Yansheng Zhang<sup>1,3</sup>

<sup>1</sup> CSIRO Process Science and Engineering, Clayton, VIC, 3169, Australia

<sup>2</sup> Key Laboratory of Biometallurgy, Ministry of Education, China

<sup>3</sup> School of Minerals Processing and Bioengineering, Central South University, Changsha, China

<sup>4</sup> Department of Microbiology, Soochow University, Tai Bei, Taiwan

zengweimin1024@gmail.com

A mixed culture of moderately thermophilic microorganisms was used to bioleach chalcopyrite concentrate in a stirred tank reactor. The results show that up to 84.7% of copper extraction could be achieved in 24 days at a pulp density of 4%. The leaching rate of chalcopyrite concentrate tended to increase with an increase of dissolved total iron concentration. Furthermore, the extracellular polymeric substance (EPS) on the surface of the chalcopyrite concentrate was extracted and analysed. EPS was extracted at the 1<sup>st</sup>, 3<sup>rd</sup>, 8<sup>th</sup>, 16<sup>th</sup> and 24<sup>th</sup> day during bioleaching, which mainly consisted of proteins, lipids, sugars and ferric ions. After the 8<sup>th</sup> day the total amount of EPS remained relatively constant. However, the amount of ferric ion in the EPS decreased in a large scale. The ore residue analysis indicates that the decrease of ferric ion was mainly due to the formation of jarosite on the mineral surface.

## An Investigation of the Pulp Chemistry and Structural Network of an Isothermally Leached Muscovite Clay Suspension

Terry Dermis, William M. Skinner and Jonas Addai-Mensah

*Ian Wark Research Institute, University of South Australia, Mawson Lakes, SA, 5095, Australia*

Terry.Dermis@postgrads.unisa.edu.au

Clay and oxide gangue minerals play a critical role in extractive metallurgical processing of ores containing valuable minerals (e.g. Cu and Au). Under certain dispersion conditions, aqueous gangue clay systems can exhibit a wide variety of structures (house of cards, banding and gels) and rheological properties (viscoelastic and thixotropy), making extraction of the valuable mineral and pulp handling more difficult. In aqueous media, natural plate-like clay particles have been shown to exhibit gel characteristics [1, 2], resulting from anisotropic charge distributions at different faces of the particles. The presence or absence of specific ions, as a result of isomorphous substitution, determines this charge disparity associated with the particle mineralogy. This study explores how dissolved ion species might form simple and/or complex molecular structures in solution, via poly-condensation reactions, which can specifically adsorb to particle surfaces, effectively bridging particles together to form stable 3-D network structures.

Model muscovite mineral dispersions were agitated at 500 rpm under fundamentally and industrially relevant processing conditions (pH 7 vs. 1; 25 °C vs. 70 °C) over a 4 h period. The solution chemistry of the leach liquor as well as bulk and surface chemical and structural characteristics of leached solid residues was investigated. The results reveal incongruent leaching of cationic species into solution, which may form poly-condensed network structures (e.g. Al-O-Al, Si-O-Si and Al-O-Si). Low pH leaching accentuates dealumination of the muscovite tetrahedral layer via protonation. This variable results in the exposure of the framework ions in the tetrahedral-octahedral clay structure. Spectroscopic analysis concludes surface layers are transformed from amorphous to more well-defined 3-D cross-linked networks, and gives insight to an adsorption mechanism relationship between activated surface sights and these poly-condensed structures.

1. Çınar, M.; Can, M. F.; Sabah, E.; Karagüzel, C.; Çelik, M. S. *Applied Clay Science* **2009**, 42(3-4), 422
2. Neaman, A.; Singer, A. *Soil Science Society of America Journal* **2000**, 64(1), 427

## Nano-Mechanical Behaviour of Living Cancer Cell Surface Using Atomic Force Microscopy

Thakshila Balasuriya<sup>1</sup>, Geoffery<sup>1</sup> Stevens, Franz Grieser<sup>1</sup>, Michelle de Silva<sup>1</sup>, Elizabeth Williams<sup>2</sup> and Raymond R Dagastine<sup>1</sup>

<sup>1</sup>*Particulate Fluids Processing Centre, University of Melbourne, Parkville, VIC, 3052, Australia*

<sup>2</sup>*Centre for Cancer Research, Monash Institute of Medical Research, Monash University, Clayton, VIC, 3168, Australia*

t.balasuriya@pgrad.unimelb.edu.au

The dynamic interaction forces between living cells mediate or control a large range of biological processes as well as in numerous applications using biomolecular additives in soft matter systems such as emulsions and foams. Living cellular systems are far more complex, but hold common themes with the drops and bubbles due to their deformable nature. Living cells are studied in an attempt to translate the fundamental understanding of dynamic forces in soft matter systems to complex challenges in biology.

This presentation will focus on the probing the nano-mechanical behaviour of living cancer cell surface using the Atomic Force Microscope. B2-P32 strain of human bladder cancer cells which originate from the bladder muscle were used in this study. The Atomic Force Microscope was used to characterize their elastic behaviour by performing various indentations on the cells. A numerical model based on the Hertz model was used to analyse the data and obtain cell elasticity.

## Multifunctional Polymeric Surface Coatings via Brominated Plasma Polymers

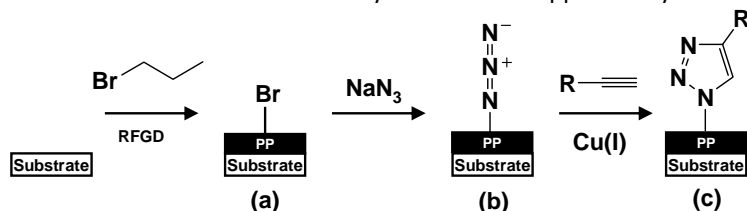
Rodney Chen<sup>1,2</sup>, Ben W. Muir<sup>2</sup>, Georgina K. Such<sup>1</sup>, Almar Postma<sup>2</sup>, Richard A. Evans<sup>2</sup>, Keith M. McLean<sup>2</sup> and Frank Caruso<sup>1</sup>

<sup>1</sup> Centre for Nanoscience and Nanotechnology, The Department of Chemical and Biomolecular Engineering, The University of Melbourne, Parkville, VIC, 3052, Australia

<sup>2</sup> CSIRO Molecular and Health Technologies, Clayton, VIC, 3168, Australia

Rodney.Chen@csiro.au

A brominated plasma polymer (BrPP) thin film was fabricated on a variety of substrate surfaces (silicon wafers, glass, gold, and polymers) via the radio frequency glow discharge of 1-bromopropane. This BrPP thin film was highly adherent and stable and was found to be a useful platform for secondary reactions, leading to surfaces with specific chemical functionalities. Following nucleophilic exchange, an azide-functionalized PP thin film was prepared that was reactive toward two different alkynes via the copper-catalyzed azide-alkyne cycloaddition



(CuAAC) reaction, a paradigm of “click” chemistry (Scheme 1) [1].

Scheme 1: Click chemistry on BrPP thin film, (a) BrPP deposition on substrates with 1-bromopropane, (b) azide functionalized PP and (c) triazole formation on PP after the CuAAC reaction.

These BrPP coatings have also been deposited on silica microparticles (3  $\mu$ M) for the fabrication of hybrid organic-inorganic Janus particles. Silica microparticles immobilized on a sodium chloride crystal, were toposelectively modified with a BrPP coating. The microparticles were recovered, modified with azide and reacted with a fluorescent alkyne through the CuAAC reaction (Fig. 1).

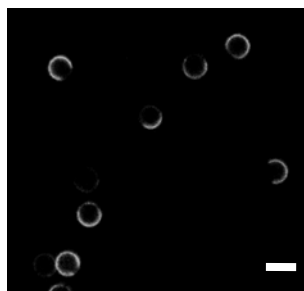


Fig. 1: Confocal laser scanning microscopy image of 3  $\mu$ M Janus particles after CuAAC reaction with fluorescent alkyne. Scale bar represents 5  $\mu$ M.

1. Chen, R.T.; Muir, B.W.; Such, G.K.; Postma, A.; Evans, R.A.; Pereira, S.M.; McLean, K.M.; Caruso, F. *Langmuir*. DOI: 10.106/la9031688

## Controlling Burst Release of Cubosomes Through Nano-Encapsulation

Chantelle Driever<sup>1,2</sup>, Xavier Mulet<sup>1</sup>, Angus Johnston<sup>2</sup>, Helmut Thissen<sup>1</sup>, Frank Caruso<sup>2</sup>,  
and Calum Drummond<sup>3</sup>

<sup>1</sup>CSIRO Molecular & Health Technologies, Clayton, VIC, 3169, Australia

<sup>2</sup>Department of Chemical & Biomolecular Engineering, University of Melbourne, VIC, 3010, Australia

<sup>3</sup>CSIRO Materials Science and Engineering, Clayton, VIC, 3168, Australia

Chantelle.Driever@CSIRO.au

Cubosomes are dispersed lyotropic liquid crystals. They exhibit several qualities which make them ideal drug delivery vehicles, such as nanoscale size (~100-300nm), mechanical rigidity, and the ability to accommodate large amounts of an extensive and diverse range of molecules [1]. Unfortunately, a large surface area to volume ratio contributes to an immediate release of the cubosomes' drug contents when they are placed into an external environment such as the body [2]. This "burst effect" can cause toxicity within the system and negative side effects to the patient [3].

We are currently investigating two approaches to minimize burst effect and achieve a sustained drug release profile. One technique involves layering polymers onto the surface of the cubosomes to form a physical barrier for the drug (fig. 1 A-C). We can tailor release through the specific polymers utilised and the number of layers added.

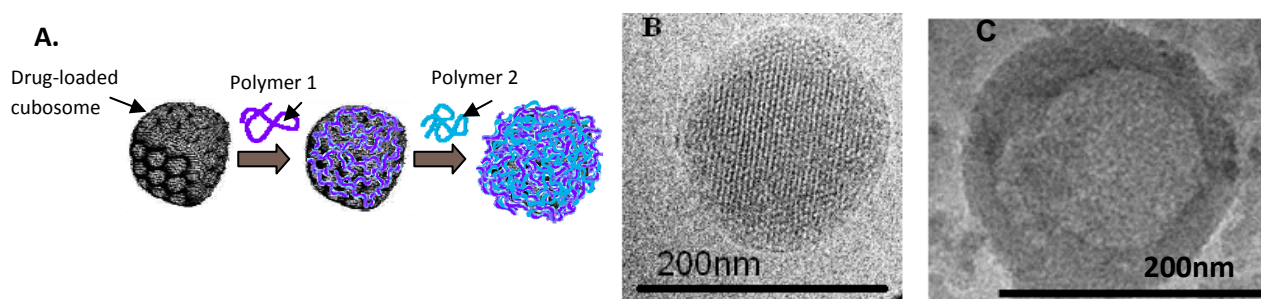


Fig. 1 A-C: A. Schematic of layering a drug loaded cubosome with polymers. B. Cryo-TEM image of an uncoated cubosome. C. Cryo-TEM image of a cubosome with seven surrounding polymer layers.

The second encapsulation technique involves coating a sacrificial core template (1-5 $\mu$ m) with layers of polymer followed by a layer of cubosomes and further polymer 'capping' layers (fig. 2). This technique may allow for a multi-functional drug release mechanism, as cubosomes loaded with different drugs can be added to separate layers of the same structure.

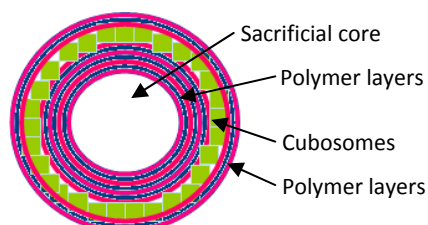


Fig. 2. Cubosomes embedded within a polymer matrix surrounding a sacrificial core.

Characterisation of these novel systems is performed with transmission electron microscopy, quartz crystal microbalance, and small angle x-ray scattering prior to drug release studies.

1. Drummond, C.J. and C. Fong, *Current Opinion in Colloid & Interface Science*, **1999**. 4(6): p. 449-456.

2. Boyd, B.J., *International Journal of Pharmaceutics*, **2003**. 260(2): p. 239-247.

3. Huang, X. and C.S. Brazel, *Journal of Controlled Release*, **2001**. 73(2-3): p. 121-136.

## In Vivo Study of Lipid-Water Cubic Formulation for Drug Delivery in Photodynamic Therapy

Hanne Evenbratt<sup>1</sup>, Charlotte Jonsson<sup>2</sup>, Jan Faergemann<sup>3</sup>, Marica B. Ericson<sup>4</sup> and Sven Engström<sup>1</sup>

<sup>1</sup> Department of Chemical and Biological Engineering, Chalmers University of Technology, Göteborg, Sweden,

<sup>2</sup> Department of Chemistry, Dermatochemistry and Skin Allergy, University of Gothenburg, Göteborg, Sweden

<sup>3</sup> Department of Dermatology, Sahlgrenska University Hospital, Göteborg, Sweden,

<sup>4</sup> Department of Physics, University of Gothenburg, Göteborg, Sweden,

hannee@chalmers.se

The objective of this study was foremost to evaluate in vivo the efficiency of certain lipid-water cubic phases, containing either of two different enhancers, as drug delivery system for topical application of  $\delta$ -aminolevulinic acid (ALA) and methylaminolevunitate (MAL) in comparison with a conventional drug (Metvix) and traditional cubic system based on GMO. Lipid-water cubic systems has been shown to have interesting properties for photodynamic therapy (PDT) [1, 2]. The cubic phase has a bicontinuous structure, suitable for accommodating both hydrophilic and hydrophobic substances. Thus it is suitable for delivery of both ALA and MAL that are photosensitisers used in PDT. PDT is based on photosensitisation of skin cells and has become an important tool for cancer treatment [3]; especially for treating superficial forms of skin disorders. When the cancerous cells are reached by the drug a photosensitive substance is formed which, when exposed to visible light, results in cell necrosis.

The formulations in this study were topically applied to live nude mice and the subsequent formation of the photosensitive substance was monitored by fluorescence measurements. It was found that particularly one cubic phase formulation was a possible alternative to use in PDT, primarily due to higher fluorescence levels observed than when monitoring the mice treated with conventional drug. Further investigation is needed in the form of a technical verification of the drug delivery potential of this specific cubic phase formulation containing ALA and MAL in humans, both healthy and cancerous skin.

1. J. Bender, M.B. Ericson, N. Merclin, V. Inani, A. Rosén, S. Engström, J. Moan, Lipid cubic phases for improved topical drug delivery in photodynamic therapy. *Journal of Controlled Release* 106 (2005) 350-360.
2. J. Kuntsche, H. Bunjes, A. Fahr, S. Pappinen, S. Rönkkö, M. Suhonen, A. Urtti, Interaction of lipid nanoparticles with human epidermis and an organotypic cell culture model. *Int J Pharmaceutics* 354 (2008) 180-195.
3. N. Fotinos, M.A. Campo, F. Popowycz, R. Gurny, N. Lange, 5-Aminolevulinic acid derivatives in photomedicine: Characteristics, application and perspectives. *Photochem Photobiol* 82 (2006) 994-1015.

## Effects of Sugars on Bilayer to Non-Bilayer Phase Transitions in Biological Membranes during Dehydration

Ben Kent<sup>1</sup>, Christopher J Garvey<sup>2</sup> and Gary Bryant<sup>1</sup>

<sup>1</sup>*Applied Physics, RMIT University, Melbourne, VIC, 3000, Australia*

<sup>2</sup>*Australian Nuclear Science and Technology Organization, Menai, NSW, 2234 Australia*

benjamin.kent@rmit.edu.au

The removal of liquid water from biological organisms – whether due to dehydration or slow freezing, can result in phase transitions in their cell lipid membranes. These transitions, induced by compressive stress in the membranes which arises when membranes are brought into close proximity, can involve the freezing of the lipids and a decrease in their lateral movement (bilayer-bilayer transition), or a rearrangement of the lipids into an inverse phase (bilayer-non bilayer transition). In both cases, the semi-permeable fluid lipid bilayer of the healthy cell is lost, impairing the function of the cell and often causing cell death.

Sugars have been shown to play an important role in the natural defences of biological organisms against freezing and dehydration damage by altering the phase behaviour of lipid membranes. Their accumulation in lipid membrane systems is known to help preserve the fluid lipid bilayer phase in low hydration lipid systems. However, the mechanisms by which this is achieved is still debated. The phase behaviour of membranes in the presence of sugars is therefore of primary importance in understanding freezing and dehydration damage.

In this paper we will present the results of small angle x-ray scattering (SAXS) and small angle neutron scattering (SANS) experiments which aim to determine the how the presence of sugars alters membrane structure. These results will be discussed in terms of the current understanding of how sugars protect membranes during dehydration.

## Ultra-Smooth Titania Surfaces for Surface Force Analysis

Rick B. Walsh and Vince S. J. Craig

*Department of Applied Mathematics, Research School of Physics and Engineering, The Australian National University, Canberra, ACT, 0200, Australia*

rbw110@physics.anu.edu.au

In order to describe the behavior of minerals in a range of separation and processing steps it is desirable to measure the forces directly, particularly under conditions of high salt concentrations and extremes of pH, which are often employed industrially. The direct measurement of interaction forces between mineral oxide surfaces has been hampered by the requirement that the surfaces are sufficiently smooth and representative of the mineral of interest. Larson et al [1] have measured the forces between a flat titania surface and a spherical titania particle however the roughness of the colloidal mineral particle influenced the data at small separations. At high salt concentrations the surface forces are short ranged and roughness adds considerable uncertainty to the interpretation of the data. Our efforts in producing extremely smooth titania surfaces suitable for force measurements will be presented along with measurements of the interaction forces.

1. Larson, I.; Drummond, C. J.; Chan, D. Y. C.; Greiser, F. J. *Am. Chem. Soc.* **1993**, Vol. 115, 11885

## Synthesis and Mechanical Characterization of Hollow Silica Shells – for the use in Total Internal Reflection Microscopy (TIRM)

Stefanie Sham and Raymond Dagastine

*Particulate Fluids Processing Centre, The University of Melbourne, VIC, 3010, Australia*

p.sham@pgrad.unimelb.edu.au

The application of hollow microspheres has attracted immense attention in recent decades. In order to gain more insights into the basic fundamentals of forces between two interacting surfaces, hollow shells will be utilized in force measurements in Total Internal Reflection Microscopy (TIRM). This presentation aims to discuss the synthesis methods that were employed in generating hollow silica shells as well as the characterization of their mechanical strength [1-8].

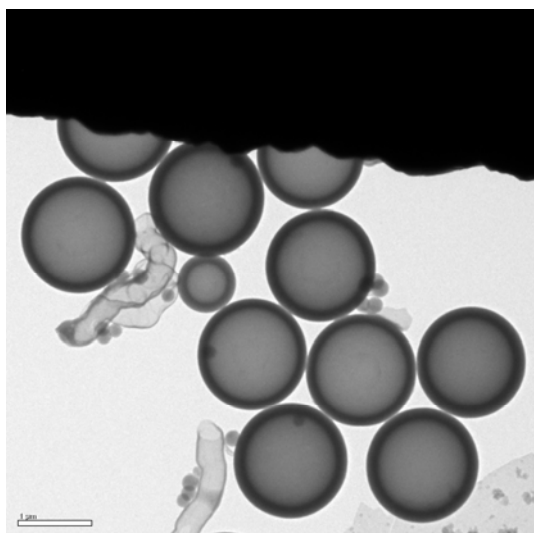


Fig. 1 Hollow Silica Shells synthesized using emulsion droplet cores (Core Size = 1.3 $\mu$ m, Shell Thickness = 93-135nm)

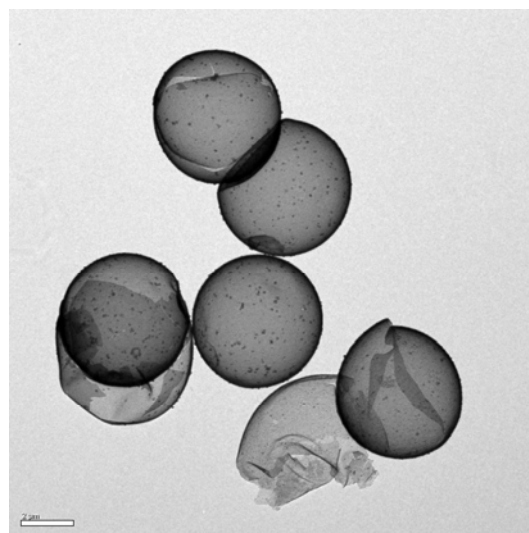


Fig. 2 Hollow Silica Shells synthesized using solid polystyrene cores (Core Size = 4.9 $\mu$ m, Shell Thickness = 40nm)

1. Zoldesi, C.I.; Imhof, A. *Advanced Materials* 17 **2005**, 924-928
2. Zoldesi, C.I.; Steegstra, P.; Imhof, A. *Journal of Colloid and Interface Science* 308 **2007**, 121-129
3. Zoldesi, C.I.; van Walree, C. A.; Imhof, A. *Langmuir* 22 **2006**, 4343-4352
4. Zoldesi, C.I.; Ivanovska, I.L.; Quilliet, C.; Wuite, G.J.L.; Imhof, A. *Physical Review E* 78 **2008**, 1-8
5. Goller, M.I.; Vincent, B. *Colloids and Surfaces A: Physicochemical and Engineering Aspects* 142 **1998**, 281-285
6. Goller, M.I.; Obey, T.M.; Teare, D.O.H.; Vincent, B.; Wegener, M.R. *Colloids and Surfaces A: Physicochemical and Engineering Aspects – Frontiers in Colloid Chemistry, an International Festschrift to Professor Stig E. Friberg* 123-124 **1997**, 183-193
7. Obey, T.M.; Vincent, B.; Krustev, R.; Muller, H. J. *Langmuir* 22 **2006**, 4343-4352
8. Zhang, L.; D'Acunzi, M.; Kappl, M.; Auernhammer, G.n.K.; Vollmer, D.; van Kats, C.M.; van Blaaderen, A. *Langmuir* 25 **2009**, 2711-2717

## Facile One-Pot Method to Synthesize Koosh Ball-Shaped Magnetite/ Lanthanide Phosphate Nanocomposites

Jie Fang<sup>1,2</sup>, Martin Saunders<sup>3</sup>, Yanglong Guo<sup>2</sup>, Guanzhong Lu<sup>2</sup>, Colin L. Raston<sup>1\*</sup> and K. Swaminathan Iyer<sup>1\*</sup>

<sup>1</sup>Centre for Strategic Nano-Fabrication, School of Biomedical, Biomolecular and Chemical Sciences, The University of Western Australia, Crawley, WA, 6009, Australia

<sup>2</sup>Key Laboratory for Advanced Materials and Research Institute of Industrial Catalysis, East China University of Science and Technology, Shanghai, 200237, P. R. China

<sup>3</sup>Centre for Microscopy, Characterisation and Analysis, The University of Western Australia, Crawley, WA, 6009, Australia

zbfountain@hotmail.com

Superparamagnetic fluorescent nanocomposites based on doped lanthanide phosphate and magnetite nanoparticles,  $\text{Fe}_3\text{O}_4@\text{SC}[6]\text{-LaPO}_4\text{:Eu}^{3+}$  or  $\text{Fe}_3\text{O}_4@\text{SC}[6]\text{-LaPO}_4\text{:Ce}^{3+}\text{:Tb}^{3+}$ , are accessible using a facile one-pot method for the first time. These multifunctional nanocomposite materials adopt a koosh ball structure incorporating magnetite nanoparticles coat with *p*-sulfonato-calix[6]arene (SC[6]). The resulting nanoparticles range in size from 200 to 300 nm, with both fluorescent and superparamagnetic properties for individual components maintained in the final nanostructure.

The SC[6] coated magnetite with multiple free upper rim  $-\text{SO}_3$  groups presumably serves as an inorganic crosslinker holding the 1D  $\text{LaPO}_4$  nanorods into a koosh nanoball structure (Fig. 1). Each magnetite nanoparticle with the structure serves as a multiple nucleation site for the growth of high aspect ratio  $\text{LaPO}_4$  nanorods. The resulting high density of nanorods within a single discrete structure may lead to a koosh nanoball spheroidal (minimum energy) structure with the nanorods growing radially outwards due to crowding.

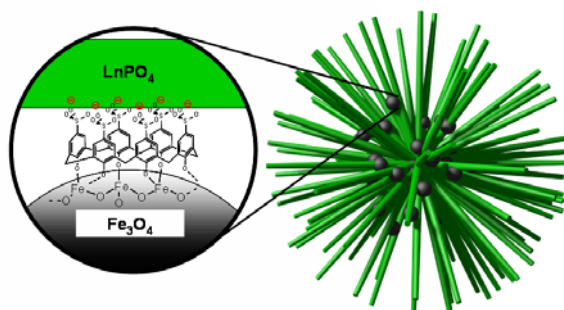


Fig. 1: A schematic representation of the Koosh nanoball structure of  $\text{LnPO}_4$  nanorods (Ln = La, Eu, Te, Ce) held together by SC[6]s stabilized  $\text{Fe}_3\text{O}_4$  nanoparticles.

## Highly Porous Alumina Bodies from Ceramic Particle Stabilized Foams

Chayuda Chuanuwatanakul, Carolina Tallon, David E. Dunstan and George V. Franks

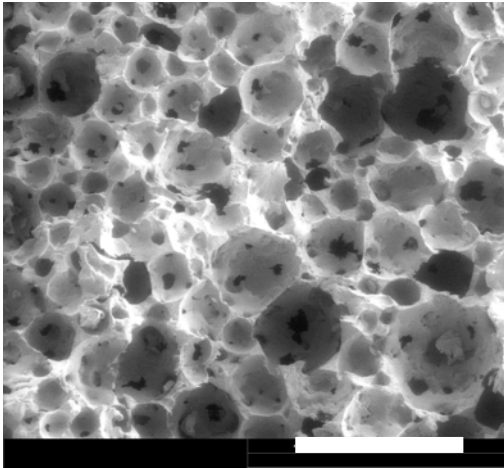
*Chemical and Biomolecular Engineering, University of Melbourne, VIC, 3010, Australia*

c.chuanuwatanakul@pgrad.unimelb.edu.au

The microstructure of gelled ceramic foams is the most important factor which influences their properties such as the mechanical strength, the permeability, and the temperature resistance. The present work studies the microstructure, such as the amount of porosity, pore size and its distribution and the morphology of alumina ( $\text{Al}_2\text{O}_3$ ) gelled ceramic foams. The microstructure of the gelled ceramic foams is affected by the surfactant concentration and type which is added to the ceramic suspension to cause the particles to become hydrophobic so that they stabilize air bubbles introduced by beating. It was found that the microstructure is changed from closed pore (bubble) morphology at the low surfactant concentration to opened pored (granular) morphology at the high surfactant concentration. (See the figures below.) The viscosity of the suspension before foaming points out that there is aggregation of the alumina particles at the higher surfactant concentrations. Moreover, the same trend of microstructure is obtained when the amount of carbon in the tail of surfactants is increased, but at the lower surfactant concentration. Also, the fired samples are observed and it is found that the microstructure of the green and fired is very similar.

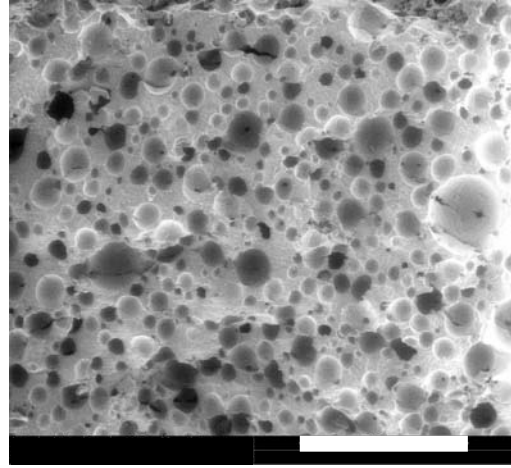
### **Green Samples**

0.1 wt% of 1-butane sulfonate at pH 2.0



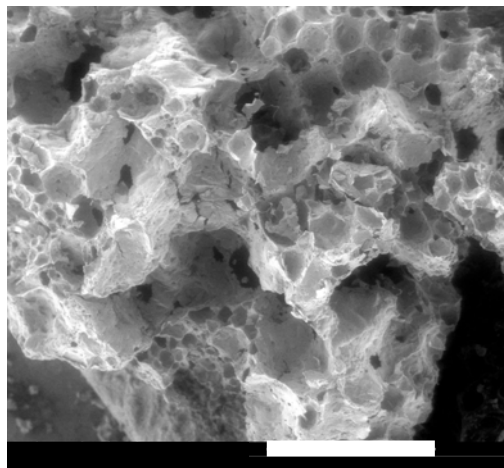
1 mm

0.7 wt% of 1-butane sulfonate at pH 2.0



1 mm

1.1 wt% of 1-butane sulfonate at pH 2.0



1 mm

## The Dependency of the Critical Contact Angle of Flotation on Particle Size - Evidence for the Non-Floatability of Fine Particles

Daniel Chipfunhu, Max Zanin and Stephen R. Grano

*Ian Wark Research Institute, ARC Special Research Centre for Particle and Material Interfaces, University of South Australia, Mawson Lakes, SA, 5095, Australia*

Daniel.Chipfunhu@postgrads.unisa.edu.au

The elementary process of flotation consists of bubble-particle collision, attachment and the formation of a stable aggregate. Flotation recovery of fine particles is poor as a result of either low collision efficiency, high critical contact angle [1,2], or both.

In this study, the flotation behaviour of methylated quartz particles of different size fractions, but all falling in the size range from 0.2 to 50  $\mu\text{m}$ , and varying contact angle, was probed in a 300  $\text{cm}^3$  mechanical flotation cell. Methyl iso-butyl carbinol (MIBC) frother was used at a concentration of 50 ppm. The results obtained show that particles in the size range studied possess different critical contact angles, which is the minimum contact angle that a particle of a particular size must attain before flotation can occur. The experimental trend is explained considering that fine particles possess low kinetic energy, which is required to expand the three phase line of contact for bubble particle attachment to occur [3]. As well, fine particles have low collision efficiency with bubbles since they do not have enough energy to exit fluid streamlines. For particles of size less than 10  $\mu\text{m}$  the Scheludko et al. (1976) model [3] shows reasonable agreement with the experimental results.

1. Crawford, R. & Ralston, J. (1988) The influence of particle size and contact angle in mineral flotation. *International Journal of Mineral Processing*, 23.
2. Miettinen, T. (2007) Fine Particles Flotation. *PhD Thesis*. Mawson Lakes, University of South Australia.
3. Scheludko, A., Toshev, B. V. & Bojadjev, D. T. (1976) Attachment of Particles to a Liquid Surface (Capillary Theory of Flotation). *Journal of the Chemical Society, Faraday Transactions 1: Physical Chemistry in Condensed Phases*, 72, 2815-2828.

## Method for Determination of The Contact Angle of Individual Particles by ToF-SIMS Surface Analysis

Susana Brito e Abreu and William Skinner

*Ian Wark Research Institute, University of South Australia, Mawson Lakes, SA, 5095, Australia*

Susana.BritoEAbreu@postgrads.unisa.edu.au

Froth flotation involves three sub-processes: particle-bubble collision, particle-bubble attachment and particle-bubble stability. The attachment ( $E_a$ ) and stability ( $E_s$ ) efficiencies are dominated by the hydrophobicity of particles [1], which is a function of surface chemistry. Particles will attach to bubbles if they possess sufficient hydrophobicity, which can be enhanced by adsorbing selected collectors and controlling the oxidation products at the surface of the minerals. The attachment efficiency of the particles to an air bubble is determined by the hydrophobic/hydrophilic ratio of the species on the surface and is measured by the contact angle. Thus, surface chemistry of minerals is the basis of mineral flotation.

Time of Flight Secondary Ion Mass Spectrometry (ToF-SIMS) has been used as a technique to correlate the surface chemistry of chalcopyrite particle ensembles, with their average contact angle measured by the Washburn method. Samples were prepared, oxidised and/or covered with collector (sodium dicesyl dithiophosphate) in different proportions to achieve different hydrophobicities. Three particle size fractions 20-38  $\mu\text{m}$ , 75-105  $\mu\text{m}$  and 150-210  $\mu\text{m}$  were used, covering a range of contact angles between 20° and 90°. Multivariate statistical techniques (principal components analysis, cluster analysis and regression analysis) were applied to the ToF-SIMS data in order to identify structure in the data and the surface species contributing most to surface chemistry variation, and hence, hydrophobicity. An innovative method to calculate the contact angle of chalcopyrite particles by ToF-SIMS surface analysis has been developed using only three secondary ions: oxygen, sulphur and a thiol collector fragment (Eq.1). This approach is based solely on the surface chemical contribution to the contact angle, regardless of surface roughness and particle size. This method introduces two new concepts in surface science: 1) the individual particle contact angle and 2) the distribution of contact angles (heterogeneity) within particle ensembles [1] and across individual surfaces. The methodology has also been validated for flat chalcopyrite surfaces, enabling more rapid surface chemistry-hydrophobicity correlation to be made on a wide range of mineral-reagent systems.

$$\theta = 45.74 - 1.208I_O + 3.065I_S + 15.82I_{Coll} \quad (\text{Eq.1})$$

Flotation studies have been conducted using the ToF-SIMS method capabilities. Surface chemistry-recovery comparisons enable the investigation of the effect of collector addition and particle size in the floatability of particles.

1. Duan, J.; Fornasiero, D.; Ralston, J. *Int. J. Min. Proc.*, **2003**, 72, 227-237

## Developing Natural Diatomaceous Earth (DE) Particles for Process Water Treatment Application

Yang Yu, Jonas Addai-Mensah and Dusan Losic

*Ian Wark Research Institute, University of South Australia,, Mawson lakes, SA, 5095, Australia*

yuyyy021@students.unisa.edu.au

The unique structural properties of natural, silica-based diatomaceous earth (DE) materials formed during fossilization of diatoms have been recognized as promising mesoporous substrates for the development of new nanomaterials. In this study, pre-treatment and characterization of the structural and chemical properties of nano-colloidal DE particles together with pH-mediated purification of synthetic saline water in the presence and absence of the DE particles are performed. The results show that the structures of pristine and acid treated DE materials were mineralogically and chemically complex, comprising predominantly amorphous SiO<sub>2</sub> and other oxide phases in minor to trace amounts. The crystallo-chemical structure and interfacial chemistry of the purified product are similar to that of silica particles in terms of pH-dependent particle zeta potentials which indicated an isoelectric point (iep) of pH 2. In synthetic solutions containing 10<sup>-1</sup> M KNO<sub>3</sub> salt, the alkali metal ion was observed to specifically adsorb onto the DE particles, causing a shift of the iep from pH 2 to 6, contrary to expectation. The DE particles were effective in removing 49 - 89% and 57 - 72% of the monovalent K<sup>+</sup> ions, respectively, at pH 7.5 and 11 via specific metal ion adsorption. For the solutions containing hydrolysable metal ions: Mn(II), Al(III) and Pb(II), on the other hand, self-nucleation lead to the removal 36 - 100% of the species at high pH (>8) as metal hydroxide precipitates. The DE particles were effective in removing up to 59% of the cations via adsorption at lower pH values (<7.5). The overall particle zeta potential and multivalent metal ion complexation analyses indicated that, the removal of these hydrolysable metal ions from solution by DE particles occurred more predominantly via specific adsorption onto the particles' surface rather than by physisorption or electrostatic attractions. The findings highlight the importance of understanding pH-dependent, metal ion speciation and hydrolysis effects and their interactions with DE particles in the removal of unwanted metal ions from aqueous media.

## Dewatering of Cyanobacteria-Rich Sludges

Feng Qian<sup>1</sup>, Peter J. Scales<sup>1</sup>, David R. Dixon<sup>1</sup> and Gayle Newcombe<sup>2</sup>

<sup>1</sup>*Particulate Fluids Processing Centre, Department of Chemical and Biomolecular Engineering, The University of Melbourne, VIC, 3010, Australia*

<sup>2</sup>*Australian Water Quality Centre, GPO Box 1751, Adelaide, SA, 5001, Australia*

fqian@unimelb.edu.au

Cyanobacteria, or blue-green algae, are now recognized as a serious water quality problem for drinking water supplies in Australia. Under a combination of high nutrient loadings and water stable conditions they can grow excessively and form blooms. When the cyanobacterial cells are stressed and damaged, they release metabolites that give water an earthy and musty taste. More importantly, some metabolites have been identified as toxic and pose potential health threats to animals and humans. This study aims to determine the factors that influence the viability of cyanobacteria and its metabolite release during water treatment processes including coagulation, sedimentation, filtration and waste stream processing. This work focuses on the dewatering characterisation of cyanobacteria-rich sludges. Time has been shown to be a critical factor in sludge management. The timescale of cyanobacteria-rich sludges in each processing step can be determined from the dewatering characteristics of the sludges. Models can then be developed to optimise the treatment processes for minimal cyanobacterial metabolite contamination.

The cyanobacterial species of most concern in Australia is *Microcystis aeruginosa*, *Anabaena circinalis* and *Cylindrospermopsis raboriskii*. These three species were cultivated in the laboratory to produce artificial alum sludges that mimic the sludges generated from a typical water treatment plant (WTP) if it were to treat water in the presence of a cyanobacterial bloom. The dewatering characteristics of these sludges were examined and compared with a range of biological and non-biological materials. Cyanobacteria rich alum sludges have demonstrated poor dewaterability. They show low compressibility, similar to WTP sludges. In addition, the sludges show permeability characteristics of typical biological sludges. Such sludges are highly impermeable once reaching a certain solids concentration.

# Poster Index

---

<b>P01</b>	<i>The Newly Designed Surface Force Apparatus for Friction Measurements</i> J. S. Park, S. Ohnishi and R. Horn	page 59
<b>P02</b>	<i>The Nature of Hydrogen Bonding in Molecular Adhesion</i> P. Tayati and T. Senden	page 60
<b>P03</b>	<i>Reliable Measurements of Slip using the AFM</i> C. Neto, L. Zhu and P. Attard	page 61
<b>P04</b>	<i>The Origin of the Contact Electrification of Insulators</i> T. Lee, P. Harrowell, C. Neto	page 62
<b>P05</b>	<i>Dynamics of Liquid-Liquid Displacement on Nanorough Substrates</i> M. Ramiasa, R. Fetzer and J. Ralston	page 63
<b>P06</b>	<i>Drop Wetting on Porous Powder Beds</i> X. Bian, C. Whitby, R. Sedev and J. Ralston	page 64
<b>P07</b>	<i>Capillaries with Chemically Patterned Interior Walls: Fabrication and Applications</i> M. O'Loughlin, C. Priest, M. Popescu, R. Sedev, J. Ralston	page 65
<b>P08</b>	<i>Comparison of Colloidal Lithography Strategies for Fabrication of Two-dimensional Arrays</i> A. Pegalajar Jurado, R. J. Crawford, P. G. Hartley, Ch. D. Easton and S. L. McArthur	page 66
<b>P09</b>	<i>Engineering the Nanostructures and Chemistry of Nanoporous Alumina Membranes for Loading and Release of Poorly Soluble Drugs and Drug Carriers</i> M. S. Aw, S. Simovic, K. Dhiraj, J. Addai-Mensah and D. Losic	page 67
<b>P10</b>	<i>Cyclic Voltammetry of Ferrocene in Ionic liquids</i> V. Vancea, V. Lockett, R. Sedev and J. Ralston	page 68
<b>P11</b>	<i>Alternative Functionalizable Steric Stabilizers for Non-Lamellar Liquid Crystalline Particles</i> J. Y. T. Chong, B. J. Boyd and C. Drummond	page 69
<b>P12</b>	<i>Surprising Particle Stability and Rapid Sedimentation Rates in an Ionic Liquid</i> J. A. Smith, O. Werzer, G. B. Webber, G. G. Warr and R. Atkin	page 70
<b>P13</b>	<i>Preparation of Porous Poly(dimethylsiloxane) (PDMS) Membrane by Polymeric Microemulsion</i> S. Peng, P. Hartley, T. Hughes and Q. Guo	page 71
<b>P14</b>	<i>Nanostructured Nanoparticulate Inorganic Contrast Agents for Medical Imaging</i> N. M. K. Tse, D. F. Kennedy, C. J. Drummond and R. A. Caruso	page 72
<b>P15</b>	<i>Lyotropic Liquid Crystals Responsive to Light Stimuli</i> W. K. Fong, T. Hanley, B. Thierry, N. Kirby and B. J. Boyd	page 73
<b>P16</b>	<i>Investigations of Lipid Exchange between Liquid Crystal Nanostructured Particles and Triglyceride Submicron Emulsions</i> A. Tilley and B. Boyd	page 74
<b>P17</b>	<i>Molecular Dynamics study of Protein Adsorption at Fluid/Solid Interfaces</i> M. Penna and M. J. Biggs	page 75
<b>P18</b>	<i>Effect of Water Temperature on Sphalerite Flotation</i> T. Albrecht, D. Fornasiero and J. Addai-Mensah	page 76

<b>P19</b>	<i>Effect of Water Quality on Copper and Molybdenite Flotation</i> M. Sinche Gonzalez and D. Fornasiero	page 77
<b>P20</b>	<i>Fundamental Study of the Mechanism and Kinetics of Nucleation and Growth of Electrocrystallization of Copper onto Glassy Carbon and Gold Electrodes</i> B. Tadesse, J. Addai-Mensah, D. Fornasiero and J. Ralston	page 78
<b>P21</b>	<i>Measuring the Critical Strain of Flocculated Particulate Networks</i> A. Kumar, A. Kilcullen, J. Foong and P. J. Scales	page 79
<b>P22</b>	<i>Modeling of Dewatering Using the Discrete Element Method (DEM)</i> B. B.G. van Deventer, P. J. Scales and M. Rudman	page 80
<b>P23</b>	<i>Development of a Novel Near Net Shaping Method in Ceramic Processing: Influence of Dispersant Size on Rheology of Non-Aqueous Suspensions</i> S. Tanurdjaja, C. Tallon, P. J. Scales and G. V. Franks	page 81
<b>P24</b>	<i>Synthesis and Characterisation of Oligomeric Surfactants</i> N. M. Baptista and G. G. Warr	page 82

# The Newly Designed Surface Force Apparatus for Friction Measurements

Jin Sung Park, Satomi Ohnishi and Roger Horn

Ian Wark Research Institute, University of South Australia, Mawson Lakes, SA, 5095, Australia

JinSung.Park@postgrads.unisa.edu.au

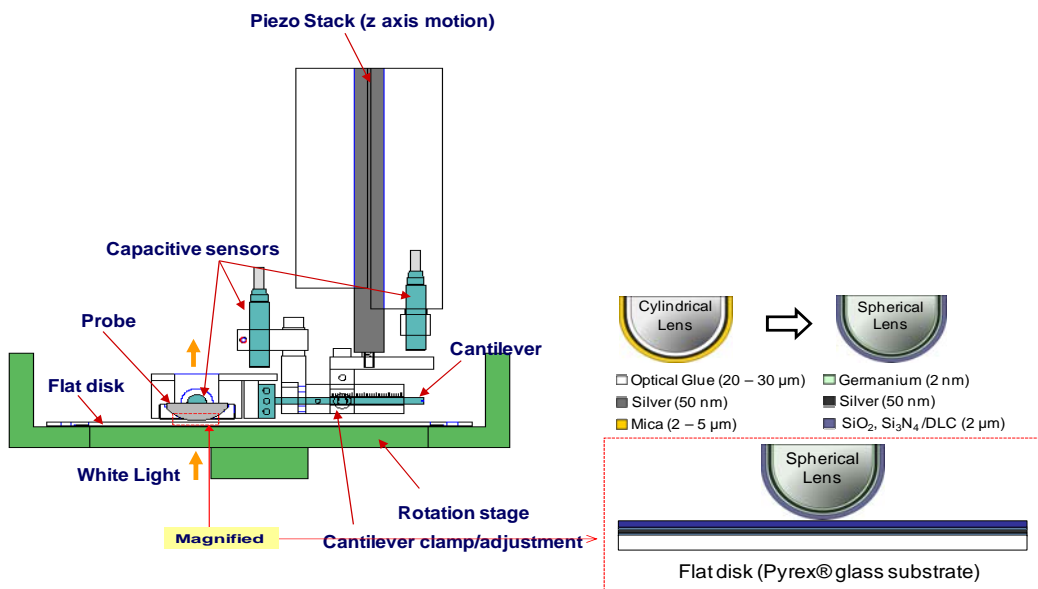
In nanotribology studies there are three main kinds of measurement, namely Surface Force Apparatus (SFA), Atomic Force Microscopy (AFM) and Ball on Disk Tribometry, sometimes utilized with optical interference [1]. In this work, we present an extension of SFA (Fig 1), which allows us to study a variety of materials under conditions closer to practical friction situations. In order to extend versatility beyond the current limitations of SFA, whilst retaining its advantages, we employ ball on disk contact geometry instead of the two cylindrical cross contact geometry used in conventional SFA. Ball on disk contact is particularly useful for thin film studies of elastohydrodynamic lubrication.

The extended SFA has three capacitive sensors. Two capacitive sensors are used for measuring the surface forces and friction force under constant applied load in the normal direction before and after contact, and one more capacitive sensor for feedback control of normal direction motion of a piezoelectric actuator stack. The instrument retains the optical interference method (FECO in reflection) of measuring surface separation and deformation.

With this system, we can use not only mica surfaces (typical substrates for SFA) but also materials applied widely in industry, such as silicon oxide, silicon nitride [2] and diamond-like carbon (DLC). These materials are deposited on spherical lenses and flat glass substrates to configure ball on disk contact. By doing so, the optical adhesive used to glue silvered mica substrates can be eliminated, thus removing the effect of the large deformation of the optical adhesive layer. This is desirable because the large deformation is out of practical friction conditions between two rigid surfaces which are generally used for friction performance.

After completing the construction of this extended SFA, surface, adhesion and friction forces in ball on disk contact between two silicon oxide/nitride/DLC surfaces will be measured as a function of sliding speed, humidity and normal load.

Fig. 1 The schematic of the extended SFA



1. R.P. Glovnea, A.K. Forrest<sup>1</sup>, A.V. Olver<sup>1</sup> and H.A. Spikes. *Tribol. Lett.* **2003**, 217
2. Y. Golan, N.A. Alcantar, T.L. Kuhl, and J. Israelachvili. *Langmuir*, **2000**. 16(17), 6955.

## The Nature of Hydrogen Bonding in Molecular Adhesion

Ponlawat Tayati and Tim Senden

*Department of Applied Mathematics, Research School of Physics and Engineering, The Australian National University, Canberra, ACT, 0200, Australia*

pjt110@physics.anu.edu.au

With the advent of the Atomic Force Microscope (AFM) [1] and the Optical Tweezers (OTs) [2], researchers can readily manipulate molecular systems ranging from motor proteins [3,4] to classical polymer chains [5,6]. Mechanical stretching of single polymer chains has long been the focus of research in many areas including polymer physics, protein energetics and surface chemistry. In the simplest single polymer chain AFM experiment, polymer chains bridging the AFM tip and a surface can be stretched while the force-separation profile is recorded. Depending on the solvency condition, the force-separation profile may be non-linear (in good solvency condition, corresponding to the conformational straightening of the chain) or linear (in poor solvency, corresponding to the removal of the monomers from the adsorbed layer).

In the present study, we use the polymer 'pull-out' AFM experiment to probe the role of surface chemical groups in the adhesion of polymer chains to the surface, especially via hydrogen bonding (H-bonding). With the ability to change the surface as well as varying the surface chemical groups, many combinations are possible. Some preliminary results will be presented.

As well as presenting the polymer-related work outlined above, we will also present a novel technique in (dynamic) atomic force microscopy. Developed within the Department of Applied Mathematics (in conjunction with Department of Physics, ANU), the technique utilises the concept of photon pressure where a modulated laser beam is used to oscillate an AFM cantilever [7]. By monitoring the dynamic deflection signal of the cantilever, the sensitivity of the AFM can be improved by at least ten-fold. Nano-mechanical properties of molecular systems may also be investigated.

1. Bining, G.; Quate, C. F. *Physical Review Letters* **1986**, 56(9), 930–933.
2. Ashkin, A. *Physical Review Letters* **1970**, 24(4), 156–159.
3. Fisher, T. E.; Oberhauser, A. F.; Carrion-Vazquez, M.; Marszalek, P. E.; Fernandez, J. M. *Trends in Biochemical Sciences* **1999**, 24(10), 379–384.
4. Fisher, T. E.; Marszalek, P. E.; Fernandez, J. M. *Nature Structural Biology* **2000**, 7(9), 719–723.
5. Senden, T. J.; di Meglio, J. M.; Auroy, P. *The European Physical Journal B* **1998**, 3, 211–216.
6. Smith, S. B.; Cui, Y.; Bustamante, C. *Science* **1996**, 271(795-798).
7. Tayati, P. *The Application of Photon Pressure in Force Microscopy*. Honours thesis. The Australian National University, **2008**.

## Reliable Measurements of Slip using the AFM

Chiara Neto, Liwen Zhu and Phil Attard

*School of Chemistry, The University of Sydney, NSW, 2006, Australia*

zhu\_l@chem.usyd.edu.au

In macroscopic systems, the traditional assumption of a no-slip boundary condition at the liquid /solid interface provides a good description of liquid flow. However, recent research has shown that under some circumstances interfacial liquid slip can occur. In these cases, the slip boundary condition gives a better description of liquid flow on the microscopic scale, and extent of slip can be quantified using the slip length, the distance within the solid surface at which the liquid velocity becomes zero. The occurrence of interfacial slip is important in confined geometries [1, 2], such as in microfluidic systems.

The slip length measured in a system has been observed to depend on several factors, such as surface properties, liquid viscosity, and shear rate. However, there is no universal agreement on the occurrence of slip and on the factors that most affect it. Inherent characteristics of the employed techniques<sup>3</sup> and the presence of contaminants or nanobubbles have been used to explain the apparent discrepancies in the magnitude of slip.

Here we report a new study on the boundary conditions for flow obtained by measuring hydrodynamic drainage forces using the colloid probe Atomic Force Microscope (AFM). In this work we provide new experimental data and a new theoretical approach to fitting the data (Fig. 1).

On the one hand, we measured hydrodynamic forces using an improved experimental protocol. In earlier work, sucrose aqueous solutions were used as viscous liquids to measure the hydrodynamic force. These liquids are not ideal, because potentially depletion of the sucrose from the solid surface could cause a viscosity gradient between the surface region and the bulk. This could be the cause of the apparent slip length. Here we used a one component liquid with high viscosity (dioctyl phthalate) to measure the hydrodynamic force. We also monitored the temperature of the liquid throughout the experiment *in situ* to get accurate viscosity values. Secondly, we employed a closed loop AFM scanner, which ensures constant drive velocity and reliable tracking of the scanner position.

On the other hand, we developed a new method to simulate the theoretical no-slip and slip hydrodynamic forces to obtain a more accurate slip length. This is an improvement over previous theoretical treatments which employed experimental data, such as the driving rate and the surface separation, to calculate the no-slip and slip hydrodynamic forces, which introduced noise. Here we calculated the theoretical force independently, which allows the no-slip force to be calculated without introducing errors from the experiments, and which allows the slip regime to be unambiguously identified. We included the van der Waals forces in the theory, and for the first time simultaneously fitted both the approach and the retraction force curves, including the adhesion.

We also developed new methods to analyse the experimental data. We corrected the experimental data for laser drift, the drag force on the cantilever, and friction artefacts in the constant compliance region. We took special care to measure the temperature and the spring constant, since the fitted slip lengths are very sensitive to these. We present evidence for contamination by nanoparticles in one case, and show that the force is well-fitted by slip theory with a large apparent slip length if the presence of a particle is overlooked. We suggest that some large slip lengths measured in the past might be due to nanoparticle contamination.

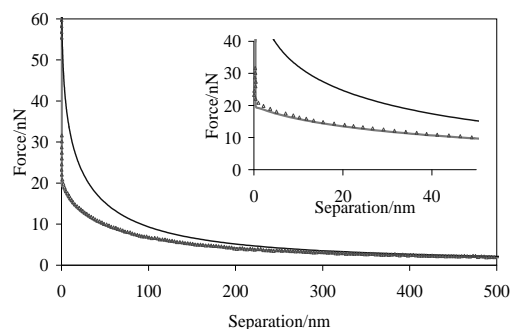


Fig.1: Hydrodynamic force measured in dioctyl phthalate using colloid probe AFM, experimental data (triangles), no-slip theoretical force (blue line), and slip theoretical force (green line). A silicon wafer surface with an OTS coating was used as a substrate. Drive velocity is 19.6  $\mu\text{m/s}$ , the radius of microsphere is 6.9  $\mu\text{m}$ , the viscosity is 61.46 mPas, and the fitted slip length is 29 nm.

1. Neto, C.; Evans, D. R.; Bonaccorso, E.; Butt, H. J.; Craig, V. S. J., *Reports on Progress in Physics* **68**, 2859-2897 (2005).
2. Bonaccorso, E.; Butt, H. J.; Craig, V. S. J., *Physical Review Letters* **90**, 144501-1-144501-4, (2003).
3. Honig, C. D. F.; Ducker, W. A., *Journal of Physical Chemistry C* **112**, 17324-17330, (2008).

## The Origin of the Contact Electrification of Insulators

Thomas Lee, Peter Harrowell and Chiara Neto

*School of Chemistry, The University of Sydney, NSW Australia 2006*

t.lee@chem.usyd.edu.au

The generation of electrostatic charges when two surfaces are rubbed together is known as contact electrification, and was first reported by the ancient Greeks 2500 years ago [1]. In modern times this phenomenon has become important in a range of commercial and industrial processes, including xerography [2], coal processing [3], and drug delivery [4]. Despite this long history and wide application, the mechanism behind contact electrification of insulating materials remains unknown. Even the nature of the charge carriers involved – whether they are ions or electrons – remains a source of controversy [5]. We review the evidence gathered for and against these theories over the past several decades.

Recently, polymer surfaces have been found to initiate electrochemical reduction of species in solution, such as protons and metal cations [6-8]. It has been proposed that this reactivity is linked to the mechanism of insulator contact electrification. We found that the evidence for such a link was lacking, and investigate this further by measuring the effect of depleting a surface of its electrochemical activity on the contact electrification of that surface. We observed that the contact electrification of poly(methyl methacrylate) can be strongly affected by contact with other materials, including Kimwipe® tissue, cotton, and nitrile rubber, as well as chemical treatments such as washing with butylamine and water. With these treatments we were able to alter both the magnitude and sign of the charge generated on PMMA surfaces. We propose that these effects are more consistent with an ion transfer mechanism, compared with the electron transfer alternative.

1. Bailey, A. G., The charging of insulator surfaces. *Journal of Electrostatics* **2001**, 51-52, 82-90.
2. Schein, L. B., Recent advances in our understanding of toner charging. *Journal of Electrostatics* **1999**, 46 (1), 29-36.
3. Dwari, R. K.; Rao, K. H., Fine coal preparation using novel tribo-electrostatic separator. *Minerals Engineering* **2009**, 22 (2), 119-127.
4. Hoe, S.; Traini, D.; Chan, H.-K.; Young, P. M., Measuring charge and mass distributions in dry powder inhalers using the electrical next generation impactor (engi). *European Journal of Pharmaceutical Sciences* **2009**, 38 (2), 88-94.
5. McCarty, L. S.; Winkleman, A.; Whitesides, G. M., Ionic electrets: Electrostatic charging of surfaces by transferring mobile ions upon contact. *Journal of the American Chemical Society* **2007**, 129 (13), 4075-4088.
6. Liu, C.; Bard, A. J., Electrostatic electrochemistry at insulators. *Nature Materials* **2008**, 7 (6), 505-509.
7. Liu, C.; Bard, A. J., Chemical redox reactions induced by cryptoelectrons on a pmma surface. *Journal of the American Chemical Society* **2009**, 131 (18), 6397-6401.
8. Liu, C.; Bard, A. J., Electrons on dielectrics and contact electrification. *Chemical Physics Letters* **2009**, 480 (4-6), 145-156.

## Dynamics of Liquid-Liquid Displacement on Nanorough Substrates

Melanie Ramiasa, Renate Fetzter and John Ralston

Ian Wark Research Institute, University of South Australia, Mawson Lakes, SA, 5095, Australia

Melanie.Ramiasa@postgrads.unisa.edu.au

In many processes of technological interest wetting occurs in systems consisting of two liquids in contact with a solid surface. The latter is likely to be heterogeneous. In light of this, the following study investigates the specific effect of nano-roughness on liquid-liquid displacement dynamics.

The spreading of a dodecane droplet on a range of nano-textured silane coated substrates surrounded by water has been studied experimentally, Fig.1. The capillary driven liquid-liquid displacement is investigated by means of optical high speed video microscopy. The nanorough surfaces are specially designed for the experiment by deposition of spherical silica nanoparticles on a smooth glass slide and followed by a homogeneous silane coating. The topographic profile of the surfaces can be modified in a controlled fashion by varying the nanoparticle diameters and lateral densities on the substrate, Fig.2. New insights into the impact of substrate roughness on contact line dynamics in liquid-liquid systems are provided.

Independent of substrate chemistry and topography, the spreading data exhibit two distinct velocity regimes, characterised by qualitatively different dynamics. Hydrodynamic models [1] apply to the fast stage of initial spreading; assuming that viscous shear is the only significant source of dissipation, while the molecular kinetic theory [2], based on non-hydrodynamic dissipation sources captures the dynamics in a final stage at low speed. However, the value of the parameters obtained when fitting the experimental results with the theoretical models display some unexpected discrepancies and do not show a systematic dependence on substrate wettability or roughness. This result is discussed in relation to additional effects such as inertia and local contact line pinning [3]. For both velocity regimes, the relevance and interdependency of the microscopic parameters introduced by the theoretical models seems deeply altered when dealing with liquid-liquid systems. Further investigations are ongoing in order to clarify these open questions.

Fig.1

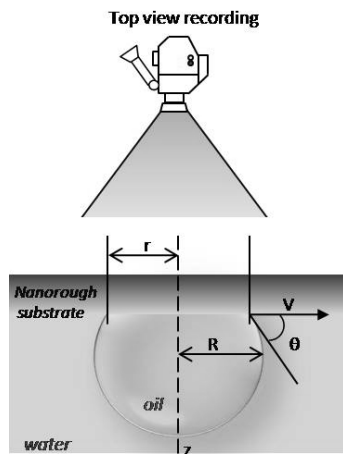
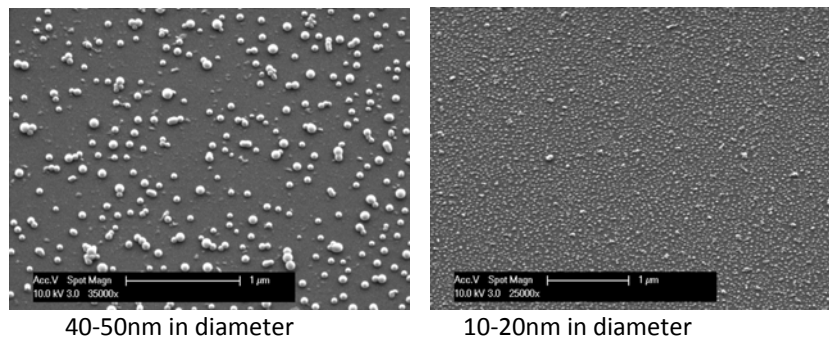


Fig.2: SEM images of silica nanoparticles deposited on smooth glass



1. Cox, R.G., *J. Fluid Mech*, **1986**, 168, 169
2. Blake, T.D.; Haynes, J.M. *J. Colloid Interface Sci.* **1969**, 30, 421
3. Fetzter, R.; Ramiasa, M.; Ralston, J. *Langmuir* **2009**, 25(14), 8069

## Drop Wetting on Porous Powder Beds

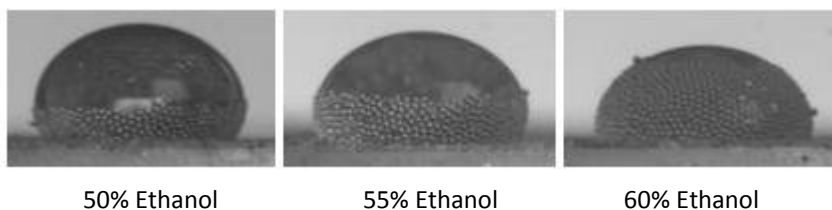
Xun Bian, Catherine Whitby, Rossen Sedev and John Ralston

*Ian Wark Research Institute, University of South Australia, Mawson Lakes, SA, 5095, Australia*

Xun.Bian@postgrads.unisa.edu.au

The wetting behavior of drops of aqueous solutions of ethanol on a bed of hydrophobic particles has been investigated. Glass spheres (90-106  $\mu\text{m}$  in diameter) coated with trichloro (1H, 1H, 2H, 2H-perfluorooctyl) silane were used as the model particles. The packed particle bed was 25 mm in diameter and 11 mm in height. The aqueous solutions were prepared at ethanol concentrations ranging from 50 to 100 vol%, corresponding to surface tensions from 29.4 to 22.4  $\text{mNm}^{-1}$ . Drops of ethanol-water solutions (10  $\mu\text{L}$  in volume) were placed on the particle bed and the drop wetting behaviour recorded using a video camera.

At ethanol concentrations from 70 to 100 vol%, the drops penetrate the powder bed within one second. For ethanol concentrations of 50 to 60 vol%, the drops remain on the porous surface. Particles spontaneously spread over the drop surface, coating the drops as shown in the figure below. At 65 vol% ethanol, the particles fully cover the droplet surface. After the coating is complete, the liquid starts to slowly penetrate into the particle bed. Penetration takes more than 5 minutes. The effect of the drop surface tension on the rate at which the powder coats the drop surface has been studied.



## Capillaries with Chemically Patterned Interior Walls: Fabrication and Applications

Muireann O'Loughlin, Craig Priest, Mihail Popescu, Rossen Sedev and John Ralston

*Ian Wark Research Institute, University of South Australia, Mawson Lakes SA 5095, Australia.*

Muireann.O'Loughlin@postgrads.unisa.edu.au

Chemically engineering and tuning the surface wettability by hydrophobic/hydrophilic patterning is of great importance in microfluidic systems. In particular, localised hydrophilic/hydrophobic patterns can be used to stabilize liquid flow or to encourage droplet formation in microfluidic devices. While patterning methods are currently available for modifying open channels, chemical patterning *inside* closed channels remains a significant challenge.

We have developed a method to chemically pattern and, therefore, tune surface wettability inside capillaries and closed channels using the photocatalytic properties of titania nanoparticles. The internal surface of the capillary was coated with titanium dioxide and a self-assembled monolayer of octadecyltrihydrosilane (OTHS) to make the surface hydrophobic. Through the photocatalytic decomposition of the OTHS monolayer (by the titania layer) and photomasking techniques, we have patterned the internal surface of capillaries and achieved the creation of geometrically well defined regions with a controlled hydrophilic character.

As a first application, we have engineered capillary tubes with distinct wetting properties in ring-like regions. Using the Wilhelmy balance technique we have measured the dynamics of capillary rise in these chemically patterned capillaries, which allowed us to investigate the influence of designed surface wettability on the characteristics of the liquid flow.

## Comparison of Colloidal Lithography Strategies for Fabrication of Two-dimensional Arrays

Adoracion Pegalajar Jurado<sup>1</sup>, Russell J Crawford<sup>2</sup>, Patrick G Hartley<sup>3</sup>, Christopher D Easton<sup>1</sup> and Sally L McArthur<sup>1</sup>

<sup>1</sup>*Faculty of Engineering and Industrial Sciences, Swinburne University of Technology, Hawthorn, Victoria 3122, Australia.*

<sup>2</sup>*Faculty of Life and Social Sciences, Swinburne University of Technology, Hawthorn, Victoria 3122, Australia.*

<sup>3</sup>*CSIRO Molecular and Health Technologies, Clayton, Victoria 3168, Australia.*

djurado@swin.edu.au

A variety of lithography and nano-fabrication techniques have been used to create nano-scaled patterned surfaces for use in a number of applications including biosensors, low dimensional electronics and nanofluidic devices. Among these techniques, colloidal lithography has emerged as a possible alternative route to replace complex and high-cost techniques.

Colloidal lithography can produce surfaces with regular, well-defined nanotopography along the three axes (i.e. x, y, and z), and can be applied to relatively large surface areas. It provides many advantages when compared to alternative techniques, as it is a quick, low-cost, reproducible method for fabricating nano-scaled patterned surfaces. The colloidal particles are arranged into well ordered structures through a self-assembly process. These well ordered structures are commonly used as a mask for etching or sputtering processes.

Two-dimensional colloid arrays can be constructed using different approaches, ranging from drop-coating, dip-coating, spin-coating, drip-drawing and tiled-drain. This work presents a critical review of the different strategies for fabricating two-dimensional arrays using polystyrene nanoparticles. Criteria relating to defect to surface area ratio, surface coverage and number and complexity of fabrication steps will be used to compare these techniques.

*Keywords: colloidal lithography, nanotopography, colloidal particles*

## Engineering the Nanostructures and Chemistry of Nanoporous Alumina Membranes for Loading and Release of Poorly Soluble Drugs and Drug Carriers

Moom Sinn Aw, Spomenka Simovic, Kumar Dhiraj, Jonas Addai-Mensah and Dusan Losic

*University of South Australia, Ian Wark Research Institute,  
Mawson Lakes Campus, Mawson Lakes, SA 5095*

Moomsinn.Aw@postgrads.unisa.edu.au

A range of nano-scale materials have been explored in the past few years to address problems associated with conventional drug therapies, such as limited drug solubility, poor biodistribution, lack of selectivity and unfavourable pharmacokinetics. Among them, nanoporous anodized alumina oxide (AAO) prepared by electrochemical anodization with ordered and controlled pore structures (10-400 nm), high surface area to volume ratio, biocompatibility, have attracted substantial attention, particularly for implantable drug delivery systems [1-3]. In this work we present drug loading and release studies of AAO nanoporous platform for delivery of drugs and drug carriers with a particular focus on the influence of nanopore structure and surface chemistry. Nanoporous AAO with pore diameters ranging from 60 nm to 150 nm and thickness of 20  $\mu\text{m}$  were prepared by electrochemical anodisation aluminium foils using two steps anodisation process in oxalic acid (0.3 M) [4]. Several surface chemistry within the pores were generated, namely, oxidation by hydrogen peroxide, silanisation using hydrophilic (3-aminopropylethoxy silane, APTES) and hydrophobic (penta-fluorophenylpropyl dimethyl chloro silane, PFPTES) silane. Indomethacin, an anti-inflammatory drug, was used as a model of poorly soluble drug [5]. Three types of polymeric micelles (TPGS, Pluronic F127 and PEO-PPO-PEO) which are nanoscopic co-polymeric structures with hydrophobic cores are selected as drug carriers with size between 20 to 80 nm. Loading of the drug and drug carriers into AAO was confirmed by TGA analysis and the release rates were characterized by observation of the appearance of the drug in solution by UV-vis absorption spectroscopy. Similar to other nanoporous platforms, the AAO showed characteristic release pattern which consists an initial burst release for about the first 30 minutes followed by sustained a slow release over 5 days. In case of indomethacin drug (small molecule) we could not observe considerable impact of pore diameters (60 -150 nm) on release kinetics. Contrarily in case of drug carriers (micelles) regarding their considerable large size, the release behaviour was significantly influenced by the pore diameters of AAO. The importance of surface chemistry and interfacial properties of pores for drug release characteristic was demonstrated for both drug (indomethacin) and series of micelles. Drug release was faster from PFPTES modified AAO than the one modified with APTES which is explained by interaction of drug with hydrophobic properties and pore modified with APTES with hydrophilic properties which lowered the release rate.

1. A. S. Hoffman, *J. Controlled Rel.*, 2008, vol. 132, p. 153.
2. D. Losic, S. Simovic, *Expert Opin. Drug Deliv.*, 2009, DOI: 10.1517/17425240903300857.
3. G. Geneviève et al., *J. Controll. Rel.*, 2005, vol. 109, 169–188.
4. D. Losic, M. Lillo and D. Losic, Jr., *Small*, 2009, vol. 5, p.1392.
5. A. M. Md. Jani, E. J. Anglin, S. J. P. McInnes, D. Losic, J. G. Shapter, N. H. Voelcker, *Chem Commun*, 2009, 3062.

## Cyclic Voltammetry of Ferrocene in Ionic liquids

Valentin Vancea, Vera Lockett, Rossen Sedev and John Ralston

*Ian Wark Research Institute, University of South Australia, Mawson Lakes Campus, South Australia 5095, Australia*

vanvy007@students.unisa.edu.au

There is an increased interest in ionic liquids, substances that can potentially replace aqueous solutions in many industrial processes. In order to develop a better understanding of these solutions, their electrokinetic properties have to be understood.

The electrochemical behaviour of ferrocene in [C<sub>4</sub>mpyr][NTf<sub>2</sub>] (Merck high purity) is investigated using cyclic voltammetry and chrono-amperometry on gold electrode. The ionic liquid is purified using adsorption with high purity charcoal, extraction with high purity water and evaporation under vacuum. The electrode is polished with alumina, and then sonicated for 30 minutes in water. The solution is purged with high purity nitrogen for 30 minutes before experiment and blanketed during the experiment.

To investigate the effect of viscosity on the diffusion coefficient, these results will be compared with others obtained from experiments done in non-aqueous substances of similar viscosity. Because of ionic liquids different molecular structure, it is important to know if there are other properties than viscosity that could influence their diffusion coefficients.

## Alternative Functionalizable Steric Stabilizers for Non-Lamellar Liquid Crystalline Particles

Josephine Y.T. Chong<sup>1,2</sup>, Ben J. Boyd<sup>1</sup> and Calum Drummond<sup>2</sup>

<sup>1</sup>*Drug Delivery, Disposition and Dynamics, Monash Institute of Pharmaceutical Sciences, Monash University, Parkville, VIC, 3052, Australia*

<sup>2</sup>*CSIRO Materials Science and Engineering, Clayton, VIC, 3168, Australia*

josephine.chong@csiro.au

Stabilizers have an essential role in colloidal drug delivery systems (DDS) providing a steric barrier between particles, preventing flocculation and aggregation initiated by van der Waals forces. The stabilizer also plays an important role where targeting of the carrier to specific tissues is required – the stabilizer helps to avoid recognition of the particles by opsonin proteins *in vivo*, allowing them to circulate through the bloodstream for extended periods of time, and ‘home’ in on particular tissue types. Several nano-particle DDS, such as liposomes, polymeric micelles and micro-emulsions, have utilized stabilizers in their design and composition.

Non-lamellar liquid crystalline particles (i.e. cubosome and hexosomes) are receiving particular attention as potential DDS to encapsulate either hydrophilic or hydrophobic therapeutic agents. It is apparent that although the internal mesophase of liquid crystalline particles is thermodynamically stable and is often identical to that of the bulk non dispersed phase, the dispersions are inherently colloidally unstable [1]. As such, preparation of liquid crystalline particles for research includes the incorporation of steric stabilizers, mainly Pluronic® 127.

Pluronic® 127 or Poloxamer 407 is a synthetic tri-block copolymer consisting of hydrophilic ethylene oxide (EO) and hydrophobic propylene oxide (PO) blocks arranged in a basic A–B–A structure: PEO–PPO–PEO. Poly(ethylene oxide), also known as poly(ethylene glycol) or PEG has the ability to provide stealth to a DDS, significantly prolonging the circulation of nano-particles *in vivo* [2]. However this is a passive targeting system with no distinction between healthy and damaged tissue [3]. The ability to target specific cells (i.e. tumour cells) is the next stage forward to enhancing DDS. Functionalizing PEG to allow ligand coupling is challenging as they do not possess reactive groups in their structure [4]. Other disadvantages of using Pluronic® F127 is that it is non-biodegradable [5,6] and there is currently an investigation suggesting it may have poor particle affinity and poor surface residence, resulting in a very small fraction actually contributing to stabilization [7].

There have only been a limited amount of investigations on alternate stabilizers for these types of particles. Consequently, this study seeks to (i) understand the structural requirements to provide effective steric stabilizers for liquid crystalline particles using cubosomes as a model structure, while providing a ‘handle’ with which to functionalise the particles and (ii) develop novel stabilizers with the capability of targeting particular cell types, using a HER2 antibody as a model targeting moiety.

This study will use two approaches to identify appropriate stabilizers for the liquid crystal particles with the essential features of imparting steric stabilization, stealth behaviour and functionalization. Firstly, existing stabilizers will be investigated. Second, novel alternative stabilizers will be prepared using RAFT [8], to permit structure-property relationships to be developed to optimize the mentioned attributes. Properties of particles that will be used to determine candidate stabilizers include; size distribution and morphology (by DLS and cryo-TEM, see Fig. 1), internal liquid crystal phase structure (using small angle x-ray scattering), chemical stability, adsorption isotherms (by observing protein binding, using biological screening), circulation time *in vivo*, and targeting efficiency in cell culture and *in vivo*.

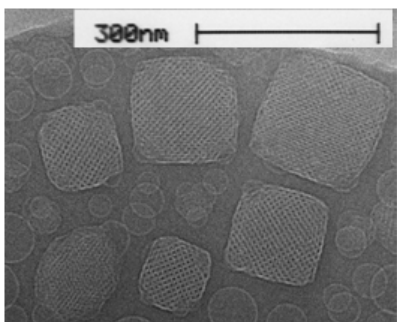


Fig. 1: Example of a Cryo-TEM image of phytantriol cubosomes [1]

1. Boyd, B.J. , Y.-D. Dong, and T. Rades. *Journal of Liposome Research*, **2009**, 19(1),12.
2. Gref, R., *et al. Science*, **1994**, 263(5153), 1600.
3. Moghimi, S.M., A.C. Hunter, and J.C. Murray. *Pharmacological Reviews*, **2001**, 53(2), 283.
4. Gref, R., J. Rodrigues, and P. Couvreur. *Macromolecules*, **2002**, 35(27), 9861.
5. Jeong, B., *et al. Nature*, **1997**, 388(6645), 860.
6. Y. Cha, Y.K Choi, Y.H Bae, 1997. US Patent 5 702 717.
7. Tilley, A.J., Boyd, B.J. PhD study, unpublished.
8. Rizzardo, E., *et al. Macromolecule Symposium*, **2001**, 174, 209.

## Surprising Particle Stability and Rapid Sedimentation Rates in an Ionic Liquid

Jacob A. Smith<sup>1</sup>, Oliver Werzer<sup>1</sup>, Grant B. Webber<sup>2</sup>, Gregory G. Warr<sup>3</sup> and Rob Atkin<sup>1</sup>

<sup>1</sup> *Centre for Organic Electronics, The University of Newcastle, Callaghan, NSW 2308, Australia*

<sup>2</sup> *Centre for Advanced Particle Processing, The University of Newcastle, Callaghan, NSW 2308, Australia*

<sup>3</sup> *School of Chemistry, The University of Sydney, NSW, 2006, Australia*

Jacob.A.Smith@studentmail.newcastle.edu.au

Recent work has demonstrated that particle suspensions in room temperature ionic liquids differ from aqueous suspensions in some surprising and remarkable ways. Two results are of key importance. Firstly, suspensions of 1  $\mu\text{m}$  diameter silica spheres do not aggregate in pure ethylammonium nitrate (EAN) despite interparticle electrostatic repulsions being completely screened by its 11M ionic strength. However these dispersions become unstable in the presence of small amounts of water. Using silica colloid probe atomic force microscopy (AFM), optical microscopy and dynamic light scattering we show that this unusual stability is imparted by repulsions between well formed solvation layers, which decreases in number and strength upon addition of water. Secondly, particle suspensions in pure EAN settle six times more rapidly than predicted by the hindered Stokes equation. This remarkable result is unprecedented to our knowledge, and could foreshadow interesting lubrication effects for surfaces in EAN.

## Preparation of Porous Poly(dimethylsiloxane) (PDMS) Membrane by Polymeric Microemulsion

Shuhua Peng<sup>1,2</sup>, Patrick Hartley<sup>1</sup>, Tim Hughes<sup>1</sup> and Qipeng Guo<sup>2</sup>

<sup>1</sup>CSIRO Molecular and Health Technologies, Bayview Avenue, Clayton South, Victoria 3169, Australia

<sup>2</sup>Centre for Material and Fibre Innovation, Deakin University, Geelong, Victoria 3217, Australia

[Shuhua.Peng@csiro.au](mailto:Shuhua.Peng@csiro.au)

Poly(dimethylsiloxane) (PDMS) has numerous applications owing to its specific properties: super hydrophobicity, high optical transparency, biocompatibility, high thermal resistance, and high permeability toward gases [1-3]. These properties have promoted a variety of applications such as long-term delivery of drugs [4], dense membrane processes for volatile organic compound removal [5], water repellent coatings [6], electrical insulation, and so forth. In those applications, porous PDMS materials are of interesting for tuning physical properties, increasing interfacial area, and enhancing internal transfer [7].

PDMS can be prepared via the polymerization or crosslinking of various siloxane monomers. There are also several ways to prepare porous PDMS materials. PDMS vulcanizate having pores formed by hydrogen foams during hydrosilylation cure has been developed by Kobayashi [8]. Apart from that, some other methods relevant to the production of porous PDMS matrices include *in situ* hydrogen bubble generation by a hydrosilylation reaction [9], vacuum drying of dispersed water droplets from a water in PDMS emulsion [10], and solvent curing induced demixing [11] and so on.

However, reports on the preparation of porous PDMS matrix are still limited and control over the porous structure of PDMS is not satisfactory. Based on the above consideration, this work attempts to generate porous PDMS membranes from a siloxane based microemulsion system consisting of polymeric siloxanes, water and surfactant. The microemulsion was characterized using small angle X-ray scattering, rheological and conductivity measurement. The relationship between microemulsion structure and PDMS morphology was also investigated.

Polymeric siloxanes were produced as the basis of the oil phase in a microemulsion system. Figure 1 shows the synthesis route of a siloxane macromonomer from monomer D4 and it was characterized by NMR. The obtained methacrylate-terminated PDMS can be self-cured without an external crosslinking agent. As for the surfactant, teric G9A8 was selected for stabilizing the microemulsion with isopropanol as co-surfactant.

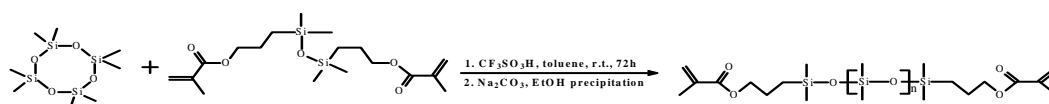


Fig. 1

Synthesis of methacrylate-terminated PDMS

1. Noll, W. Chemistry and Technology of Silicones; Academic: New York, 1968.
2. Whitesides, G. M. Nature 2006, 442, 368.
3. El-Ali, J.; Sorger, P. K.; Jensen, K. F. Nature 2006, 442, 403.
4. McGinity, J. W.; Hunke, L. A.; Combs, A. B. J Pharm Sci 1979, 68, 662.
5. Paul, D. R., Yampol'skii, Y. P., Eds.; CRC Press: Boca Raton, FL, 1994.
6. Eckberg, R. P.; Lake, P. U.S. Pat. 4, 256, 870, 1981.
7. Dufaud, O.; Favre, E.; Sadtler, V. J Appl Polym Sci, 2002, 83, 967.
8. Kobayashi, T.; Saitoh, H.; Fujii, N. J Appl Polym Sci, 1994, 51, 483.
9. Kobayashi, T.; Saitoh, H.; Fujii, N.; Hoshino, Y.; Takanashi, M. J Appl Polym Sci 1993, 50, 971.
10. Martina, A. D.; Kiefer, J.; Hilborn, J. G.; Hedrick, J. L.; Miller, R. D. ACS Symp Ser 1997, 575, 320.
11. Kiefer, J.; Hilborn, J. G.; Hedrick, J. L. Polymer 1996, 37, 5715.

## Nanostructured Nanoparticulate Inorganic Contrast Agents for Medical Imaging

Nicholas M.K. Tse<sup>1,2</sup>, Danielle F. Kennedy<sup>2</sup>, Calum J. Drummond<sup>2,3</sup> and Rachel A. Caruso<sup>1,3</sup>

<sup>1</sup>PFPC, School of Chemistry, The University of Melbourne, Parkville VIC 3010, Australia

<sup>2</sup>CSIRO Molecular and Health Technologies – Clayton, Clayton VIC 3168, Australia

<sup>3</sup>CSIRO Materials Science and Engineering – Clayton, Clayton VIC 3168, Australia

nicholas.tse@csiro.au

Magnetic resonance imaging (MRI) is routinely used as a medical diagnostic technique and it is becoming an integral part of preventative healthcare of the 21st century. Despite the use of non-ionizing radiation for image acquisition and high spatial resolution, in the micrometer range [1], the lack of contrast makes differentiation of biological environments difficult [2]. Contrast agents (CA) are therefore routinely administered to enhance the radio signals in MR images. The two types of CA are in the form of paramagnetic materials and ferromagnetic materials. The former is known as a longitudinal relaxation ( $T_1$ ) enhancing CA where as the latter is the transverse relaxation ( $T_2$ ) enhancing CA [3].

Currently all commercial  $T_1$  CA are in the form of a metellochelate complex, problems associated with this includes the inability to provide a high enough local concentration to greatly enhance medical images, this is especially true when monitoring molecular activities in techniques such as functional MRI (fMRI). Strategies undertaken to improve relaxivity include added bioselectivity, an increase in water exchanges and an increase hosting of paramagnetic species per molecule [4]. Nanoparticulate CAs have been shown to satisfy these requirements, and recent reviews by Na *et al.* provide a great overview in this area of research [5, 6].

Lin *et al.* demonstrated an inorganic nanostructured nanoparticulate  $T_1$  CA. Mesoporous gadolinium silicate was synthesised, and up to 6.8 wt% of gadolinium was successfully incorporated in the biocompatible silica matrix. The combination of porosity and high paramagnetic species in the particle was shown to have a 6 fold increase in  $T_1$  relaxation time when compared to the commercial product Magnevist®.

In this study, the effect of varying pore sizes, shapes and pore hierarchy will be correlated to the relaxivity measurements. Colloidal silica with different amounts of gadolinium doping will be synthesised *via* various acid-catalysed hydrolysis-condensation approaches. Samples will then be characterised to determine corresponding parameters that are most effective in making an inorganic CA.

1. Jacques, V.; Desreux, J. F., "New Classes of MRI Contrast Agents," *Top. Curr. Chem.*, 2002, 221, pp. 123-164.
2. Lauffer, R. B., "Paramagnetic metal complexes as water proton relaxation agents for NMR imaging: theory and design," *Chem. Rev.* 1987, 87, (5), pp. 901-927.
3. Pankhurst, Q. A.; Connolly, J.; Jones, S. K.; Dobson, J., "Applications of magnetic nanoparticles in biomedicine," *J. Phys. Appl. Phys.*, 2003, 36, (13), pp. 167-181.
4. Caravan, P., "Strategies for increasing the sensitivity of gadolinium based MRI contrast agents," *Chem. Soc. Rev.* 2006, 35, (6), pp. 512-523.
5. Na, H. B.; Hyeon, T., "Nanostructured T1 MRI contrast agents," *J. Mater. Chem.*, 2009, 19, (35), pp. 6233-6428.
6. Na, H. B.; Song, I. C.; Hyeon, T., "Inorganic Nanoparticles for MRI Contrast Agents," *Adv. Mater.*, 2009, 21, (21), pp. 2133-2148.

## Lyotropic Liquid Crystals Responsive to Light Stimuli

Wye Khay Fong<sup>1</sup>, Tracey Hanley<sup>2</sup>, Benjamin Thierry<sup>3</sup>, Nigel Kirby<sup>4</sup> and Ben J. Boyd<sup>1</sup>

<sup>1</sup>*Drug Delivery, Disposition and Dynamics, Monash Institute of Pharmaceutical Sciences, Monash University (Parkville Campus), Parkville, VIC, 3052, Australia.*

<sup>2</sup>*Bragg Institute, Australian Nuclear Science and Technology Organisation*

<sup>3</sup>*Ian Wark Research Institute, University of South Australia, Mawson Lakes Campus, South Australia 5095, Australia*

<sup>4</sup>*SAXS/WAXS Beamline, Australian Synchrotron*

Wye.Fong@pharm.monash.edu.au

Stimuli responsive systems have the potential to improve drug delivery by providing pulsatile active release 'on demand'. The ability to control when and where the drug releases allows for greater control over the efficacy of the therapy by e.g. maximising longevity in the body and/or minimising toxicity issues associated with concentrated doses of some therapeutics.

Lipid-based liquid crystal systems (LLCs) are ideal for triggered release as they are biocompatible, can provide sustained delivery of a wide range of drug molecules [1] and have thermodynamically stable nanostructures which determine drug release rate [2]. Using SAXS, we have previously shown that reversible control over the nanostructure and drug release rates of modified bulk GMO and phytantriol liquid crystal systems is possible through the use of temperature change *in vitro* and *in vivo* [3], by 'switching' between bicontinuous cubic and reversed hexagonal phases. However, for some applications such as ocular drug delivery, direct application of heat is not practical and using a different stimulus, such as light would be a preferable trigger for drug release.

To address these issues, we have taken two approaches to facilitate external activation of changes in lipid packing and hence induce phase changes and drug release, namely incorporation of photochromic dyes and hydrophobic gold nanorods. We have prepared LLCs containing varying concentration of the photo-sensitive additives and irradiated while following evolution of nanostructure using SAXS. Preliminary results indicate a shift in nanostructure of the systems anticipated from 1) the influence of the photoisomerisation of the photochromics on the packing geometry of the materials and 2) the photothermal activation of gold nanorods causing thermotropic phase changes in the LLCs.

1. Clogston J, Caffrey M. Controlling release from the lipidic cubic phase. Amino acids, peptides, proteins and nucleic acids. *J Controlled Release* 2005;107(1):97-111.
2. Lee KWY, Nguyen T-H, Hanley T, Boyd BJ. Nanostructure of liquid crystalline matrix determines *in vitro* sustained release and *in vivo* oral absorption kinetics for hydrophilic model drugs. *Int J Pharm* 2009;365(1-2):190-9.
3. Fong W-K, Hanley T, Boyd BJ. Stimuli responsive liquid crystals provide 'on-demand' drug delivery *in vitro* and *in vivo*. *J Controlled Release* 2009;135(3):218-26.

## Investigations of Lipid Exchange between Liquid Crystal Nanostructured Particles and Triglyceride Submicron Emulsions

Adam Tilley and Ben Boyd

*Faculty of Pharmacy and Pharmaceutical Sciences, Monash University, 381 Royal Pde, Parkville, VIC, 3052*

Adam.Tilley@pharm.monash.edu.au

Liquid crystal nanostructured particles (LCNP) have been shown to provide properties that are advantageous for delivery of pharmaceutical and agricultural active ingredients. The amphiphilic nature of these self-assembled lipid systems allow both hydrophilic and hydrophobic drug incorporation and their internal nanostructure has been shown to provide controlled release of active ingredients. However this internal nanostructure can be lost when molecules become incorporated with it, therefore causing a loss in the controlled release properties of the LCNP. Such molecules include lipids found on surfaces to which these particles may adsorb, such as the skin or the wax layer of a leaf. We investigated the exchange of lipidic materials between LCNP and triglyceride submicron emulsions (TSEs) to better understand this phenomenon.

Liquid crystal nanoparticles were made by dispersing 10% w/v phytantriol in solutions of the steric stabiliser Pluronic F127 giving bicontinuous cubic phase ( $v_2$ ) LCNP known as cubosomes. at F127 was present at concentrations of 10, 20 and 30% w/v; importantly we know from previous studies that the cubic phase structure is independent of stabilizer concentration with F127 in this range, providing an identical starting point from an internal phase structure perspective. These coarse dispersions were then ultrasonicated to give particles of approximately 200 nm in diameter. The triglyceride submicron emulsions were prepared via the same procedure, with the lipid and 20% w/v F127 solution being heated to 85°C prior to ultrasonication. The triglycerides used were tristearin (C18), trilaurin (C12) and tricaprylin (C8). A vitamin E acetate emulsion was also prepared and used as a control, as the phytantriol/vitamin E acetate phase behaviour is already well known, hence the liquid crystalline structure of the particles could be interpreted in terms of composition. Synchrotron small angle x-ray scattering (SAXS) was then used to follow the kinetics of evolution of the liquid crystal phase of the LCNP upon addition of the TSEs on the assumption that lipid transfer between particles will alter the liquid crystalline nanostructure of the particles. This was done by circulating 1.5 ml of the LCNP through a flow-through capillary in the SAXS/WAXS beamline at the Australian Synchrotron, and remotely mixing 0.5 ml TSE into the LCNP dispersion while acquiring scattering patterns for 1 sec every 20 seconds.

Tristearin TSE caused no change to the  $v_2$  phase structure of the LCNP, suggesting that there was no exchange of lipid occurring. However trilaurin and tricaprylin both induced a complete loss of  $v_2$  phase structure in the LCNP over time. Interestingly trilaurin induced a more rapid loss of  $v_2$  structure than tricaprylin despite its longer chain length.

Increasing the concentration of F127 increased the rate of disappearance of the  $v_2$  phase, consistent with the hypothesis that F127 micelles act as a reservoir during lipid transfer between TSE and LCNP particles.

This study has provided an insight into the lipid exchange between LCNP and TSEs, with the size of the lipid and the amount of F127 found to be influencing factors on the rate of lipid exchange. Further work is required to gain a better understanding of these factors, including if they have the same influence when the triglycerides are presented as a layer as would be the case during application.

## Molecular Dynamics study of Protein Adsorption at Fluid/Solid Interfaces

Matthew Penna and Mark J. Biggs\*

*School of Chemical Engineering Engineering North Building, The University of Adelaide, Adelaide 5005.*

matthew.penna@adelaide.edu.au and \*mark.biggs@adelaide.edu.au

Protein adsorption is of relevance in a number of diverse fields. Examples included the response of the body to foreign materials (e.g. prostheses or nanoparticles), controlled cell deposition in tissue scaffolds, heat exchanger fouling and bone growth. One application of particular interest here is the use of designed synthetic peptides for the self-assembly of nanoscale entities such as nanotubes and nanoparticles to form complex nanostructured materials and systems; materials and systems that could be assembled in this way include complex functional nanoporous solids and nanoelectronic devices.

Peptides that have varying degrees of binding affinity and selectivity for range of inorganic solid materials of interest for nanotechnology (e.g. platinum, gold, graphitic carbon), have been identified experimentally by a number of groups around the World. Due to the inability of current experimental techniques to probe peptide/solid surface systems on a molecular level, fundamental understanding of the adsorption of these peptides is limited, however. Molecular simulation provides an alternate avenue for investigating the adsorption process which can be used in conjunction with experimental results to gain a greater understanding of the underlying physics of adsorption.

We are developing the application of molecular dynamics simulation to elucidate the fundamentals of adsorption of peptides at fluid/solid interfaces and design of peptides that recognise particular inorganic surfaces and entities. In this poster, we will present preliminary work on the study of the adsorption behaviour of experimentally-identified binding peptides on a platinum surface. The conformation of the peptide at the surface and the impact of the ordered water layers at the platinum surface on adsorption will be presented. In addition to investigating the nature of adsorption in a qualitative way, a comparison between the predicted and experimentally determined adsorption free energies and relative selectivities of different peptides for the platinum surface will be presented.

## Effect of Water Temperature on Sphalerite Flotation

Trent Albrecht, Daniel Fornasiero and Jonas Addai-Mensah.

*Ian Wark Research Institute, University of South Australia, Mawson Lakes Campus, South Australia 5095, Australia*

Albty001@students.unisa.edu.au

Water is a vital part of the mining and mineral processing industry. The issue of water and its importance in mineral processing is becoming more and more a hot topic, due to increased water scarcity and the demand for mining companies to manage their water use more attentively [1,2]. The proposed research project will investigate the effect of pulp temperature on sphalerite flotation. The research was conducted using a series of chemical and surface analysis techniques as well as laboratory flotation tests.

Preliminary results have shown that flotation of copper-activated sphalerite at pH 10.5 was much reduced when temperature was below 12°C in agreement with observation at Bolindén plants (Sweden) that zinc recoveries are lower in winter than in summer. It was also found that zinc hydroxide and copper hydroxide precipitation in solution increased with temperature, which may affect sphalerite depression in the copper/lead circuit and activation in the zinc circuit, respectively in alkaline pH conditions. Furthermore, it was observed that more zinc hydroxide formed at the sphalerite surface with an increase in temperature. It is possible that a high temperature may promote the exchange at the sphalerite surface of zinc by copper and therefore copper-activation of sphalerite.

Recent and current events of droughts and water shortages have demanded that the way water is used and utilised by large industries be scrutinised and tougher regulations imposed on water management. The current pressures on water supply are anticipated to increase in the future. Thus water availability and cost are likely to drive changes in water consumption within the minerals industry [3]. A “fit for purpose” water strategy should be adopted by mining, mineral processing and metal production operations [3]. The proposed research project will endeavour to increase our understanding on how water quality affects mineral separation processes. This will help operators to minimise adverse effects while maintaining the best utilisation of available water as a valuable resource [4].

1. Rao, S.R. and Finch, J.A., (1989). A review of water re-use in flotation. *Minerals Engineering*, 2, 65-85.
2. Hoover, M.R., (1980). Water chemistry effects in the flotation of sulphide ores – a review and discussion for molybdenite. In *Complex Sulphide Ores* (M.L. Jones, Ed.). Inst. of Mining and Metal., London, pp. 100-112.
3. Norgate, T.E. and Lovel, L.L., 2004, 'Water Use in Metal Production: A Life Cycle Perspective'. CSIRO Minerals, Report DMR-2505.
4. Schumann, R., Levay, G. and Dunne, R., 2002, 'Process Water Chemistry Influences in Base Metal Sulphide Flotation'. Ian Wark Research Institute, University of South Australia.

## Effect of Water Quality on Copper and Molybdenite Flotation

Maria Sinche Gonzalez and Daniel Fornasiero

*Ian Wark Research Institute, University of South Australia, Mawson Lakes Campus, South Australia 5095, Australia*

MariaMargarita.SincheGonzalez@postgrads.unisa.edu.au

The separation process of valuable mineral from gangue mineral in a liquid phases through flotation is ruled by complex reactions and interaction between water and its species with mineral particles, air bubbles and reagents. Water is extremely important in the separation of minerals as it controls mineral hydrophobicity [1] and because of the large amount of water used in the flotation circuit.

In this study, the effect of water quality on chalcopyrite and molybdenite flotation in the Cerro Verde ore and in single mineral experiments was investigated.

Preliminary results show that chalcopyrite flotation was strongly depressed at pH 9.3 by aluminum and iron species in solution but less depressed by magnesium species and not affected by calcium and sulphate species. Molybdenite flotation was strongly depressed by sulphate, iron and manganese species in solution but less depressed by aluminum and magnesium species and not affected by calcium species. The interpretation of the zeta potential of these sulphide minerals indicates that the cause of the decrease in flotation is the precipitation/adsorption of metal hydroxides on the chalcopyrite and molybdenite surfaces [2, 3].

With the Cerro Verde ore, it was found that Cu and Mo flotation recoveries were affected by the type of water used at the plant site, particularly for molybdenite flotation. Grade and recovery of molybdenite were strongly depressed by the water from a river which has a high amount of coliforms and dissolved organic carbon. A correlation between flotation results and the species present in the water will be performed to identify the species responsible for the decrease in flotation performance.

Results obtained in this study suggest that the floatability of sulphide minerals is adversely influenced by changes in water quality and concentration of its constituents, especially when water is recycled and/or is supplied from different sources of water.

1. Wills, B.A., Napier-Munn, T., (2006). Mineral Processing Technology, seventh ed. Julius Kruttschnitt Mineral Research Centre.
2. Hoover, M. R., (1980). Water chemistry effects in the flotation of sulphide ores a review and discussion for molybdenite, *Complex Sulphide Ores*, 100-112.
3. Fuerstenau, M.C; Miller, J.D. and Kuhn, M.C. (1985) *Chemistry of Flotation*, Amer. Inst. Min. Metall. Pet. Eng., New York, pp 1-45.

## Fundamental Study of the Mechanism and Kinetics of Nucleation and Growth of Electrocrystallization of Copper onto Glassy Carbon and Gold Electrodes

Bogale Tadesse, Jonas Addai-Mensah, Daniel Fornasiero and John Ralston

*Ian Wark Research Institute, University of South Australia, Mawson Lakes Campus, Mawson Lakes, Adelaide, SA 5095, Australia*

Bogale.Tadesse@postgrads.unisa.edu.au

Electrocrystallization involves the formation and growth of crystals at electrochemical solid/solution interfaces and is a powerful method for various technological applications such as fabrication of metallic alloys, semiconductors, magnetic and non-magnetic layers, nano-particles, ultrathin films, electroplating and electrowinning of metals [1]. The early stages of electrochemical phase transformations can be readily controlled by the current density and applied potential and thus various outputs can be obtained as desired. Although electrocrystallization processes have been studied for long time, fundamental understanding still persists in the mechanism and kinetics of nucleation and growth of crystals at the substrate surfaces. For instance, there is disagreement in values of the critical nucleus size obtained from electrochemical experiments using 3D electrodeposition models and those obtained by direct microscopic observation at the electrodes. The overpotential, pH, electrolyte concentration, substrate surface roughness and additives are found to affect the morphology and quality of the crystal obtained during electrocrystallization [2]. Although some additives have beneficial effects (brightening and smoothing of deposit), their mechanism of action has yet not been completely elucidated. The focus of this work is to investigate the effect of deposition potential, pH, additives and electrolyte concentration on the nucleation mechanism and kinetics of electrocrystallization of copper onto glassy carbon and gold electrodes. The preliminary results obtained from cyclic voltammetric and chronoamperometric experiments will be presented.

1. G. Staikov, *Electrocrystallization in Nanotechnology*, WILEY-VCH Verlag GmbH & Co. KGaA, Weinheim, 2007.
2. M.R. Majidi, K. Asadpour-Zeynali, B. Hafezi, *Electrochimica Acta* 54, 1119-1126, 2009

## Measuring the Critical Strain of Flocculated Particulate Networks

Ashish Kumar, Adam Kilcullen, Jonathan Foong, and Peter Scales

*Particulate Fluids Processing Centre, Department of Chemical and Biomolecular Engineering, The University of Melbourne, VIC, 3010, Australia*

a.kumar3@pgrad.unimelb.edu.au

The measurement of the rheology and flow behaviour of flocculated particulate suspensions has been the subject of extensive research aimed at predicting and optimising suspension transport and handling processes such as pipelining, mixing, solid-liquid separation and pumping. These suspensions encompass materials such as mineral slurries, biomass, pigments and mine tailings; the efficient processing of which is significant from an economic standpoint. As the particulate concentration of these suspensions increase, they reach a critical concentration at which they become networked and are characterised by a yield stress and non-Newtonian flow behaviour.

Measurement of the yield stress of these suspensions is important to the prediction and design of a range of processes such as the start up of pipelines (shear yield stress) and the dewatering of suspensions (compressive yield stress). In some instances, such as in dewatering in the presence of shear, knowledge of the effect of shear processes on compression is critical. However, there is little known about the relationship between the shear and compressive yield stress of these suspensions and systematic experimental evidence is scant. It has been suggested that the ratio between the two parameters will depend strongly on the critical strain,  $\gamma_c$ . This parameter is well known in the characterisation of polymer melts but its measurement as the deformation at the transition from linear to non-linear viscoelastic behaviour of coagulated suspensions has not been reported systematically for a range suspension conditions. It has been proposed that at low to moderate solids concentrations (relative to close packing), that the critical strain will scale as the inter-particle force between two particles.

Measurement of the critical strain is facilitated through small angle oscillatory shear (SAOS) using a stress-controlled rheometer (AR-G2, TA Instruments) incorporating a vane. Analysis of the resulting data through Lissajous plots and Fourier transform of the rheometer output to study the development of higher order harmonics provides graphical evidence for the onset of non-linear viscoelastic deformation, indicating critical stress and critical shear stress values. Initial results show the critical stress to be lower than might be expected from conventional shear yield stress measurements using a vane.

## Modeling of Dewatering Using the Discrete Element Method (DEM)

Ben B.G. van Deventer, Peter J. Scales and Murray Rudman

*Particulate Fluids Processing Centre, Department of Chemical & Biomolecular Engineering, The University of Melbourne, VIC, 3001, Australia*

b.vandeventer@prad.unimelb.edu.au

The dewatering process aims to increase the concentration of solids within particulate suspensions. Separation through dewatering relies on the difference in density between the solids and liquid phases; dewatering performance is indeed proportional to this difference. Discrepancies exist between theoretical dewatering behaviour, and actual performance. Such discrepancies have been attributed to various shear and compression induced effects.

In order to capture complex particle-fluid behaviour, it is possible to combine the discrete element method (DEM) with computational fluid dynamics (CFD), using what has been termed the Combined Continuum and Discrete Model (CCDM). To develop a fundamental understanding of the behaviour of particles undergoing dewatering, CCDM will be used.

CCDM allows the development of a particle scale model, allowing the input of fundamental information such as particle size, particle size distribution, material elasticity, bonding strength, and attractive and repulsive forces such as van der Waals. Through the modelling of batch settling (Fig. 1), the effect of these particle scale properties on dewatering behaviour can be investigated through traditional dewatering parameters such as the hindered settling function. Additionally, through the modelling of aggregate structures, the effect of shear on these aggregate structures can be used to investigate the theory of shear induced aggregate densification.

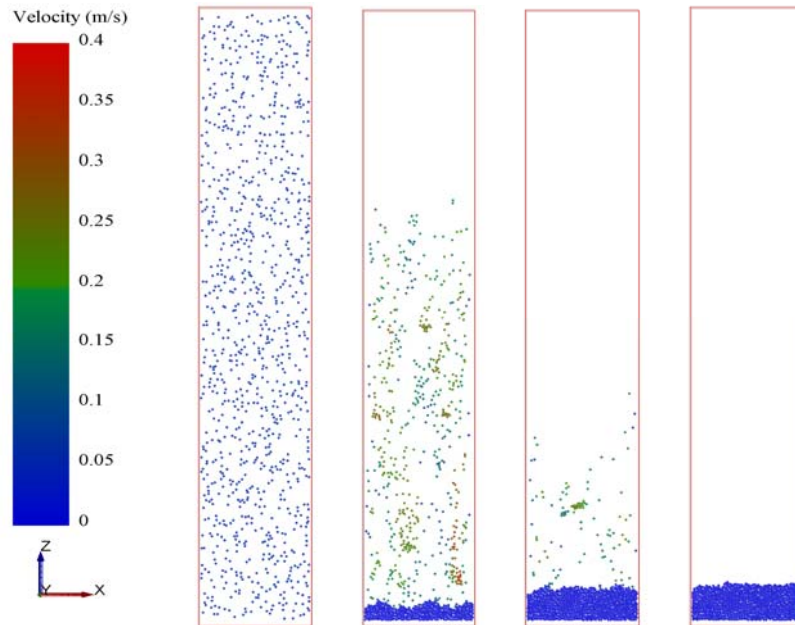


Fig. 1. Images of transient particle sedimentation, from left to right, the sedimentation times are 0.01, 0.6, 1.2 and 1.8 seconds respectively. The colours of the particles represent their sedimentation velocities.

## Development of a Novel Near Net Shaping Method in Ceramic Processing: Influence of Dispersant Size on Rheology of Non-Aqueous Suspensions

Stephen Tanurdjaja, Carolina Tallon, Peter Scales and George V. Franks

*University of Melbourne, Parkville, VIC,3052, Australia*

stanu@unimelb.edu.au

Recent developments in ceramic shaping methods have enabled the formation of not only strong but also corrosion proof, high temperature and wear resistant ceramics, called advanced ceramic materials. Examples of these shaping methods are gel casting, freeze casting or direct coagulation casting. These shaping methods have the potential to cut cost by producing complex ceramic articles which are close to their final shapes; thus, reducing machining steps.

We are developing a new route for shaping ceramic materials through dispersion of ceramic particles in a non-aqueous medium. The key to develop this new method is in understanding and controlling colloidal interactions in the ceramic suspensions. The surface of ceramic particles, which is hydrophilic in general, is modified by adsorption of polymer (physisorption) or by alkylation reaction with alcohol (chemisorption) to enable dispersion in this medium. Alumina particles and a linear alkane have been used in this study as a model. Rheological measurements of ceramic suspensions indicate that it may be possible to achieve high solid loading (50%vol) with relatively low viscosity (0.253 Pa.s at  $100\text{s}^{-1}$ ). Preliminary results have shown that these conditions enable preparation of green bodies with high density. Interaction potential between particles has been calculated to model the observed rheological behaviour.

## Synthesis and Characterisation of Oligomeric Surfactants

Natalie M. Baptista and Gregory G. Warr

*School of Chemistry, The University of Sydney, NSW, 2006, Australia*

n.baptista@chem.usyd.edu.au

Oligomeric surfactants have many desirable properties including very low critical micelle concentrations and a high surface activity which makes them good potential candidates for a variety of applications. Oligomeric surfactants are composed of two or more amphiphilic monomers joined by spacer groups. Here we use a linkage elimination/addition reaction to produce oligomeric cationic alkylpyridinium surfactants [1].

The aims of this project are to synthesise 2-(2-hydroxyethyl)-*N*-dodecylpyridinium chloride (2HEDPC) and to study the rate of oligomerisation in methanol at various pH's over time. This would allow us to identify and produce a particular oligomeric distribution for a given pH and reaction time. In water, the 2HEDPC monomer forms micelles above the critical micelle concentration, whereas in methanol it is free surfactant in solution. Polymerisation in both water and methanol will allow us to compare the resulting morphology of the oligomers obtained and deduce whether this is affected by the self-assembled structures present in the initial solution.

1. K. White, K., G. G. Warr, 'Linkage by elimination/addition: A simple synthesis for a family of oligomeric alkylpyridinium surfactants'. *J. Colloid Interface Sci.* **2009**, *337*, 304–306.

# Experimental Techniques

## Atomic Force Microscope (AFM)

The Atomic Force Microscope is one of a family of Scanned Probe Microscopes derived from the Scanning Tunnelling Microscope. They all share three attributes: a mechanism for translating a surface in three dimensions typically with the precision on the atomic scale, a probe which is sensitive to a particular surface phenomenon which decays as a function of distance normal to a surface, and a feedback mechanism which can couple the previous two elements. In AFM the translating element is piezoelectric element, and the probe is comprised of either (i) a sharp tip or (ii) particle (so-called "colloid probe") affixed to the free end of a cantilever.

Laser light from a solid state diode is reflected off the back of the cantilever and collected by a position sensitive detector (PSD) consisting of two or four closely spaced photodiodes whose output signal is collected by a differential amplifier. Angular displacement of cantilever results in one photodiode collecting more light than the other photodiode, producing an output signal (the difference between the photodiode signals normalized by their sum) which is proportional to the deflection of the cantilever. It detects cantilever deflections  $<1 \text{ \AA}$  (thermal noise limited) - see Fig. 1. A long beam path (several cm) amplifies changes in beam angle. Because of AFM's versatility; it has been applied to a large number of research topics. The AFM has also gone through many modifications for specific application requirements.

### Measuring forces

Because the atomic force microscope relies on the forces between the tip (or "colloid probe") and sample, knowing these forces is important for proper imaging. The force is not measured directly, but calculated by measuring the deflection of the lever, and knowing the stiffness of the cantilever. Hook's law gives  $F = -kz$ , where  $F$  is the force,  $k$  is the stiffness of the lever, and  $z$  is the distance the lever is bent. Typical force curve is presented in Fig. 2.

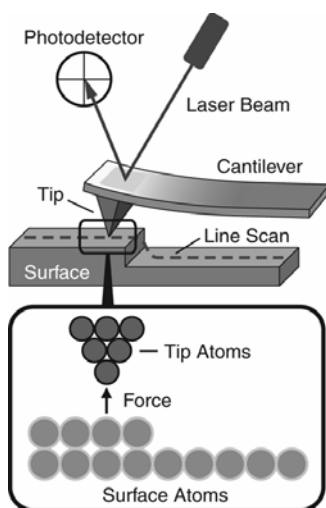


Fig. 1. Schematic of AFM

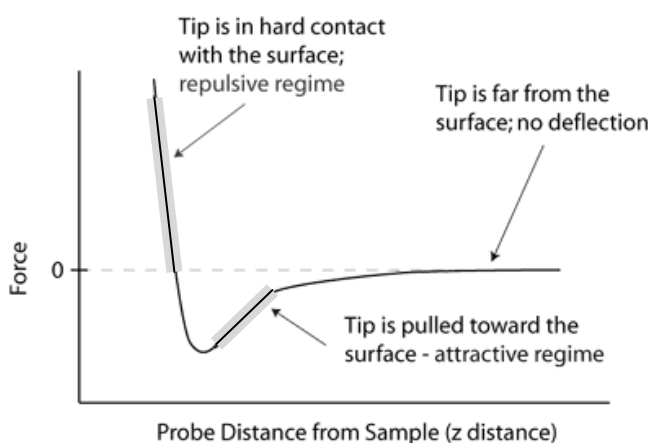


Fig. 2. Typical force curve

Binnig, Quate, and Gerber invented the Atomic Force Microscope (AFM) in 1985. Their original AFM consisted of a diamond shard attached to a strip of gold foil. The diamond tip contacted the surface directly, with the interatomic van der Waals forces providing the interaction mechanism. Detection of the cantilever's vertical movement was done with a second tip - an STM placed above the cantilever.

## Cyclic Voltammetry (CV)

Cyclic Voltammetry is an electrochemical technique that is the most widely used to obtain qualitative information about electrochemical reactions. It offers a rapid location of redox potentials of the electroactive species, and evaluation of the effect of media upon the redox process. CV can also provide information on the thermodynamics of redox processes and the kinetics of heterogeneous electron-transfer reactions as well as on coupled chemical reactions and adsorption processes.

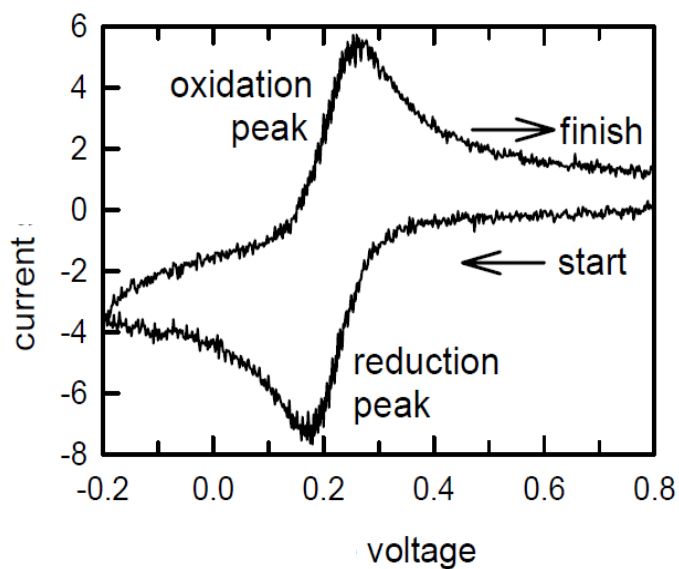


Fig. 1. A typical voltammogram of a reversible redox process

*Summary provided by Vera Lockett*

## Dynamic Light Scattering

The Dynamic Light Scattering (DLS) technique measures particle size. Sub-micrometre sized particles in a dispersion move constantly in a random, Brownian motion. When a laser beam is shone through the dispersion, the light is scattered by the particles. The Brownian movement of the particles causes the intensity of the scattered light to fluctuate. By measuring the rate of fluctuation, the speed at which the particles are diffusing (the diffusion coefficient) is determined. Using the Stokes Einstein equation the particle diameter ( $d$ ) is calculated from the particle diffusion coefficient.

DLS measures the hydrodynamic diameter of the particles. That is the size of a particle with the same diffusion coefficient as the scattering particles. The particle shape is assumed to be spherical. The hydrodynamic diameter includes molecules adsorbed to the surface and the solvation layer that moves with the particle. The diffusion coefficient of the particles, and hence the hydrodynamic radius, can be sensitive to changes in the ionic strength of the dispersion and conformational changes of adsorbed species on the particles.

DLS instruments use a correlator to construct a correlation function of the intensity of the light scattered by the particles. The correlation curve is fitted to an exponential function. The diffusion coefficient is proportional to the lifetime of the exponential decay. The particle size distribution obtained from the correlation function is an intensity size distribution, a plot of the relative intensity of light scattered by particles in various size classes. The intensity of light scattered by a particle is proportional to  $d^6$  (Rayleigh approximation). Thus the intensity size distribution tends to be biased towards the larger particle sizes in a polydisperse distribution.

*Summary provided by Catherine Whitby*

## Electrokinetic Sonic Amplitude Effect “AcoustoSizer”

The application of an AC voltage across a colloidal dispersion causes the particles to vibrate at a velocity dependent upon their size, zeta potential and the applied frequency. At the high frequencies employed in the “AcoustoSizer”, typically around MHz, the particles emit acoustic waves in response to the alternating voltage. By pulsing the voltage signal the acoustic response or electrokinetic sonic amplitude (ESA) of the particles can be recorded as a function of frequency. The ESA signal is a linear function of the applied voltage and hence a Fourier transform of the recorded acoustic response is required.

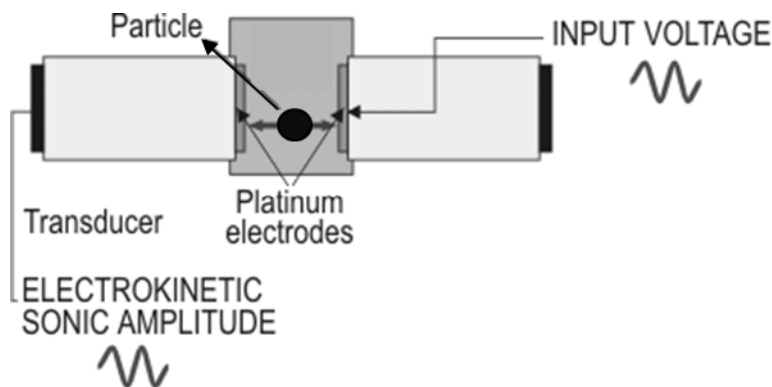


Fig. 1 Schematic diagram of the AcoustoSizer showing how zeta potential can be measured.

From the ESA spectrum the dynamic mobility is obtained from which the size and charge of the particles can be determined. The larger the difference between the densities of the fluid electrolyte and the colloid, or the larger the volume fraction the greater the ESA signal.

The dynamic mobility is a complex quantity equal in magnitude to the ratio of the particle velocity divided by the applied field. It is complex because there is a phase lag between driving frequencies and the response of the particles to that field. As the applied field tends to zero the mobility becomes a real quantity, equal to the electrophoretic mobility defined for a static (DC) applied field. Field strengths are in the order of  $100\text{Vm}^{-1}$ , and at MHz frequencies typical particle displacements are in the order of  $10^{-13}\text{m}$ . At low frequencies the inertia of particles is not sufficient to cause a large enough phase lag to connect dynamic mobility with particle size, and only zeta potential is accessible. However, as the frequency increases the particle motion lags more and more behind the field and both size and zeta potential become available. At higher frequencies the ESA effect is too small to give a measurable signal. It is observed for many colloid systems that the equations governing the dynamic mobility simplify such that the size is determined solely by the argument and the zeta potential from the magnitude of this complex quantity. Unlike traditional electrokinetic measurements this technique is well suited to concentrated dispersions.

## Flotation

Flotation or froth flotation is a simple and inexpensive process used for the separation of particles (smaller than 500  $\mu\text{m}$ ) based on hydrophobicity contrast of their surfaces. Only hydrophobic particles attach to gas bubbles (smaller than 2mm) rising through the mineral pulp. At the top of the flotation cell, these gas bubbles break up allowing the floated particles to be recovered. In froth flotation, the floated particles are trapped in the froth at the top of the flotation cell before being recovered; the froth constitutes an additional separation process.

To increase the mineral separation, a variety of reagents are added to the mineral pulp. Collectors are added to increase the surface hydrophobicity of valuable material particles and therefore increase their attachment to gas bubbles (only a few minerals are naturally hydrophobic, for example talc, sulphur or molybdenite). Collectors are surfactants which consist of a head group which attaches to specific sites on the mineral surface and a hydrocarbon chain or tail which impacts hydrophobicity of the mineral surface. On the other hand, depressants such as inorganic ions or polymers are added to make the mineral surface more hydrophilic and, therefore, to depress the flotation of these minerals.

Flotation has also been used in the treatment of waste water, coal, clays, corn, proteins, dyes, rubber, glass, plastic, etc.

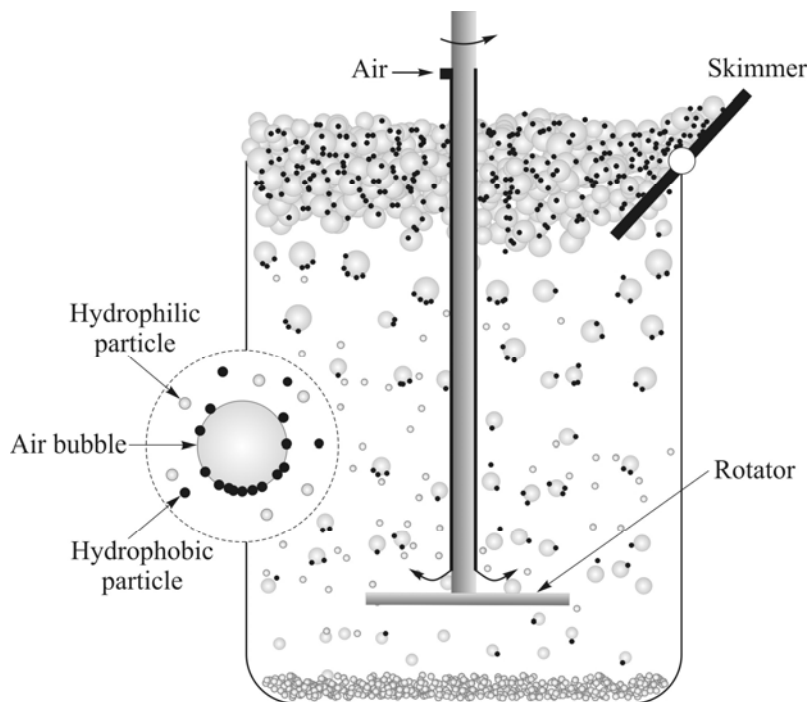


Fig. 1 A very simplified schematic of a flotation cell

*Summary provided by Daniel Fornasiero*

## Neutron and X-ray reflectivity

**Neutron reflectivity** is a technique which provides structural information about surfaces and thin films. The technique involves shining a highly collimated beam of neutrons onto an extremely flat surface and measuring the intensity of reflected radiation as a function of angle or neutron wavelength. The exact shape of the reflectivity profile provides detailed information about the structure of the surface, including the thickness, density, and roughness of any thin films.

Neutron reflectivity is a specular reflection technique, where the angle of the incident beam is equal to the angle of the reflected beam. The reflection is usually described in terms of a momentum transfer vector, denoted  $Q_z$ , which describes the change in momentum of a neutron after reflecting from the material. Conventionally the z direction is defined to be the surface normal direction, and for specular reflection, the scattering vector has only a z-component. A typical neutron reflectivity plot displays the

reflected intensity (relative to the incident beam) as a function of the scattering vector,  $Q = \frac{4\pi \sin \theta}{\lambda}$ , where  $\lambda$  is the neutron wavelength. The reflected intensity is a function of the scattering length density,  $\rho = \sum_i n_i b_i$ , where  $n_i$  is the number density of each component and  $b_i$  is its scattering length, and the variation in reflectivity with  $Q$  is a function of the adsorbed layer thickness,  $\tau$ .

Neutron reflectivity is sensitive to contrast arising from different nuclei, and the feature that makes this technique so powerful is the difference in scattering lengths of hydrogen ( $-0.374 \times 10^{-12}$  cm) and deuterium ( $0.676 \times 10^{-12}$  cm). Hence, selective deuteration allows certain parts of molecules or ions to be highlighted, whilst the chemistry is unaltered.

<http://www.isis.stfc.ac.uk/instruments/reflectometry2594.html>

**X-ray reflectivity** is used to probe the structure of surfaces, thin-films or buried interfaces as well as processes occurring at surfaces and interfaces such as adsorption, adhesion and interdiffusion. The technique directs a beam of x-rays on a surface and measures the intensity of x-rays reflected in the specular direction. If the interface is not perfectly sharp and smooth then the reflected intensity will deviate from that predicted by the law of Fresnel reflectivity. The deviations can then be analyzed to obtain the density profile of the interface normal to the surface.

A beam of x-rays is directed at the interface at an incident angle,  $\theta$ . The reflected beam intensity,  $R$ , is measured as a function of the change in momentum transfer normal to the

surface,  $Q = \frac{4\pi \sin \theta}{\lambda}$ , where  $\lambda$  is the wavelength of the beam. The reflected intensity is a function of the scattering length density profile perpendicular to the interface. The scattering length density,  $\rho$ , of a

given species depends on its electron density, and is given by  $\rho = \frac{\sum_i z_i r_e}{V_m}$ , where  $z_i$  is the atomic number of an element  $i$ ,  $V_m$  is the molecular volume and  $r_e$  is the Compton radius. The reflectivity profile can reveal oscillations in the reflection intensity, which arises from the interference of waves reflecting from the different layers within the system. The periodicity of these KIESSIG fringes is related to the thickness of the film.

*Summary provided by Deborah Wakeham*

## Particle-Film ATR FTIR Spectroscopy

Fourier transform infrared spectroscopy (FTIR) is a powerful and versatile technique for the characterization of molecules and their environment [1]. The benefits of the technique for studying molecular systems have resulted in many applications to interfacial systems [2, 3]. However, the use of FTIR in wet surface chemistry is sometimes hindered by issues of sampling and spectral interference from solution species, and the bulk liquid and solid phases associated with wet interfaces. One successful method of applying infrared spectroscopy for in situ adsorption studies is attenuated total reflection FTIR [1, 4]. Passage of the probe infrared radiation through an IR transparent crystal allows light delivery to the interfacial region between the crystal and a solution without the beam undergoing attenuation by reaching the interface through the liquid phase. If an adsorbate is present in significant amounts at the interface, the internal reflection of the IR light is attenuated at the characteristic frequencies of the adsorbate molecular vibrations, resulting in the acquisition of the spectrum of the adsorbate by the FTIR spectrometer. Provided that the solution concentration of the adsorbate is below the detection limit of the instrument in ATR mode, the signal detected is solely from the adsorbed species, i.e. the technique is surface selective and surface sensitive.

Whereas ATR crystals provide ideal substrates for many in situ interfacial spectroscopic investigations, they do limit the number of substrates that can be studied (eg. IR transparent crystal materials such as germanium, silicon, zinc sulfide or selenide, etc.). One means by which users can extend this range of substrates is to use deposited films of particles atop the ATR crystal [5]. Provided that the film is stable, thin enough (i.e. sub-micron), continuous, and not too optically dense, the ATR experiment can proceed as before, but this time the interface probed is the particle-solution interface. Another advantage of the particle film approach is that the available surface area of the substrate for adsorption is increased, resulting in higher sensitivity for detection of the adsorbate, which in many cases allows in situ kinetic studies of adsorption to be performed [6].

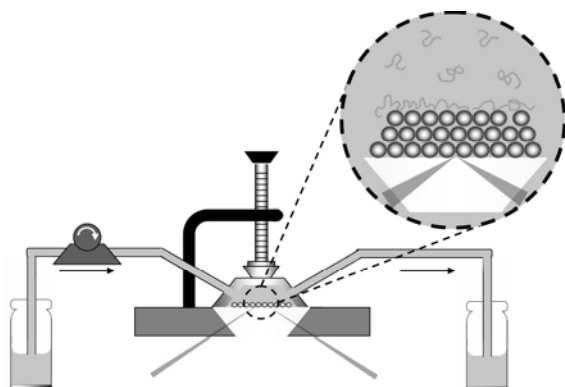


Fig. 1 – Schematic of experimental set-up for an in situ adsorption experiment using particle film ATR FTIR. The infrared beam comes from the spectrometer IR source and bounces off the crystal/particle film – liquid interface and is sent to the spectrometer detector. Diagram produced by Audrey Beaussart.

### References:

- [1] P.R. Griffiths, J.A. De Haseth, Fourier transform infrared spectrometry. 2nd ed., Wiley, Hoboken, New Jersey, 2007.
- [2] J.T. Yates, T.E. Madey, Vibrational spectroscopy of molecules on surfaces. Plenum Press, New York, 1987.
- [3] R. Aroca, Surface enhanced vibrational spectroscopy. Wiley, Hoboken, NJ, 2006.
- [4] N.J. Harrick, Internal Reflection Spectroscopy. Wiley, New York, 1967.
- [5] A.J. McQuillan, Adv. Mater. 13 (2001) 1034.
- [6] L.T. Cuba-Chiem, L. Huynh, J. Ralston, D.A. Beattie, Langmuir 24 (2008) 8036.

*Summary provided by David Beattie*

## Positron Annihilation Lifetime Spectroscopy (PALS)

Positron annihilation lifetime spectroscopy (PALS) is a technique which utilises positrons to directly probe and thus characterise condensed media. It has been used extensively to characterise metals, ceramics and polymers and to some extent soft matter materials such as self-assembled amphiphile systems. Positrons are formed when radioactive isotopes such as  $^{22}\text{Na}$  undergo radioactive decay. Figure 1 presents the nuclear decay scheme of  $^{22}\text{Na}$ .

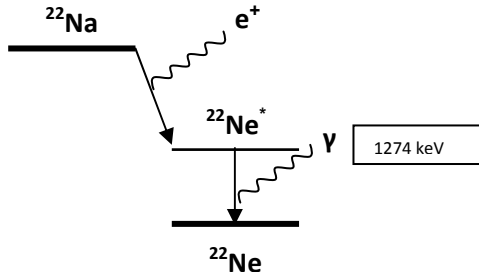


Fig. 1 - Schematic of  $^{22}\text{Na}$  decay pathway. The birth of the positron and the emission of a gamma ray occur within 3 ps of each other and usually assumed to be a simultaneous process.

The emission of the positron and photon is regarded to occur simultaneously. Thus, the detection of the 1274 keV photon is used to tag the ‘birth’ of the positron. When the positron encounters the material of interest, it will accumulate in areas of low electron density (void space). The positron will then annihilate with an electron from the sample, and emission of two 511 keV photons signals the ‘death’ of the positron. The time difference between the 1274 and 511 keV photons provide information regarding the lifetime of the positron. The positron lifetime or in other words, the rate of positron annihilation is affected by the medium in which the positron annihilates. By measuring the lifetime of the positron in the sample, information regarding both the physical and chemical nature of the medium can be obtained. Figure 2 is a representation of a PALS experimental setup.

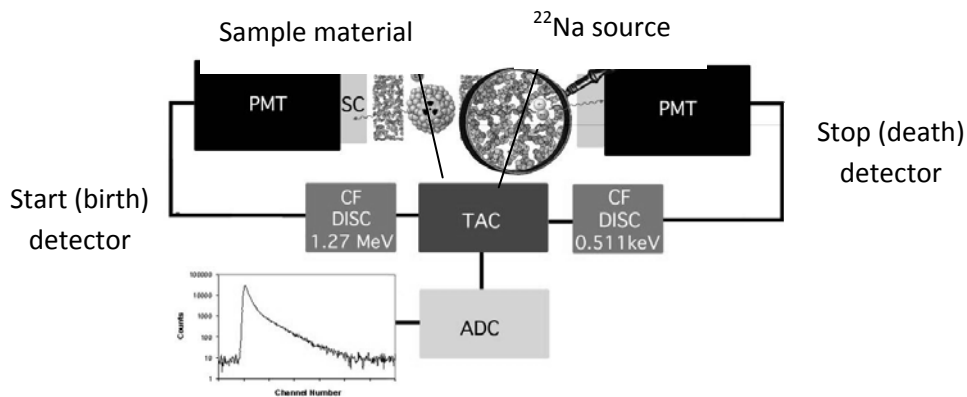


Fig. 2 - Schematic of the PALS spectrometers and electronics. The resulting PALS spectrum is a histogram of the number of counts with a particular lifetime.

Following analysis with the appropriate fitting programs two parameters can be obtained from the raw PALS spectrum –  $\tau$  and  $I$ .  $\tau$  represents the lifetime of the positron and is an indication of the pore size in solid state materials, while  $I$  corresponds to intensity which provides information on the number density of the pores, or in other words the porosity of the material.

*Summary provided by Aurelia Dong*

## Small-Angle X-ray scattering (SAXS)

Static small angle scattering methods allow the characterization of structures and their organization in the mesoscopic and microscopic size range, which makes these methods important and popular for the investigation of e.g. complex fluids, colloidal suspensions, synthetic and biological macromolecules or porous materials. While light scattering is used to explore rather large length scales, the mesoscopic size range can usually only be investigated using x-rays or neutrons. The choice of the technique depends on the particular properties of the sample since some samples have a high contrast for neutrons whereas other samples have a high contrast for X-rays. The analysis of the measured angular dependence of the scattered intensity provides information on size, structure and interaction of the scattering objects.

In a typical SAXS experiment, a highly monochromatic X-ray beam is focused on the sample. Due to inhomogeneities of the electron density of the sample, X-rays are scattered and collected using a 2-dimensional multidetector. The basic principle of a SAXS experiment is also illustrated in Fig. 1.

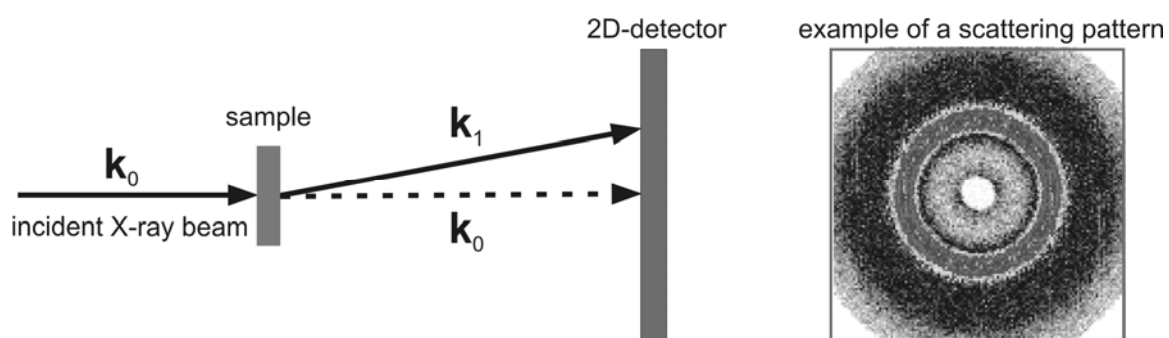


Fig.1 A typical SAXS experiment: The incident X-ray beam passes the sample and X-rays are scattered. A 2D-detector measures the scattered X-rays and a characteristic scattering pattern of the sample can be recorded. The shown pattern on the right is an example for an isotropic scatterer.

Most of the SAXS experiments can be performed without the need of large-scale facilities (as needed for experiments with neutrons) by using laboratory SAXS instruments. However, if X-rays with higher brilliance and a much higher focus are required, synchrotron sources have to be employed. A disadvantage of X-ray scattering experiments is the low scattering contrast for light atoms, since X-rays are scattered by electrons. Therefore, SAXS cannot be used for many organic samples. Another problem is damage to the sample due to the high energy of X-rays.

*Summary provided by Matthias Karg*

## Surface Force Apparatus (SFA)

Forces are measured as a function of distance between typically two crossed mica sheets, which were back-silvered and glued onto cylindrical silica discs (Fig.1 - part 1). The forces between mica surfaces are measured from the deflection of a cantilever spring that supports the lower surfaces (Fig.1 - part 2). The separation between surfaces is determined interferometrically by using fringes of equal chromatic order (FECO) (Fig.1 - part 3). The shape and pattern of optical fringes provide information about separation between surfaces, contact geometry such as contact area and deformation, and events happening between surfaces such as condensation, adsorption, and most unwelcomed surface contamination! The distance between surfaces is controlled by a series of coarse and fine micrometers connected to stepping/DC motors or a piezo drive (Fig.1 - part 4), with a synchronous motor coupled by a cantilever spring to the other surface. Number of modified versions has been developed to extend the SFA method such as for friction measurements.

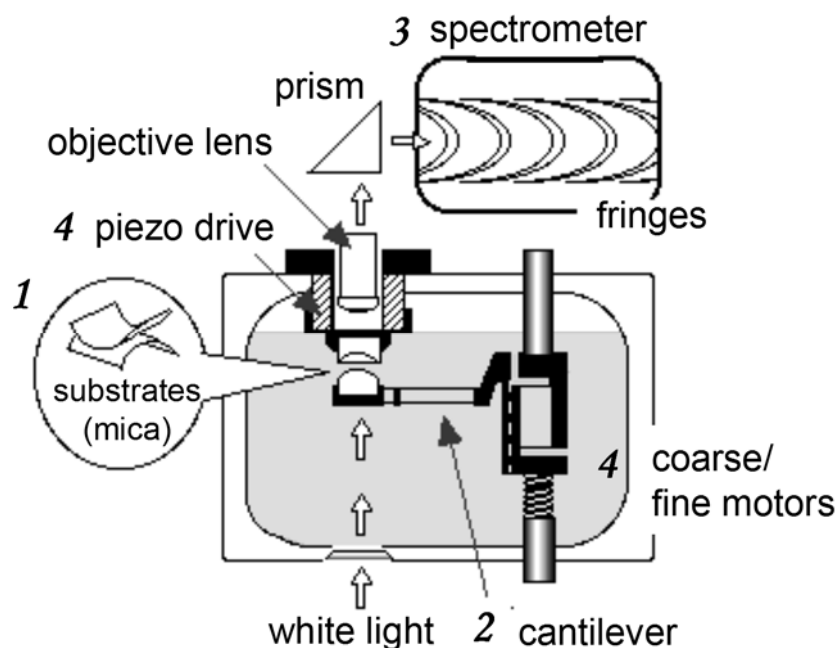


Fig.1 Surface Force Apparatus (SFA), "legendary" Mark II

*Summary provided by Satomi Onishi*

## Time-of-Flight Secondary Ion Mass Spectrometry (ToF-SIMS)

ToF-SIMS is an analytical technique for obtaining elemental and molecular information from surfaces with detection limits in the parts per billion range. In a ToF-SIMS measurement, the sample is placed in an ultrahigh vacuum (UHV) environment where a pulsed beam of primary ions bombard the surface ejecting atoms, molecular fragments and molecules. A small portion of these “secondaries” are in an charged state (positive and negative) and are extracted into a time of flight mass spectrometer and mass spectra are built up with each pulse of the primary beam. The primary beam currents employed are so low as to only remove perhaps 1 in a 1000 species from the top few monolayers of the surface, leaving the surface essentially undamaged. Secondary ion images may be obtained by scanning, or “rastering” the primary beam and collecting mass spectra as a function of beam position. Typical spatial resolution can be better than 0.5  $\mu\text{m}$ . Additionally, depth profiles may be acquired by alternating analysis and sputtering cycles using either the same primary beam or a second, sputtering ion source.

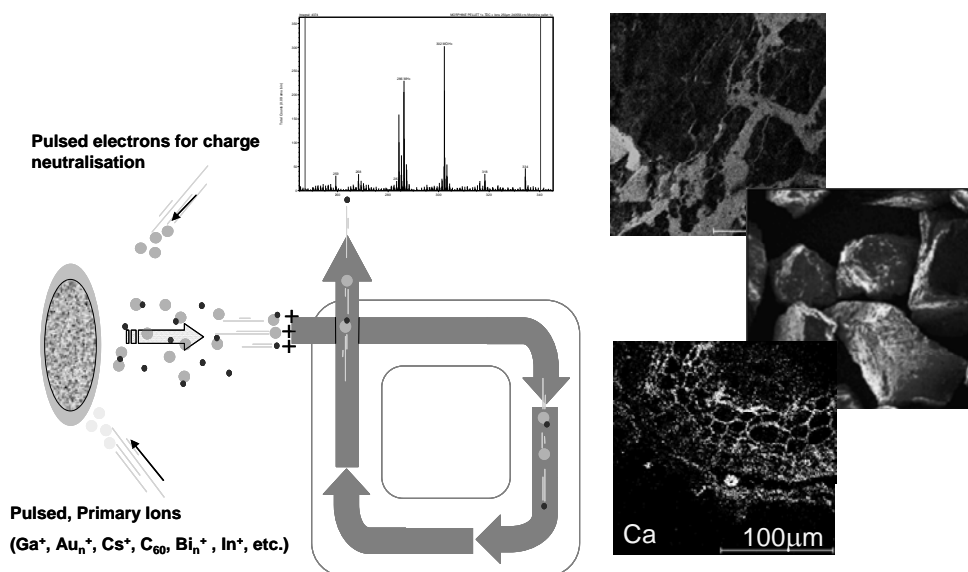


Fig. 1 Schematic of ToF-SIMS instrument with example data. Images are (clockwise from top) copper distribution in mineral section (200  $\mu\text{m}$  view), 20-38  $\mu\text{m}$  soil particles and Ca distribution in a tree root.

Primary beams available for modern ToF-SIMS instruments include – gallium ( $\text{Ga}^+$ ), gold and gold Cluster ( $\text{Au}^+$ ,  $\text{Au}_n^+$ ), bismuth and bismuth cluster ( $\text{Bi}^+$ ,  $\text{Bi}_n^+$ ), cesium ( $\text{Cs}^+$ ), indium ( $\text{In}^+$ ), argon ( $\text{Ar}^+$ ), oxygen ( $\text{O}^+$ ,  $\text{O}^-$ ),  $\text{SF}_6$ , etc. More recently, fullerene,  $\text{C}_{60}$ , primary ion sources have become available.  $\text{C}_{60}$  beams enhance the sputtering of large molecular weight molecular fragments and molecules and are therefore extremely useful analytical beams for organic materials and adsorbates.

In most ToF-SIMS instruments, samples may be cooled to liquid nitrogen temperatures to preserve species that may be volatile under UHV conditions, and insulating surface may be analysed using advanced charge neutralising electron flooding.

### Suggested reading:

Vickerman, J. C.; Briggs, D. D. *ToF-SIMS: Surface analysis by mass spectrometry*, Chichester, Surface Spectra and IM Publications, 2001

*Summary provided by Bill Skinner*

## Total Internal Reflection Microscopy (TIRM)

Total Internal Reflection Microscopy (TIRM), developed by Prieve *et al*<sup>1, 2</sup>, is a force measurement tool that uses Brownian motion to gauge the forces between a colloidal particle levitated above a plate. Compared to force balance methods that use mechanical springs such as atomic force microscopy (AFM) and the surface force apparatus (SFA) the TIRM is much more sensitive. On a force scale, TIRM is three and five times more sensitive than AFM and SFA, respectively<sup>2</sup>.

TIRM is an optically noninvasive experimental technique that measures the interaction potential energy of a levitated colloidal particle (typically 3-5 microns in diameter). The particle is illuminated by an evanescent wave created at the solid liquid interface above the critical angle, as shown in Figure 1. The intensity of the scattered light,  $I(h)$ , varies exponentially with the elevation with the evanescent wave decay length,  $\beta^1$ . The decay length is on the order of 100 nanometers, which translates into a separation distance resolution on the order of 1 nanometer.

The energy is measured by tracking the particle motion. The changes in particle elevation are measured using the evanescent wave. A large number of elevations are recorded over time and used to construct a probability density function of the particle residing at any elevation above the surface. The probability density function is related to the particle potential energy using a Boltzmann distribution according to

$$p(h) = Ae^{\left(\frac{-\phi(h)}{k_b T}\right)} \quad (1)$$

where  $p(h)$  is the probability density function of heights,  $f(h)$  is the interaction potential energy, and  $A$  is a normalization constant. Optical tweezers are also employed for solution changes and to bias the heights the particle samples to better elucidate different regions of the potential energy diagram.

A range of phenomena have been examined using TIRM including the diffusion of a particle near an interface, depletion force that arise from particles or polymers, retarded van der Waals-Casimir-Lifshitz forces, steric forces and electrical double layer forces<sup>1</sup>.

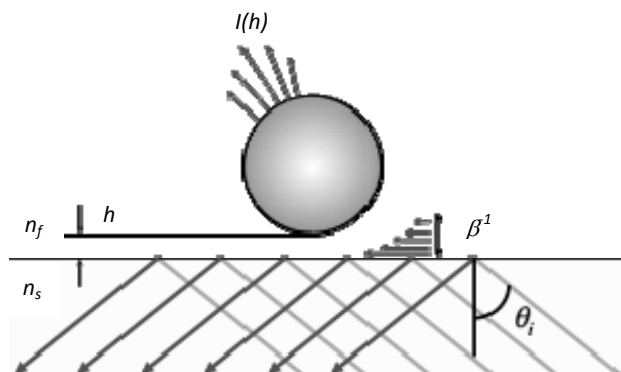


Fig. 1. A schematic of the TIRM showing a particle scatter the light from an evanescent wave generated at the solid liquid interface

### References:

- [1] D. C. Prieve, F. Luo and F. Lanni, *Faraday Discussions of the Chemical Society*, 1987, **83**, 297-307.
- [2] D. C. Prieve, *Advances in Colloid and Interface Science*, 1999, **82**, 93-125.

*Summary provided by Raymond Dagastine*

## Vibrational Sum Frequency Spectroscopy (VSFS)

Vibrational Sum Frequency Spectroscopy (VSFS) is a nonlinear optical technique used to study the details of molecular structure and dynamics at surfaces and interfaces. The extremely high surface selectivity of the VSFS process allows the thin layer of a few atoms or molecules near the interface to be probed. The surface selectivity is due to even-order nonlinear processes such as VSFS being forbidden, in the electric dipole approximation in media with inversion symmetry, e.g. gases, liquids, and isotopic solids. At an interface between two such media, the inversion symmetry is broken, and the VSFS optical signal can be generated and detected.

The VSFS technique involves two laser beams, a fixed visible beam and a tunable infrared beam, which are overlapped in space and time on the sample surface. A third beam is generated due to nonlinear effects, which carries information about the interfacial molecules. The intensity of this laser beam is proportional to the intensities of the incoming beams  $I_{IR}$  and  $I_{Vis}$  and the square of the nonlinear

susceptibility  $\chi^{(2)}$ ,  $I_{SFG} \propto \left| \chi_{eff}^{(2)} \right|^2 I_{IR} I_{Vis}$ .

An important aspect of VSFS is its ability to directly measure the orientation of molecules and even fragments of molecules (e.g. methyl groups, carbonyl groups, etc.) at the surface. This is achieved by performing the measurement with different polarizations of the two incoming beams, and the generated sum frequency beam.

*Summary provided by Deborah Wakeham*

# Index of Presenters

---

<b>Name</b>	<b>Presentation</b>	<b>Page</b>
Albrecht, Trent	<b>P18</b>	76
Aw, Moom Sinn	<b>P09</b>	67
Balasuriya, Thakshila	<b>O27</b>	44
Baptista, Natalie	<b>P24</b>	82
Bian, Xun	<b>P06</b>	64
Brito e Abreu, Susana	<b>O37</b>	54
Chatjaroenporn, Khwanrat	<b>O22</b>	39
Chen, Rodney	<b>O28</b>	45
Chen, Zhengfei	<b>O15</b>	32
Chipfunhu, Daniel	<b>O36</b>	53
Cho, Kwun Lun	<b>O02</b>	19
Chong, Josephine	<b>P11</b>	69
Chuanuwatanakul, Chayuda	<b>O35</b>	52
Del Castillo, Lorena	<b>O10</b>	27
Dermis, Terry	<b>O26</b>	43
Dong, Aurelia	<b>O20</b>	37
Driever, Chantelle	<b>O29</b>	46
Evenbratt, Hanne	<b>O30</b>	47
Fang, Jie	<b>O34</b>	51
Fong, Wye Khay	<b>P15</b>	73
Haebich Annette	<b>O18</b>	35
Harrington, Wendy	<b>O07</b>	24
Hayes, Robert	<b>O14</b>	31
Jiang, Li	<b>O13</b>	30
Kent, Ben	<b>O31</b>	48
Kumar, Ashish	<b>P21</b>	79
Lee, Thomas	<b>P04</b>	62
Li, Hua	<b>O17</b>	34
Lim, Josephine	<b>O08</b>	25
Liu, Connie	<b>O21</b>	38
Lockie, Hannah	<b>O19</b>	36
Manor, Ofer	<b>O09</b>	26
Niecikowska, Anna	<b>O12</b>	29
Nosrati, Ataollah	<b>O23</b>	40
O'Loughlin, Muireann	<b>P07</b>	65
Palmer, Lauren	<b>O03</b>	20
Paneru, Mani	<b>O01</b>	18
Park, Jin Sung	<b>P01</b>	59
Pegalajar Jurado, Adoracion	<b>P08</b>	66

Peng, Shuhua	<b>P13</b>	71
Penna, Matthew	<b>P17</b>	75
Pericet-Camara, Ramon	<b>PL</b>	17
Puah, Lee San	<b>O04</b>	21
Qian, Feng	<b>O39</b>	56
Ramiasa, Melanie	<b>P05</b>	63
Sham, Stefanie	<b>O33</b>	50
Sinche Gonzalez, Maria	<b>P19</b>	77
Smith, Jacob	<b>P12</b>	70
Tadesse, Bogale	<b>P20</b>	78
Tanurdjaja, Stephen	<b>P23</b>	81
Tayati, Ponlawat	<b>P02</b>	60
Teh, E-Jen	<b>O05</b>	22
Tilley, Adam	<b>P16</b>	74
Tse, Nicholas	<b>P14</b>	72
van Deventer, Ben	<b>P22</b>	80
Vancea, Valentin	<b>P10</b>	68
Wakeham, Deborah	<b>O16</b>	33
Walsh, Rick	<b>O32</b>	49
Xu, Danfeng	<b>O11</b>	28
Yeap, Kai Ying	<b>O06</b>	23
Yu, Yang	<b>O38</b>	55
Zeng, Weimin	<b>O25</b>	42
Zhang, Yansheng	<b>O24</b>	41
Zhu, Liwen	<b>P03</b>	61

